CHARACTERISATION OF ONCOGENIC LMP1 AND CD40 SIGNALS IN PRIMARY GERMINAL CENTRE B CELLS AND THEIR RELEVANCE TO THE PATHOGENESIS OF HODGKIN'S LYMPHOMA.

BY

ESZTER NAGY

A thesis submitted to The University of Birmingham

for the degree of DOCTOR OF PHILOSOPHY

School of Cancer Sciences

College of Medical and Dental Sciences

University of Birmingham

September 2013

Abstract

Latent membrane protein 1 (LMP1) is an oncogene expressed in a subset of germinal centre (GC)-derived lymphomas including Hodgkin's lymphoma (HL) and diffuse large B cell lymphoma (DLBCL). However, LMP1 shares functional homology with CD40, a receptor required for normal GC B cell development. Dissecting how LMP1 functions differently from CD40 in GC cells is central to a better understanding of lymphomagenesis and is the subject of this thesis.

In Chapter 3, I show that GC B cells can be successfully isolated from normal human tonsils and that these cells retain a GC phenotype upon short-term culture.

In Chapter 4 I explore how the transcriptional programmes of LMP1 and CD40 differ in GC B cells and identify a subgroup of genes regulated by LMP1 but not by CD40, which are also concordantly regulated in primary HL cells from which I focus on sphingosine-1-phosphate receptor 2 (S1PR2). I confirm that S1PR2 is an LMP1 target in GC B cells and show that it is not expressed in the tumour cells of the majority of cases of HL and DLBCL. In DLBCL, S1PR2 loss is associated with LMP1 expression. I also provide preliminary evidence that the over-expression of S1PR2 can inhibit the HL cell migration.

In Chapter 5, I report my initial attempts to optimise a method for the measurement of the activity of transcription factors in GC B cells which can be used to delineate those pathways activated by LMP1, but not by CD40, in GC B cells.

Acknowledgements

I would like to acknowledge the University of Birmingham for supporting my stipend and Leukaemia and Lymphoma Research whose support of the Murray lab made my research possible.

I would like to thank my supervisors Dr Martina Vockerodt and Professor Paul Murray for all their support. I am especially grateful for the patience with which you imparted your advice over the last four years, even if I may not have shown it at the time. Further thanks to Dr Vockerodt for introducing me to an eclectic repertoire of music in tissue culture.

I would also like to say thanks to all members of the Murray group past and present who not only supported me through my time in the lab, but made the last four years enjoyable. I would especially like to say thanks to Dr Zumla Cader, Dr Jenifer Anderton and Dr Jessica Edwards who were always ready to console and offer me their wisdom in times of need. Special thanks to Naheema Gordon and Daniela Liebelt and who were always there to listen (and provide the occasional distraction when needed).

Lastly, I would like to thank my friends and family, without who I would not be where I am today. In particular I want to thank my parents and my sister for their unconditional love and support. I could not have done it without you.

Table of Contents

List of Figures

List of Tables

List of common abbreviations

ABC	activated B cell like
AID	activation-induced cytidine deaminase
APC	allophycocyanin
ATF2	activating transcription factor 2
BCR	B cell receptor
BL	Burkitt's lymphoma
CD40L	CD40 ligand
CHOP	C/EBP homologous protein
CSR	class-switch recombination
CTAR	carboxy-terminal activating region
CXCL	CXC chemokine ligand
CXCR	CXC chemokine receptor
DLBCL	diffuse large B cell lymphoma
EBV	Epstein-Barr virus
FDC	follicular dendritic cell
FITC	fluorescein isothiocyanate
GC	germinal centre
GCB	germinal centre B cell like
HL	Hodgkin's lymphoma
HRS	Hodgkin and Reed-Sternberg
Ig	immunoglobulin
IHC	immunohistochemistry
IL	interleukin
JAK	janus kinase
JNK	c-Jun N-terminal kinase
LCL	lymphoblastoid cell line
LMP	latent membrane protein
MAPK	mitogen-activated protein kinase
mRNA	messenger-RNA
NF-κB	nuclear factor kappa –light chain- enhancer of activated B cells
PE	phycoerythrin
PI3K	phosphatidylinositol 3–kinase
qPCR	quantitative polymerase chain reaction
S1P	sphingosine 1 phosphate
S1PR	Sphingosine 1 phosphate receptor
SHM	somatic hypermutation
STAT	signal transducer and activator of transcription
Tfh	T follicular helper
TRAF	tumour necrosis factor receptor associated factor

Chapter 1

Introduction

1 Introduction

1.1 The germinal centre reaction

The germinal centre (GC) reaction takes place in secondary lymphoid organs and is the process in which naïve B cells encountering antigen proliferate, undergo somatic hypermutation and class-switch recombination to give rise to antigen specific plasma and memory B cells (MacLennan, 1994, Klein and Dalla-Favera, 2008). Several types of lymphoma derive from GC B cells. They include: Hodgkin's lymphoma, Burkitt's lymphoma, follicular lymphoma, post-transplant lymphomas and a subset of diffuse large B cell lymphomas (Kuppers, 2005). In order to understand the pathogenesis of these lymphomas, it is important to consider the GC reaction and how the disruption of the processes involved can lead to lymphomagenesis.

1.1.1 Entry into the GC

B cells produced in the bone marrow exit as mature B cells that express surface immunoglobulin (Ig)M. They are referred to as naïve B cells and upon exit from the bone marrow they migrate to lymphoid organs where they can interact with antigen presenting cells. Upon entry into a lymphoid organ, through the high endothelial venules (HEV), these naïve B cells migrate towards the outer follicle. This migration is a chemotactic response mediated by two receptors expressed on the surface of naïve B cells, CXCR5 and Epstein-Barr virus induced molecule 2 (EBI2), the ligands for which are produced by cells in the follicle (Cyster et al., 2000, Gatto and Brink, 2013).

Once a naïve B cell encounters its cognate antigen (presented by dendritic cells residing in the outer follicle), it up-regulates specific chemokine receptors that enable it to home

to the T cell zone of the follicle (Cyster, 2010, MacLennan, 1994, Pereira et al., 2010). These receptors include CCR7 which responds to the chemokines CCL19 and CCL21 produced in the T cell zone (Reif et al., 2002). In the T cell zone, the B cells become fully activated through their interactions with $CD4^+$ T follicular helper (Tfh) cells, and the GC reaction is initiated. One of the most important interactions for GC B cell survival and differentiation within the GC occurs between the CD40 receptor on B cells and its ligand (CD40 ligand, CD40L also known as CD154) on Tfh cells.

Following B cell activation by cognate antigen the cells migrate away from the T cell zone into the outer follicle. This migration is initiated by the EBI2 receptor in response to its ligand 7α,25-dihydroxycholesterol (Pereira et al., 2009, Gatto and Brink, 2013). The B cells then either differentiate into low affinity plasma cells directly in the extra follicular areas or mature into GC precursor B cells and migrate to the primary follicle (Klein and Dalla-Favera, 2008). B-cell lymphoma 6 (BCL6) is essential for GC formation and is highly expressed in GC B cells. It has been shown to be induced in activated B cells located in the outer follicle (Kitano et al., 2011). BCL6 can down-regulate EBI2 (Shaffer et al., 2001), leading to migration to the follicle centre where the GC reaction takes place (Pereira et al., 2009, Gatto et al., 2009).

Once in the primary follicle, the GC B cells undergo rapid proliferation, pushing the surrounding cells aside which form the mantle zone, forming the secondary follicle. Following further proliferation and differentiation the GC structure fully develops, displaying the dark and light zones.

1.1.2 Overview of the GC reaction

The GC reaction takes place within the dark and light zones of the GC, home to centroblasts and centrocytes respectively, depicted in Figure 1.1 (MacLennan, 1994).

The process of somatic hypermutation (SHM) occurs in the rapidly proliferating centroblasts and results in variation in the immunoglobulin (Ig) genes of centroblasts (Klein and Dalla-Favera, 2008). The process of SHM starts with the production of double strand breaks in the DNA induced by the activity of activation-induced cytidine deaminase (AID). This is followed by the error prone repair of the break, which leads to the introduction of mutations into the DNA, thus leading to somatically mutated heavy and light chain immunoglobulins.

SHM also induces mutations in non-Ig genes, for example, BCL6 and CD95 (Pasqualucci et al., 1998, Müschen et al., 2000). The importance of SHM of non-IG genes in lymphoma development is highlighted by the finding that in over 50% of diffuse large B cell lymphomas one or more non-Ig genes are hypermutated, for example MYC, paired box protein 5 (PAX5) and proto-oncogene serine/threonine-protein kinase 1 (PIM1) (Pasqualucci et al., 2001).

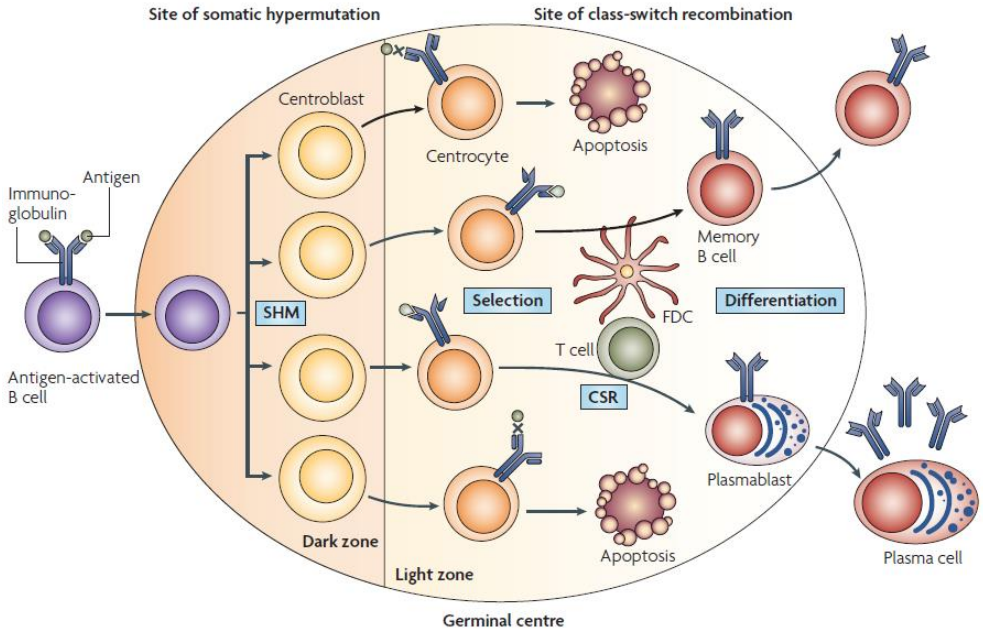

Figure 1.1: The germinal centre reaction (Klein and Dalla-Favera, 2008)
Following antigen encounter, naïve B cells enter the primary follicle and initiate the GC reaction, resulting in the formation of the characteristic GC structure composed of the mantle zone, dark zone and light zone. The dark zone is home to the highly proliferative centroblasts and is where clonal expansion and somatic hypermutation occur. The light zone GC B cells are the centrocytes and this is the site of affinity maturation, positive selection by follicular dendritic and follicular T helper cells, and class switch recombination. Throughout the process, cells with disadvantageous mutations are induced to undergo apoptosis.

Centroblasts express telomerase and their DNA damage response is suppressed in order to support their proliferation (Klein and Dalla-Favera, 2008). BCL6 is important for the suppression of the DNA damage response, firstly by suppressing p21, a key molecule involved in the initiation of cell cycle arrest and secondly, by down-regulating p53, a molecule involved in DNA damage mediated apoptosis (Phan et al., 2005, Phan and Dalla-Favera, 2004).

Centrocytes are smaller, non-proliferating cells undergoing selection for high affinity antibodies and class-switch recombination (CSR) before they are permitted to differentiate into either memory B cells or plasma cells (MacLennan, 1994). This selection process is crucial, as GC B cells have been shown to be highly prone to apoptosis (Liu et al., 1989). It has been shown that many anti-apoptotic molecules are down regulated in GC B cells, such as B-cell lymphoma 2 (BCL2), whereas pro-apoptotic molecules are up regulated, for example Bcl-2-associated X protein (BAX) and Bcl-2-associated death promoter (BAD) (Martinez-Valdez et al., 1996, Peperzak et al., 2012).

Selection for high affinity antibodies is a dual process requiring both FDCs and Tfh cells (Zotos and Tarlinton, 2012). First, centrocytes with B cell receptor (BCR) that binds the antigens presented on FDCs receive a survival signal upon successful interaction of the BCR with FDCs. Second, centrocytes with high affinity for antigen receive further survival signals through CD40 engagement by CD40L present on Tfh cells. Additionally, GC B cells have a high expression of CD95/Fas, a key receptor involved in apoptosis (Martinez-Valdez et al., 1996, Takahashi et al., 2001). The ligand for CD95 (CD95L/FasL) is found on T cells and can induce apoptosis in GC B cells that recognise self-antigens. This tight

control allows for the selection of B cells with a functional BCR and high affinity for antigen, but which are not auto reactive. Any GC B cell that does not meet these criteria fails to receive these survival signals and undergoes rapid apoptosis.

Centrocytes then undergo class-switch recombination (CSR), an irreversible somatic recombination affecting the immunoglobulin heavy chain constant region. This process results in a switch of Ig class without affecting the antigen specificity of the antibody. The process of CSR can be T cell dependent or independent, but is always directed by the presence of specific cytokines and co-stimulatory molecules (Klein and Dalla-Favera, 2008). The main co-stimulatory signals include CD40-CD40L and B7-related protein-1 (B7RP)-inducible T cell co-stimulator (ICOS) interactions between B cells and T helper cells, and engagement of B cell activating factor receptor (BAFFR) and trans-membrane activator and calcium-modulating cyclophilin ligand interactor (TACI) on the B cells (McAdam et al., 2001, Tafuri et al., 2001, Castigli et al., 2005). E2A activity and interleukin (IL)-21 are also required for CSR (Bartholdy and Matthias, 2004, Linterman et al., 2010).

The process of CSR requires DNA strand breaks and therefore poses the risk of malignant translocations. Examples include the t(8;14) immunoglobulin heavy chain variable region (IgH)/c-myc chromosomal translocation in endemic Burkitt's lymphoma and the t(3;14)(q27;q32) translocation of IgH and BCL6 observed in diffuse large B cell lymphoma (DLBCL) (Haluska et al., 1987, Hartl and Lipp, 1987, Baron et al., 1993, Ye et al., 1993, Iqbal et al., 2007).

Although the GC structure is morphologically distinguishable into dark and light zones, it is now clear that centroblasts and centrocytes can move between these zones (Allen et al., 2007, Schwickert et al., 2007). This movement is achieved through the expression of specific cytokines and their receptors. Centroblasts express the CXC chemokine receptor 4 (CXCR4) which is responsive to CXC chemokine ligand 12 (CXCL12) expressed in the light zone, whereas centrocytes express CXCR5 which is responsive to CXCL13 expressed in the dark zone (Allen et al., 2004, Caron et al., 2009). The previous dogma of the GC B cell as a rather stable structure has recently been challenged by the observation that non-GC B cells can enter the GC, and on occasion other B cells with higher affinity to antigen can outgrow the GC B cell population which initiated the reaction (Schwickert et al., 2007).

For the GC reaction to take place, it is essential that the GC B cells do not differentiate. BCL6 can inhibit plasma cell and memory B cell differentiation through multiple mechanisms (Basso and Dalla-Favera, 2012). For example, BCL6 down regulates genes needed for plasma cell differentiation, such as B-lymphocyte-induced maturation protein 1 (BLIMP1) and (interferon regulatory factor 4) IRF4.

1.1.3 Control of the GC reaction

The GC reaction is also tightly controlled through a variety of mechanisms which involve the regulation of cell migration as well as survival. GC B cells, more specifically centroblasts, are rapidly proliferating cells so what is stopping these cells from outgrowing their GC niche? Recently, two molecules have been implicated in the

maintenance of GC homeostasis; sphingosine 1 phosphate receptor 2 (S1PR2) and regulator of G-protein signalling (RGS13) (Figure 1.2).

Both S1PR2 and RGS13 are highly expressed in GC B cells and they both interact with G proteins (Shi et al., 2002, Green and Cyster, 2012). S1PR2 is a G protein coupled receptor that signals mainly through $G_{12/13}$, and can inhibit GC B cell migration in response to sphingosine 1 phosphate (S1P), a molecule present at high concentrations on the outer edge of the GC, leading to the retention of these cells within the GC structure. S1PR2 has also been implicated in the regulation of GC B cell survival (Green et al., 2011); in mice, S1PR2 deficient GC B cells showed increased growth in response to antigen stimulation compared to wild type cells.

RGS13 is a negative regulator of G_{α}, a G protein involved in CXCL12 and CXCL13 signalling (Shi et al., 2002, Han et al., 2006). CXCL12 and CXCL13 are key mediators of the GC structure by homing CXCR4 expressing centroblasts and CXCR5 expressing centrocytes to distinct areas within the GC (Allen et al., 2004). As with S1PR2, the loss of RGS13 expression lead to increased GC B cell growth compared to wild type in response to antigen stimulation (Hwang et al., 2013). Thus the high expression of S1PR2 and RGS13 in GC B cells is necessary to limit GC size.

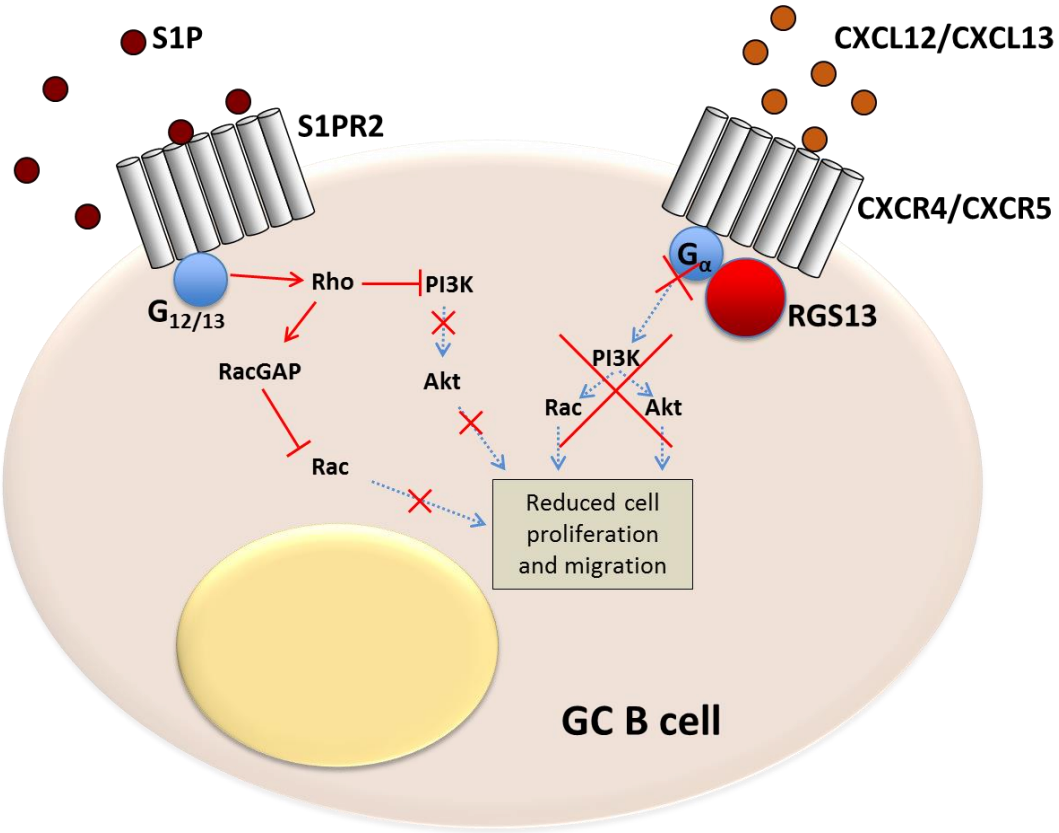

Figure 1.2: S1PR2 and RGS13 regulate GC B cell proliferation and migration
S1PR2 and RGS13 are highly expressed in GC B cells and interact with G proteins $G_{12/13}$ and G_{α} respectively.
Upon S1P binding, S1PR2 recruits $G_{12/13}$ resulting in the activation of Rho and subsequent inhibition of Rac and Akt, resulting in the inhibition of GC B cell migration. Rac inactivation is mediated by Rac GTPase proteins (RacGAP), while Akt inactivation is a consequence of Rho mediated inhibition of PI3K.
RGS13 can inhibit G_{α} and thus CXCR4 and CXCR5 signalling in GC B cells. Signalling via G_{α} activated PI3K and its down-stream effectors, such as Rac and Akt as depicted on the diagram. Inhibition of G_{α} by RGS13 results in reduced cell proliferation and migration.

1.1.4 Exit from the GC

Centrocytes can differentiate into either memory B cells or plasma cells (Figure 1.3). Not much is understood about GC B cell differentiation into memory B cell, however PAX5, CD40 signalling and phosphorylated STAT5 are all implicated in memory B cell development (Klein and Dalla-Favera, 2008, Victora and Nussenzweig, 2012).

The signals regulating plasma cell differentiation are better characterised. PAX5 inactivation and BCL6 repression appear to be involved in this process (Klein and Dalla-Favera, 2008). BCL6 repression results in increased expression of BLIMP1, a regulator of plasma cell differentiation. T cell help via CD40L is key, leading to CD40 mediated activation of NF-κB, which leads to the induction of IRF4 and the eventual down regulation of BCL6 (Sciammas et al., 2006, Klein et al., 2006). PD-1 signalling on T helper cells has recently been shown to contribute to long term plasma cell survival (Good-Jacobson et al., 2010).

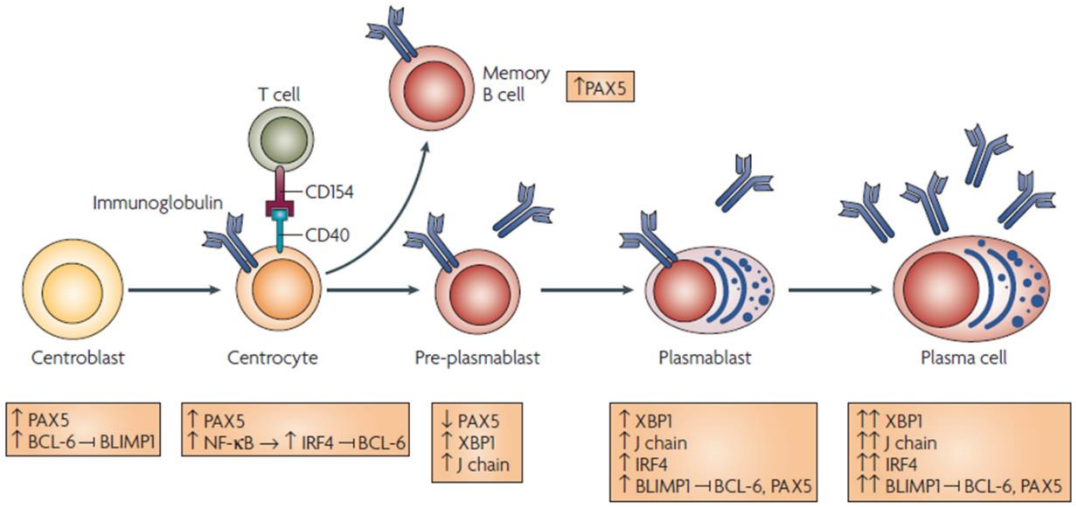

Figure 1.3: Differentiation of centrocytes (Klein and Dalla-Favera, 2008)
Centrocytes can differentiate into either memory B cells or plasma cells. Not much is understood about GC B cell differentiation into memory B cell. PAX5, CD40 signalling and phosphorylated STAT5 are all implicated in memory B cell development. The signals regulating plasma cell differentiation are better characterised. PAX5 inactivation and BCL6 repression are involved in this process. T cell help via CD40L is key, leading to activation of NF-κB, the induction of IRF4 and the eventual down regulation of BCL6 resulting in increased expression of BLIMP1, the master regulator of plasma cell differentiation.

Differentiated B cells, as well as other lymphocytes, exit from lymph nodes through the medullary sinuses into the lymphatic vessels. Lymphocyte egress is dependent on the cell surface receptor S1PR1 (sphingosine 1 phosphate receptor 1 or EDG1) and on the increased concentration of sphingosine 1 phosphate (S1P) in the blood and lymph compared to tissue (Cyster, 2005). Several studies have shown that S1P signalling through S1PR1 is essential for lymphocyte egress. The immunosuppressive S1P receptor agonist, FTY720, leads to lymphopenia in several animal models and in humans (Chiba et al., 1998, Yagi et al., 2000, Rosen et al., 2003). FTY720, when phosphorylated is a structural homologue of S1P, and leads to S1PR1 internalisation and thus inhibition of S1P signalling (Cyster, 2005). Other studies have shown that knock-down of S1PR1 in the haematopoietic cells of mice lead to B and T cell retention in the bone marrow and thymus respectively as well as in the secondary lymphoid organs (Allende et al., 2004, Matloubian et al., 2004, Allende et al., 2010).

1.2 EBV

Epstein-Barr virus (EBV), a B lymphotropic ϒ-herpesvirus, was originally identified in 1964 from Burkitt's lymphoma samples (Epstein et al., 1964). The virus has a double-stranded DNA genome of 172 kilobase pairs (Baer et al., 1984). EBV is widespread in the human population and is transmitted via the oral route. Primary infection in children is generally asymptomatic, following which the virus establishes a latent infection in B cells. When individuals are infected in adolescence or as adults, primary infection can manifest as infectious mononucleosis, a self-limiting lymphoproliferative disease (Young and Rickinson, 2004). EBV is, however, an oncogenic virus that is associated with the

development of several cancers including Hodgkin's lymphoma (HL), Burkitt's lymphoma (BL), and nasopharyngeal carcinoma (NPC) (Young and Murray, 2003).

1.2.1 EBV latency

A key feature of the EBV lifecycle is how the virus establishes latency, leading to the persistent infection of its host. The current model suggests the virus makes use of the normal B cell lifecycle to drive infected naïve B cells into the memory compartment, where the virus resides in latency (Thorley-Lawson and Babcock, 1999).

In this model EBV infects circulating naïve B cells, either during primary infection, when the virus enters the tonsillar crypts, or during persistent infection, where virus is produced by lytic replication in B cells (Thorley-Lawson, 2001, Thorley-Lawson and Babcock, 1999). Following infection, it is proposed that the naïve B cells become activated and proliferate in a manner similar to naïve B cells encountering cognate antigen for the first time. This is referred to as the virus growth programme or latency III, where all viral proteins are expressed (Babcock et al., 2000, Thorley-Lawson, 2001). In latency III all nine latent EBV genes are expressed including the six EBV nuclear antigens (EBNA1, EBNA2, EBNA3a, EBNA3b, EBNA3c and EBNA-LP) and the three latent membrane proteins (LMP1, LMP2a and LMP2b).

Following this initial activation, the EBV infected naïve B cells migrate into the follicles where they proliferate and can undergo a germinal centre reaction. During this process the viral transcription programme switches to the default programme (latency II), in which only EBNA1, LMP1 and LMP2a are expressed (Babcock et al., 2000). The germinal centre reaction leads to the clonal expansion of EBV infected B cells and to their

differentiation into memory B cells. The two latent membrane proteins of EBV, LMP1 and LMP2a, are thought to play a crucial role in this process by mimicking the key survival signals required for GC B cell survival. LMP2a can provide a B cell receptor (BCR) signal (Caldwell et al., 1998), whereas LMP1 is a functional homologue of CD40 (Gires et al., 1997).

The resulting EBV infected memory B cells express the latency programme (latency 0), where no latent viral genes are expressed (Thorley-Lawson, 2001). Thus the virus can avoid immune detection and can therefore persist for many years within long-lived memory B cells. When memory B cells are activated by antigen, they undergo terminal differentiation into plasma cells. If an EBV infected memory B cell is activated in this way the virus will undergo lytic replication and produce infectious progeny. This results in virus shedding in saliva, and may also lead to infection of new naïve B cells, thus allowing for lifelong persistence.

Furthermore, a study looking at tonsils of healthy virus carriers showed that the EBV infected B cells expressing the latency II program are not only physically located in the GCs, but they also express the phenotypic markers of GC B cells (Roughan and Thorley-Lawson, 2009). In addition, a study examining latently infected memory B cells in the peripheral blood of infectious mononucleosis patients found evidence of both somatic hypermutation and class switch recombination, which are hallmarks of the germinal centre process. (Souza et al., 2005).

However, other studies provided data which conflicts with this model. First, although LMP1 is believed to be expressed in germinal centre B cells, it has been shown to inhibit

germinal centre formation (Uchida et al., 1999). Second, a study examining tonsils from infectious mononucleosis patients found that the EBV infected B cells were not physically located in the GC (Kurth et al., 2003). Third, a recent study found that EBV infection of naïve B cells results in the outgrowth of LCLs that can express both GC and memory B cell markers without having gone through the GC reaction (Siemer et al., 2008).

1.2.2 Latent membrane protein 1

LMP1 is essential for the transformation of B cells and is expressed in Latency II and III (Kaye et al., 1993, Middeldorp and Pegtel, 2008). It is an integral membrane protein of 63kDa and is a functional homologue of CD40 (Zimber-Strobl et al., 1996, Gires et al., 1997). However, LMP1 signalling is ligand independent, and is mediated through the aggregation of its trans-membrane domain (Gires et al., 1997).

LMP1 signals through its cytoplasmic domain (C-terminal region) (Figure 1.4). This domain does not have an intrinsic kinase activity and therefore signals through a family of adaptor proteins called tumour necrosis factor receptor associated factors (TRAFs) (Lam and Sugden, 2003). The LMP1 C-terminal region contains two motifs, carboxy-terminal activating regions 1 and 2 (CTAR1 and CTAR2), which interact with TRAFs. CTAR1 preferentially recruits TRAF1-3 (Lam and Sugden, 2003). Both domains are required for efficient activation of nuclear factor kappa-light chain-enhancer of activated B cells (NF-κB) and p38/mitogen-activated protein kinase (MAPK); however the CTAR2 domain is largely responsible for canonical NF-κB activation. Additionally, the recruitment of TRAF6 by CTAR2 has been implicated in LMP1 mediated NF-κB, and p38

MAPK activation (Luftig et al., 2003, Wu et al., 2006, Wan et al., 2004, Schultheiss et al., 2001) More recently, recruitment of TRAF5 has been shown to activate c-Jun N-terminal kinase (JNK) (Kraus et al., 2009). In addition to the TRAF binding domains, LMP1 has a proposed third domain, CTAR3, located between CTAR1 and CTAR2, which interacts with Janus kinase 3 (JAK3) to activate signal transducer and activator of transcription (STAT) (Gires et al., 1999). However, the association of this domain with JAK proteins is debated (Higuchi et al., 2002).

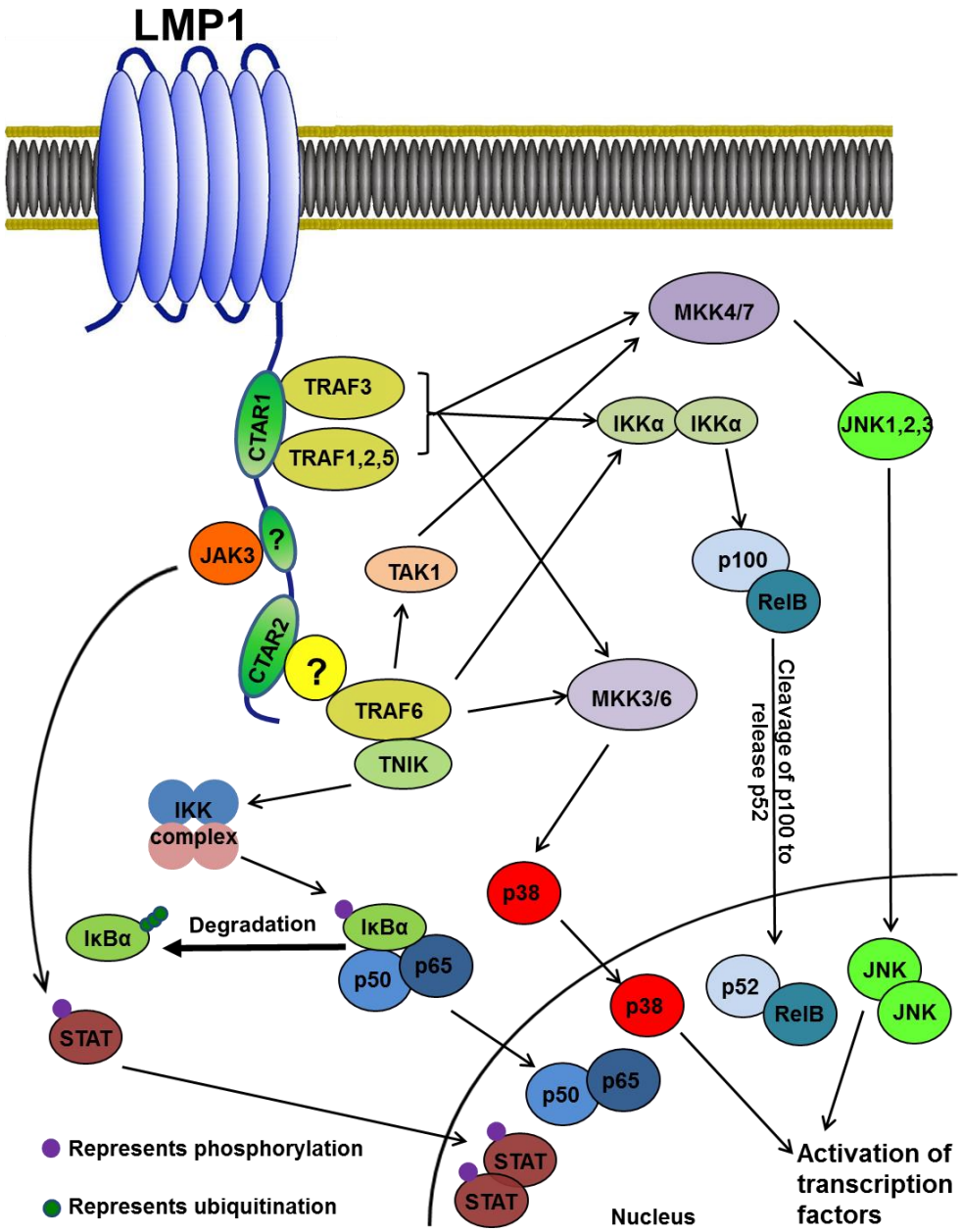

Figure 1.4: LMP1 signalling in B cells

LMP1 signals through its cytoplasmic domain consisting of CTAR1 and CTAR2 domains which recruit TRAFs. Both domains can activate the non-canonical NF-κB, JNK and p38 MAPK pathways, while the CTAR2 domain is largely responsible for the activation of the canonical NF-κB pathway. LMP1 has a proposed third domain, CTAR3, which interacts with the JAK3 leading to STAT activation.

Abbreviations: CTAR (carboxy-terminal activating regions) TRAF (tumour necrosis factor receptor associated factor), MAPK (mitogen-activated protein kinase), MKK (MAPK kinase), JNK (c-Jun-N-terminal kinase), JAK (janus kinase), STAT (signal transducer and activator of transcription).

LMP1 has a wide range of functions:

LMP1 itself is poorly immunogenic, and is suggested to have an immune modulatory function. LMP1 can affect the expression of several chemokines, cytokines, adhesion molecules, co-stimulatory molecules and also antigen presenting/processing genes (Middeldorp and Pegtel, 2008). This strongly indicates a role for LMP1 in immune evasion. LMP1 can block interferon α (IFNα) mediated antiviral activity by inhibiting tyrosine kinase 2 (Tyk2) (Geiger and Martin, 2006).

LMP1 has been shown to contribute to the regulation of EBV latency. LMP1 was found to suppress lytic cycle induction through the inhibition of the transcription of BamHI Z fragment leftward open reading frame 1 (BZLF1), an immediate early protein of EBV that is required for the induction of the lytic cycle (Adler et al., 2002).

LMP1 provides an essential proliferative signal to B cells. This has been shown by examining the growth characteristics of immortalised B cells which contained a conditional LMP1 gene. The presence of high levels of LMP1 lead to cell proliferation; however, in the presence of only low levels of LMP1 this proliferation was hardly detectable (Kilger et al., 1998).

LMP1 expression in rodent fibroblasts and endothelial cells leads to transformation of cells to anchorage-independent growth (Wang et al., 1985, Moorthy and Thorley-Lawson, 1993). NF-κB activation has been shown to play an important role in LMP1 mediated transformation of Rat-1 fibroblasts (He et al., 2000). LMP1 expression in the B cells of transgenic mice leads to a block in GC development (Uchida et al., 1999) and the development of B cell lymphomas in old age (Kulwichit et al., 1998), further underlining

the role of LMP1 in oncogenesis. These lymphomas displayed elevated levels of BCL2 and c-MYC, indicating that these genes could play a role in LMP1-mediated lymphomagenesis.

More recently, LMP1 expression in GC B cells was shown to induce a Hodgkin and Reed-Sternberg (HRS) cell like phenotype (Vockerodt et al., 2008). HRS cells are the GC B cell derived tumour cells of HL. LMP1 transfection of GC B cells up-regulated the expression of several signalling pathways including NF-κB, STAT, phosphatidylinositol 3–kinase (PI3K) and CD95 signalling components, while down-regulating several B cell phenotypic markers including BCR signalling molecules, co-receptors and downstream targets as well as B cell associated transcriptional regulators, consistent with observations made in HRS cells.

1.2.3 CD40

CD40 is a 48-kDa type 1 trans-membrane protein of the tumour necrosis factor receptor (TNFR) family (van Kooten and Banchereau, 2000, Graham et al., 2010). CD40 was originally identified as a molecule expressed exclusively on B cells. However, it is now known that CD40 is also expressed on several other cell types, such as monocytes, dendritic cells, endothelial cells and also on epithelial cells (van Kooten and Banchereau, 2000).

Activation of CD40 by its ligand CD40L results in the clustering of CD40 into lipid rafts. Lipid rafts are patches of cell membrane which contain high concentrations of cholesterol and glycosphingolipids where receptors are often found and thus are involved in the regulation of signalling. Like LMP1, the cytoplasmic signalling domain of

CD40 then recruits TRAF1, TRAF2 and TRAF3 at a distal, as well as TRAF6 at a membrane proximal site (Lam and Sugden, 2003, Graham et al., 2010, Bishop, 2004).Together these molecules lead to the activation of NF-κB, while TRAF2 activates JNK and TRAF6 activates p38 (Figure 1.5). In contrast to LMP1 signalling, CD40 signalling is self-regulated through the proteasomal degradation of TRAF2 and TRAF3 upon CD40 activation (Brown et al., 2001, Brown et al., 2002). This degradation is mediated by TRAF2.

CD40 signalling in B cells is important in T cell mediated humoural immune responses. CD40 signalling is achieved through the activation of the CD40 receptor on B cells via the CD40L, which is mainly expressed on CD4 positive T helper cells, along with the help of cytokines specifically secreted by these T cells (Carbone et al., 1995b).

The importance of this CD40-CD40L interaction in the formation of T cell dependent immune responses can be seen in patients suffering from X-linked hyper-IgM syndrome (HIGM) (Korthauer et al., 1993, DiSanto et al., 1993). HIGM is a severe immunodeficiency caused by mutations in the CD40L gene. These patients have elevated IgM levels with low levels of the other immunoglobulin types (IgA, IgG and IgE). Furthermore, these patients fail to form GCs and have impaired memory B cell formation. These effects can also been seen in CD40 and CD40L deficient mice (Kawabe et al., 1994, Renshaw et al., 1994).

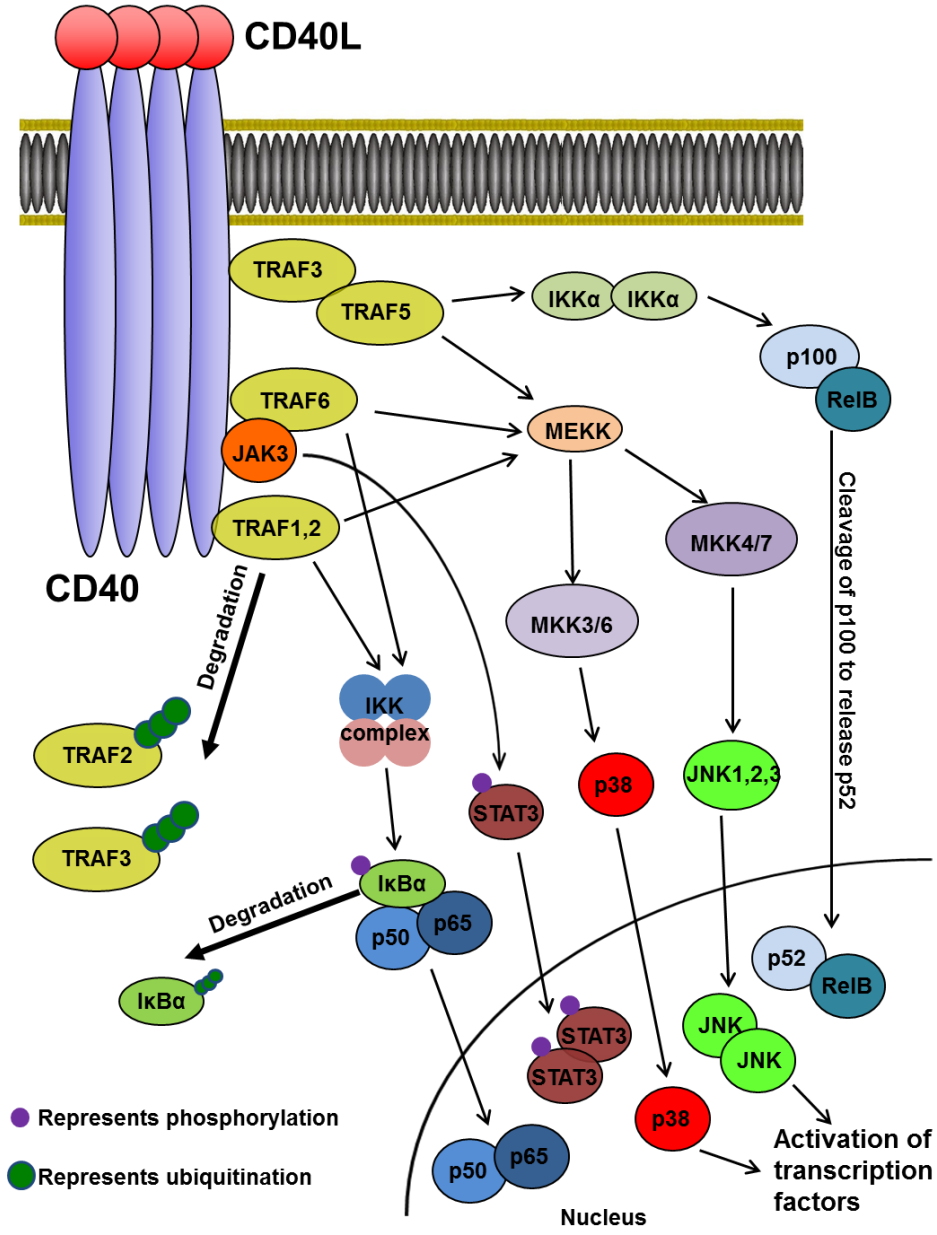

Figure 1.5: CD40 signalling in B cells

Activation of CD40 by its ligand CD40L results in the clustering of CD40 into lipid rafts and the recruitment of TRAFs. Interaction of TRAF5 with TRAF3 results in the activation of the non-canonical NF-κB pathway leading to p52/RelB accumulation in the nucleus, while TRAF6 and TRAF2 activate the canonical NF-κB pathway leading to p50/p65 accumulation in the nucleus. TRAF5, TRAF6 and TRAF2 all contribute to the activation of the JNK and p38 MAPK pathways via various MEKKs, such as ASK1/2, MLK3 and TAK1. CD40 also interacts with JAK3 leading to STAT3 activation.

CD40 signalling is self-regulated through TRAF2 mediated proteasomal degradation of TRAF2 and TRAF3. CD40 also interacts with JAK3 leading to STAT3 activation.

Abbreviations: TRAF (tumour necrosis factor receptor associated factor), MAPK (mitogen-activated protein kinase), MEKK (MAPk/ERK kinase kinase), MKK (MAPK kinase), JNK (c-Jun-N-terminal kinase), JAK (janus kinase), STAT (signal transducer and activator of transcription).

Signalling through CD40 can induce proliferation, differentiation, immunoglobulin expression and survival of B cells (van Kooten and Banchereau, 2000). Activation of CD40 induces GC formation, isotype switching, affinity maturation and selection, leading to the differentiation of B cells into memory cells. CD40 also prevents the differentiation of B cells into plasma cells.

There is evidence that alterations in this physiological CD40 signal can lead to malignant transformation of B cells. The malignant cells of HL, the Hodgkin and Reed-Sternberg (HRS) cells express functional CD40 on their cell surface and as CD40L expressing T cells are found in the tumour microenvironment, it is likely that CD40 signalling is important for HRS cell survival. In fact, a study looking at CD40L stimulation of a HL cell line, L428, showed that CD40 signalling supports cell growth (Carbone et al., 1995a). Furthermore, it has been shown *in vivo* that constitutive CD40 signalling in B cells can to lead to transformation (Homig-Holzel et al., 2008).

A study of non-Hodgkin's lymphomas identified a structure called a CD40 Signalosome within the membranes of the tumour cells (Pham et al., 2002). The formation of this structure is initiated through CD40L production by the tumour cell, leading to CD40-CD40L interaction in the membrane. This interaction results in the recruitment of scaffolding proteins that anchor it to the membrane, giving rise to the CD40 Signalosome. This prolonged CD40-CD40L interaction within the structure leads to constitutive NF-κB activation, which is of key importance in the proliferation and viability of the tumour cells.

1.2.4 Studies of LMP1 and CD40 functional homology

A number of studies have investigated the functional links between LMP1 and CD40 signalling. In 1996, it was observed that constitutive expression of LMP1 in EREB2-5 cells (EBV-immortalised B cell line) leads to a phenotype similar to CD40 stimulation (Zimber-Strobl et al., 1996). Oligomerisation of the carboxy-terminal of LMP1 is required for NF-κB activation, thus although LMP1 mimics a ligand activated receptor, itself is ligand independent (Gires et al., 1997). A different study showed that in a cell line dependent on LMP1 for proliferation, CD40 activation can replace LMP1 (Kilger et al., 1998). In a more recent study it has been shown that both LMP1 and CD40 activation can inhibit lytic cycle induction in EREB2 cells (Adler et al., 2002).

Several studies utilised LMP1 and CD40 chimeric molecules to directly compare LMP1 and CD40 signalling. For example, LMP1CD40 chimeras containing the N-terminal trans-membrane domain of LMP1 and the C-terminal signalling domain of CD40 was shown to act as a constitutively active CD40 molecule (Hatzivassiliou et al., 1998, Homig-Holzel et al., 2008, Panagopoulos et al., 2004). Expression of this chimeric LMP1CD40 construct in Rat1 fibroblasts can, like LMP1, lead to loss of contact inhibition and anchorage independent growth (Hatzivassiliou et al., 2007). This suggests that a constitutive CD40 like signal is sufficient for transformation.

Another study examined the effect in vivo of a similar chimera (Homig-Holzel et al., 2008). In transgenic mice expressing this chimera there is a strong accumulation of follicular and marginal zone B cells in secondary lymphoid organs. These B cells displayed an activated phenotype, and failed to form GC when the mice were immunised.

Furthermore, over 60% of these transgenic mice over the age of 1 year developed B cell lymphomas. Additionally, it was shown that the expression of the LMP1CD40 chimera, like LMP1, leads to constitutive activation of the non-canonical NF-κB pathway. These findings provided further evidence that constitutive CD40 signalling could be important for B cell transformation.

A second study in mice compared the effect of LMP1 and the LMP1CD40 chimera expression in B cells (Panagopoulos et al., 2004). The molecules were expressed under the control of the CD19 promoter, allowing for B cell specific expression. It was observed that LMP1CD40 expressing mice, like LMP1 expressing mice, showed similar suppression of the humoural immune response, measured by defective GC formation and antibody production when stimulated with thymus-dependent (TD) antigens. It was also observed that the expression of both LMP1 and the LMP1CD40 chimera in B cells lead to the suppression of the BCL6 promoter, thus antagonizing GC formation. However, the LMP1CD40 chimera did not fully mimic LMP1. First, its ability to suppress the humoural immune response was greater than that of LMP1. Second, expression of the chimera led to an increased accumulation of macrophages, polymorphonuclear cells and marginal zone B cells in the spleen. This alteration in B cell populations was associated with autoimmunity, and mice expressing LMP1CD40 showed signs of spontaneous inflammatory responses.

A further two studies used a different approach. In these studies, the chimeric molecules (CD40LMP1) consisted of the C-terminal signalling domain of LMP1 fused to the trans-

membrane and ligand-binding domains of CD40, allowing them to study the effects of transient LMP1 signalling.

One study used transgenic mice bred onto a CD40 deficient background, with the CD40LMP1 chimera under the control of the mouse major histocompatibility complex (MHC) class II Eα promoter (Stunz et al., 2004). This resulted in CD40LMP1 expression replacing that of physiological CD40. The results showed that the LMP1 signalling domain could replace that of CD40. However, the transgenic mice had enlarged lymph nodes and spleens with elevated serum IL-6 and increased GC formation. These mice also showed signs of autoimmunity.

Another study used transgenic mice expressing a CD40LMP1 chimera upon Cre-mediated recombination, controlled by the CD19 promoter (Rastelli et al., 2008). As with the previous study, LMP1 signalling was able to completely substitute CD40 signalling in B cells leading to normal B cell development and activation. However, as opposed to CD40 signalling, CD40LMP1 was able to induce class-switch recombination independent of cytokines. This ability of LMP1 could provide a survival advantage to infected B cells by increasing their life span and can force B cells towards becoming long lived memory B cells.

Altogether, these studies confirm the role of LMP1 as a CD40 mimic, while at the same time identify some differences in their signalling, such as LMP1 but not CD40 signalling causing cytokine independent CSR in B cells. It is becoming increasingly clear, as shown in two of the above studies, that aberrant constitutive CD40 signalling has the potential to transform B cells.

1.3 GC derived lymphomas

The GC is a site of extensive cell proliferation, SHM and CSR. As described in the previous section, all of these processes carry a high risk of inducing mutations in GC B cells. There is a tight regulation of the GC reaction, but it is not always sufficient in eliminating mutated and thus potentially cancerous cells. It is therefore not surprising that the majority of B cell lymphomas are derived from germinal centre B cells, or B cells that have undergone the GC reaction (Kuppers et al., 1999).

Lymphomas derived from GC B cells include Burkitt's lymphoma, Hodgkin's lymphoma and diffuse large B cell lymphoma (DLBCL) (Kuppers, 2005). There are several transforming processes implicated in B cell lymphomas including chromosomal translocations between immunoglobulin loci and proto-oncogenes and somatic hypermutation of non-immunoglobulin genes. In this section I will focus on two GC B cell derived lymphomas: Hodgkin's lymphoma and diffuse large B cell lymphoma (DLBCL). In particular I will highlight the involvement of EBV in these cancers.

1.3.1 Hodgkin's lymphoma

Hodgkin's lymphoma (HL) was first described in 1832 (Hodgkin, 1832). It is currently treated by chemotherapy or radiation therapy and is curable in 80-90% of cases. HL is characterised by low numbers of tumour cells (typically around 1%), surrounded by a mixed infiltrate of cells in the lymphoma tissue. The infiltrate contains non-malignant immune and inflammatory cells such as T cells, B cells, macrophages, neutrophils, eosinophils and mast cells. CD4 positive T cells are usually the largest population of reactive cells in the infiltrate (Schmitz et al., 2009b).

Hodgkin's lymphoma is subdivided into classical HL (cHL) and nodular lymphocyte-predominant HL (NLPHL). Classical HL accounts for 95% of cases, and is further divided into four subtypes; nodular sclerosis, mixed cellularity, lymphocyte depletion and lymphocyte rich, of which nodular sclerosis is the most common (Kuppers et al., 2012). Around 40% of cases of cHL are positive for EBV, and this virus is found mainly in the mixed cellularity and lymphocyte depletion subtypes (Aldinucci et al., 2010). Rare cases of HL (1-2%) originate from T cells (Muschen et al., 2000, Seitz et al., 2000, Tzankov et al., 2005).

The tumour cells of cHL are called Hodgkin and Reed-Sternberg (HRS) cells. Hodgkin cells are large mononuclear cells that have pronounced nucleoli. Reed-Sternberg cells are multinuclear cells which are generally larger then Hodgkin cells (Kuppers, 2009). HRS cells are derived from B cells but show a global loss of B cell specific gene expression and have a varied immunophenotype (Schwering et al., 2003, Tiacci et al., 2012).

The unique gene expression profile of HRS cells can in part be explained by the de-regulation of key B cell specific transcription factors in HRS cells, such as Oct-2, Pu.1 and BOB1 which are not expressed (Stein et al., 2001, Torlakovic et al., 2001) and E2A, EBF1 and PAX5, which are expressed in HRS cells and in HL cell lines, but are inactivated (Mathas et al., 2006, Renne et al., 2006, Jundt et al., 2008). The inactivation of E2A by ABF1 and inhibitor of DNA binding (ID2) has been implicated in the down-regulation of B cell specific genes (CD19, AID, CD79a and Oct-2) and the up-regulation of non-B lineage genes (transcription factor 7 (TCF7), colony stimulating factor 1 receptor (CSF1R),

musculoaponeurotic fibrosarcoma oncogene homolog (MAF) and GATA3) (Mathas et al., 2006).

CD30, CD40, RANK and CD95 are highly expressed in the majority of HRS cells (Kim et al., 2003). Despite the high expression of CD95, resistance to CD95 mediated apoptosis, through the over-expression of the FADD-like interleukin 1β–converting enzyme-inhibitory protein (c-FLIP), is a key feature of HRS cells (Dutton et al., 2004, Mathas et al., 2004). Several receptor tyrosine kinases (RTKs) not normally expressed in B cells are aberrantly expressed in HRS cells (Renne et al., 2005, Renne et al., 2007).

Several signalling pathways are aberrantly activated in HRS cells, including the NF-κB, Janus kinase (JAK)/STAT, mitogen-activated kinase (MEK)/Extracellular signal-regulated kinase (ERK) and the PI3K/AKT pathways, as displayed in Figure 1.6. Some are activated by the HRS microenvironment, while others are a result of constitutive activation through mutations.

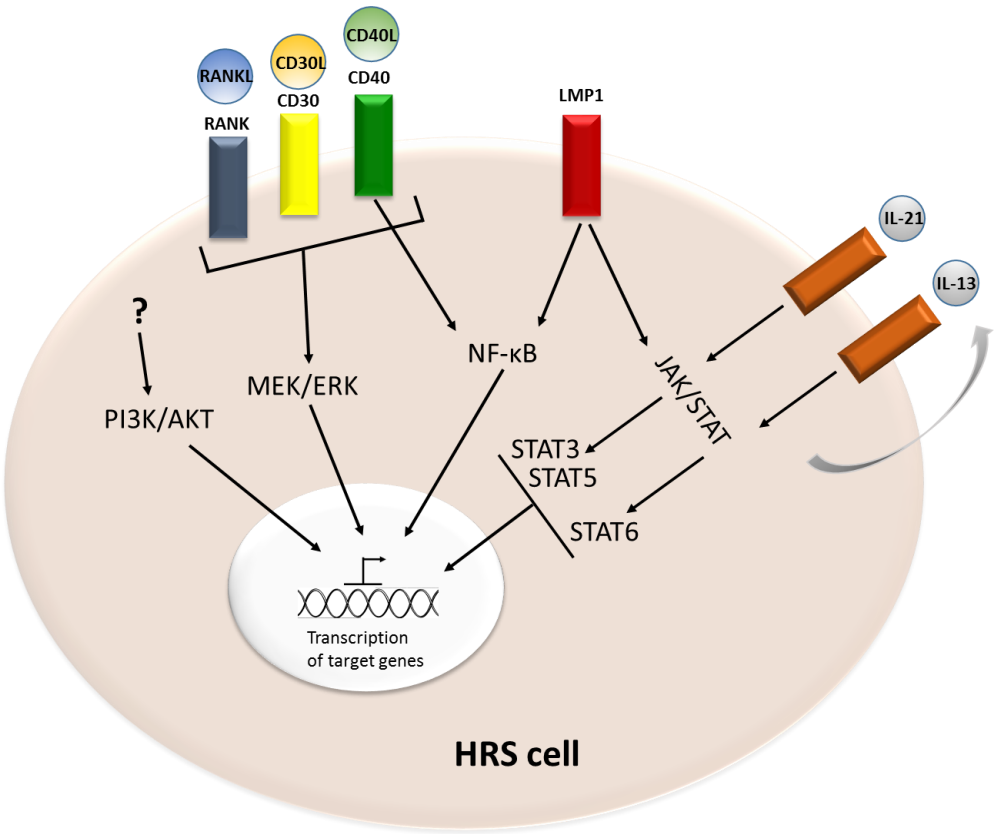

Figure 1.6: Aberrant signalling pathways in Hodgkin's lymphoma
Key pathways involved in HL pathogenesis: NF-κB pathway, PI3K/AKT pathway, MAPK/ERK pathway and JAK/STAT pathway. Activation by CD30, CD40 and RANK contribute to the aberrant activation of the MAPK/ERK pathway. The NF- κB is activated via CD40 and mutations targeting signalling components. In EBV positive cases, LMP1 contributes to NF- κB activation. LMP1 can also contribute to the activation of the JAK/STAT pathway, which is also activated by interleukins and is targeted by mutations. The PI3K pathway is also aberrantly activate in HRS cells.

The components of the NF-κB pathway are de-regulated in HRS cells, leading to constitutive NF-κB activation (Bargou et al., 1997, Krappmann et al., 1999). Two mechanisms have been described for the de-regulation of the NF-κB pathway in HRS cells. First, components of the pathway are often targeted by mutations, listed in Table 1.1. Second, CD40 signalling can contribute to the constitutive activation of NF-κB. CD40 is highly expressed on the surface of HRS cells, while CD40L is expressed on the non-malignant tumour infiltrating T cells (Carbone et al., 1995a, Carbone et al., 1995b).

STAT3, STAT5 and STAT6, components of the JAK/STAT pathway have all been shown to be constitutively activated in HRS cells and HL cell lines (Hinz et al., 2002, Kube et al., 2001, Skinnider et al., 2002). As with NF-κB, this pathway is targeted by mutations in HRS cells (Table 1.1). Autocrine and paracrine activation by interleukins (IL) also contribute to STAT activation. IL13 activates STAT6 via its receptor IL13R (Wurster et al., 2000), both of which are highly expressed in HRS cells (Ohshima et al., 2001, Kapp et al., 1999). Similarly, IL21-IL21R has been shown to activate STAT3 and STAT5 in HRS cells (Lamprecht et al., 2008, Scheeren et al., 2008).

Table 1.1: Mutations affecting the key signalling pathways in HL

Pathway	*Gene affected*	*Type of mutation*	*Outcome*	*References*
NF-κB	REL	Amplification	Constitutive NF- κB activation	(Joos et al., 2002, Martin-Subero et al., 2002)
	IκBα and IκBε	Inactivating mutations	Constitutive NF- κB activation	(Jungnickel et al., 2000, Emmerich et al., 1999, Emmerich et al., 2003, Cabannes et al., 1999)
	A20 (TNFAIP3)	Deletions, inactivating mutations, mostly in EBV negative HL	Constitutive NF- κB activation	(Schmitz et al., 2009a, Kato et al., 2009)
	NIK (MAP3K14)	Gains	Constitutive NF- κB activation	(Otto et al., 2012, Steidl et al., 2010)
JAK/STAT	JAK2	Amplification, rare translocations	Activation of STATs	(Joos et al., 2000, Van Roosbroeck et al., 2011)
	SOCS1	Inactivating mutations	Activation of STAT5 and STAT6	(Mottok et al., 2007, Weniger et al., 2006)

The activation of CD30, CD40 and receptor activator of NF-κB (RANK) all contribute to the aberrant activation of the MEK/ERK pathway in HRS cells (Zheng et al., 2003). The PI3K/AKT pathway is also constitutively active in HRS cells and HL cell lines and inhibition of this pathway leads to apoptosis in HL cell lines (Morrison et al., 2004, Dutton et al., 2005, Georgakis et al., 2006). Additionally, the EBV protein LMP1 has been shown to activate the NF-κB, JAK/STAT and JNK and p38 MAPK pathways in B cells (Lam and Sugden, 2003). As approximately 40% of cHL cases are positive for EBV, LMP1 signalling can contribute to the aberrant activation of signalling pathways in HRS cells.

Despite the varied expression of markers expressed in HRS cells, they are now known to derive from GC B cells. HRS cells are clonal and have somatically mutated and re-arranged immunoglobulin genes, indicating that these cells have undergone the GC reaction (Kuppers et al., 1994, Marafioti et al., 2000, Hummel et al., 1995, Küppers et

al., 1998). There is also evidence of immunoglobulin class switching in HRS cells (Martin-Subero et al., 2006) as well as in HL cell lines (Irsch et al., 2001).

In approximately 25% of cHL, HRS cells harbour destructive somatic mutations in their IgV genes that make the gene non-functional (Brauninger et al., 2003, Kanzler et al., 1996, Marafioti et al., 2000). These mutations are nonsense mutations or deletions that alter the reading frame of the gene and would normally result in the apoptosis of the B cell in the germinal centre (Kanzler et al., 1996). As nearly all HRS cells harbouring these crippling mutations are latently infected with EBV, the virus may have role in the rescue of these pre-apoptotic GC B cell and their transformation (Brauninger et al., 2006).

In fact, LMP2a can rescue BCR negative B cells (Caldwell et al., 1998, Casola et al., 2004). Furthermore, it has been shown in three studies that EBV infection can not only transform normal but also BCR negative GC B cells into lymphoblastoid cell lines (LCLs) (Bechtel et al., 2005, Chaganti et al., 2005, Mancao et al., 2005).

1.3.2 Diffuse large B cell lymphoma

Diffuse large B cell lymphoma (DLBCL) is highly heterogeneous and is the most common form of lymphoma (Coiffier, 2001, Frick et al., 2011). In 2008 the WHO classified DLBCL into two major groups: DLBCL associated with chronic inflammation and DLBCL not otherwise specified (NOS) (Campo et al., 2011). This latter group is further divided into: T cell/histiocyte-rich large B cell lymphoma (THRLBCL), primary DLBCL of the CNS (central nervous system), primary cutaneous DLBCL leg type and a new, provisional entry, EBV-positive DLBCL of the elderly.

Recent studies have delineated three molecular subtypes. These are germinal centre B cell like (GCB), activated B cell like (ABC) and primary mediastinal B cell lymphoma (PMBL) (Frick et al., 2011). These subtypes differ in their clinical outcomes as well as in their genetic make-up. Patients with the GCB subtype have a better prognosis (Alizadeh et al., 2000, Rosenwald et al., 2002, Wright et al., 2003).

GCB DLBCL is thought to originate from GC B cells, by virtue of their expression of several GC B cell associated genes, such as CD10, LMO2 and BCL6 (Alizadeh et al., 2000, Rosenwald et al., 2002). Furthermore, ongoing somatic hypermutation is often detected in the Ig heavy chain variable region of these lymphomas (Lossos et al., 2000). GCB DLBCL harbour several abnormalities some of which so far have not been detected in ABC type (Table 1.2). The most common genetic alterations target BCL2, PTEN, and various tumour suppressors (Rosenwald et al., 2002, Lenz et al., 2008c).

The ABC subtype is believed to originate from B cells in the process of differentiating into plasma cells, and thus is characterised by the up-regulation of many genes associated with plasma cells, such as XBP-1 (Wright et al., 2003, Rosenwald et al., 2002). However, a hallmark of ABC DLBCL is that full plasmacytic differentiation is blocked in these cells (Frick et al., 2011), probably through several genetic abnormalities directed at the PR domain zinc finger protein 1 (PRDM1) gene encoding BLIMP1 (Table 1.2). Another hallmark is the constitutive activation of the NF-κB pathway which is essential for ABC DLBCL survival (Davis et al., 2001).

Table 1.2: Genetic alterations in diffuse large B cell lymphoma (DLBCL)

DLBCL subtype	*Gene altered*	*Genetic alteration and proportion of cases harbouring mutation*	*Function/Result*	*References*
Germinal centre B cell (GCB) DLBCL	EZH2	Somatic mutation (approx. 20%)		(Morin et al., 2010)
	BCL2	t(14;18) translocation (nearly 50%)	Constitutive activation, anti-apoptotic	(Rosenwald et al., 2002)
	PTEN	deletion or miR-17-92 amplification	activation of AKT and mTOR pathways leading to cell survival, growth and proliferation	(Lenz et al., 2008c)
	TP73	Deletion	anti-apoptotic	(Lenz et al., 2008c)
	ING1	Deletion	anti-apoptotic	(Lenz et al., 2008c)
	MDM2	Amplification	negative regulator of tumour suppressor p53	(Lenz et al., 2008c)
Activated B cell (ABC) DLBCL	PRDM1 (encoding BLIMP1)	Inactivating (approx. 25%)	Regulator of plasma cell differentiation	(Pasqualucci et al., 2006, Tam et al., 2006)
	BCL6	Translocation t(3;14) (approx. 25%)	BCL6 overexpression, resulting in the repression of BLIMP1	(Iqbal et al., 2007, Frick et al., 2011)
	SPIB	Amplification (approx. 25%)	transcription factor known to repress BLIMP1	(Lenz et al., 2008c, Frick et al., 2011)
	CARD11	Activating (approx. 10%)	Activation of CBM complex, leading to NF-κB activation	(Lenz et al., 2008a, Ngo et al., 2006)
	CD79a and CD79b	Somatic/activating	BCR co-receptors. Leads to chronic BCR signalling activation of CBM complex and constitutive NF-κB signalling	(Davis et al., 2010)
	A20 (TNFAIP3)	Inactivating/deletions (approx. 30%)	negative regulator of NF-κB	(Compagno et al., 2009, Kato et al., 2009)
	MYD88	Activating (approx. 30%)	links toll-like receptor (TLR) and interleukin (IL-1 and IL-8) signalling to NF-κB activation	(Ngo et al., 2011)
	BCL2	Amplification of 18q	Overexpression, anti-apoptotic	(Lenz et al., 2008c, Bea et al., 2005)
	INKa/ARF	Deletions	Tumour suppressor	(Lenz et al., 2008c)
	FOXP1	Trisomy 3		(Lenz et al., 2008c, Bea et al., 2005)

Epstein Barr virus (EBV)-associated DLBCL of the elderly is a recently identified subtype of DLBCL (Campo et al., 2011). It was first described in 2003 (Oyama et al., 2003) and is defined as an "EBV-positive monoclonal large B-cell lymphoproliferative disorder arising in immunocompetent patients over 50 years of age" with no prior history of the disease (Ok et al., 2013). It is more frequent in Asian population, with very low frequency in western populations (Oyama et al., 2007, Park et al., 2007, Hoeller et al., 2010).

EBV-associated DLBCL of the elderly is associated with immune senescence. This tumour has a phenotype close to that of ABC DLBCL, with increased NF-κB activation as a result of LMP1 expression (Montes-Moreno et al., 2012). The tumour cells usually display a latency III expression of EBV genes, with the majority of cells positive for LMP1 and a subset also positive for EBNA2 (Oyama et al., 2003). Overall, EBV-associated DLBCL is more aggressive then EBV negative DLBCL, with more extranodal involvement and a worse clinical outcome (Park et al., 2007). Even when compared to the subtype of EBV negative DLBCL with the worst prognosis (ABC DLBCL), EBV associated DLBCL has a poorer clinical outcome (Montes-Moreno et al., 2012).

1.4 Aims

The EBV oncogene LMP1 shares functional homology with CD40, a cell surface receptor that is important for GC B cell survival and differentiation. This thesis investigates the transcriptional and signalling differences that underpin the pathogenic effects of LMP1 in GC B cells, the presumed progenitors of several important EBV-associated malignancies, including HL and DLBCL.

The specific aims of this work are to:

1. Characterise *in vitro* isolated and cultured human GC B cells

2. Compare the transcriptional programmes of LMP1 and CD40 in isolated GC B cells.

3. Investigate the expression and function of selected LMP1 target genes in B cell lymphomas.

4. Optimise a flow cytometry based method for the measurement of the phosphorylation of specific transcription factors in low numbers of GC B cells.

Chapter 2

Materials and Methods

2 Materials and methods

2.1 Cell culture

2.1.1 Maintenance of cell lines

Cell lines were maintained in RPMI 1640 medium (Gibco®, Life Technologies Ltd, Paisley, UK), supplemented with 10% v/v selected foetal calf serum (FCS; PAA the cell culture company, Somerset, UK) and 1% v/v penicillin/streptomycin (Gibco®, Life Technologies Ltd, Paisley, UK) at 37°C with a humidified atmosphere and CO_2 at 5% (Galaxy R CO_2 Incubator, RS Biotech, Livingston, UK). Information for all cell lines used are summarised in Table 2.1. To split cells and replenish media, cells were pelleted by centrifugation at 173g for 10 minutes (Eppendorf Centrifuge 5810R, Eppendorf UK Limited, Stevenage, UK), media was aspirated using a VACUSAFE aspirator (INTEGRA Biosciences AG, Zizers, Switzerland) and pellets were re-suspended at a concentration of $5x10^5$cells/ml in fresh media, pre-warmed to 37°C in a Heratherm™ Compact Microbiological Incubator (Thermo Fisher Scientific Inc, Waltham, MA, USA). All cell lines were negative for mycoplasma, tested using the MycoAlert® mycoplasma detection kit (Lonza, Slough, UK).

2.1.2 Cryopreservation and thawing of cells

Aliquots of 5 x 10^6 cells were pelleted by centrifugation at 173g for 10 minutes at 4°C and re-suspended in 500µl of chilled freezing solution (90% v/v FCS and 10% v/v dimethyl sulphoxide (DMSO; Sigma-Aldrich Ltd., Gillingham, UK). Cells were transferred to cryopreservation tubes (Nunc® Cryo Tubes®; Sigma-Aldrich Ltd., Gillingham, UK) and cooled slowly overnight to -80°C in a cryo container (Nalgene® Mr. Frosty; Sigma-Aldrich

Ltd., Gillingham, UK). Cells were subsequently stored at -80°C. Cryopreserved cells were thawed quickly to minimize exposure to DMSO. Thawed cells were re-suspended in 10ml of medium and grown in a 25 cm^3 flask overnight.

2.1.3 Cell counting

Cell concentration were determined using a Neubauer haemocytometer (Marienfeld, Harsewinkel, Germany). To exclude dead cells, directly before counting cells were mixed 1:1 with Trypan Blue (Sigma-Aldrich Ltd., Gillingham, UK) and 10µl of suspension was pipetted onto the glass slide. Live (bright) cells were counted using an Olympus CK30 inverted light microscope in four zones of the grid following which the number was averaged. This number was then multiplied by 10^4 and the dilution factor of the Trypan Blue to obtain the number of cells per ml of culture.

Table 2.1: Cell lines

Cell line	*Cancer type*	*Origin*	*References*
L591	Nodular Sclerosis HL	EBV-positive cell line originated from the pleural effusion of 31 year old female patient.	(Diehl et al., 1982)
L1236	Mixed Cellularity HL	EBV-negative cell line established from the peripheral blood of a 34 year old male patient with advanced HL.	(Wolf et al., 1996)
L540	T–cell derived Nodular Sclerosis HL	EBV-negative HL cell line derived from bone marrow of a female patient with stage IV disease.	(Diehl et al., 1982, Falk et al., 1987)
L428	Nodular Sclerosis HL	EBV-negative cell line established from the pleural effusion of a 37 year old female patient with refractory disease.	(Schaadt et al., 1980)
KM-H2	Mixed Cellularity HL	EBV-negative cell line established from the pleural effusion of a 37 year old male patient	(Kamesaki et al., 1986)
DG75	BL	Established from the pleural effusion of a 10-year-old boy with sporadic BL.	(Ben-Bassat et al., 1977)
BL2	BL	Established from the bone marrow of a relapsed 7 year old Caucasian boy with non-endemic BL.	(Cohen et al., 1987, Bertrand et al., 1981)
SUDHL4	DLBCL, GCB subtype	Established from the peritoneal effusion of a 38 year old man with B-NHL	(Epstein et al., 1978)
U2932	DLBCL, ABC subtype	Established from the ascites of a 29 year old woman with DLBCL, who 16 years earlier was diagnosed with advanced stage HL	(Amini et al., 2002)

2.2 Isolation and maintenance of primary human GC B cells

All steps of the isolation (except for Ficoll-Isopaque centrifugation) were performed on ice, with ice cold reagents to prevent the apoptosis of cells. All centrifugation steps were at 173g at 4°C for 10 minutes unless otherwise specified.

2.2.1 Tonsil specimens

Paediatric tonsils were obtained from the Birmingham Children's Hospital, under local ethics committee approval (Ref No.06/Q2702/50) and transported in cold phosphate buffered saline (PBS) on ice.

2.2.2 Purification of tonsillar mononuclear cells (TMCs)

Tonsils were minced with a scalpel in RPMI 1640 medium (Gibco®, Life Technologies Ltd, Paisley, UK), without foetal calf serum, supplemented with 0.5% ciproxin (Bayer, Newbury, UK) and 1% penicillin-streptomycin solution (Gibco®, Life Technologies Ltd, Paisley, UK), to obtain a suspension of tonsillar cells.

Mononuclear cells were then isolated by Ficoll-Isopaque centrifugation, whereby 15ml of lymphoprep solution (Axis-Shield Diagnostics Ltd. UK, Dundee, UK) was pipetted into tubes and carefully overlaid with 35ml of tonsillar cells. Tubes were centrifuged with the breaks off at 839g at room temperature for 30 minutes creating the visible layers of: plasma (top), mononuclear cells (middle), lymphoprep solution (bottom) and erythrocytes (pellet). Mononuclear cells were transferred to a fresh tube, washed twice with cold media and once with cold autoMACS solution (Miltenyi Biotec Ltd, Surrey, UK) supplemented with ciprofloxacin and penicillin-streptomycin as per RPMI and 5% MACS® BSA stock solution (Miltenyi Biotec Ltd, Surrey, UK).

2.2.3 Purification of CD10$^+$ GC B cells

Isolated TMCs were counted and cells were resuspended at a concentration of 10^7cells/100µl of autoMACS solution with anti-CD10-Phycoerythrin (PE) antibody (eBioscience, Hatfield, UK) added at a 1/50 dilution. Cells were incubated for 10 minutes at 4^{o}C in the dark and washed with 10x staining volume of autoMACS. Cells were then resuspended at a concentration of 10^7cells/100µl of autoMACS solution with anti-PE microbeads (Miltenyi Biotec Ltd, Surrey, UK) added at a 1/10 dilution. Cells were incubated for 15 minutes at 4^{o}C in the dark and washed with 10x staining volume of autoMACS.

Finally, cells were resuspended at a concentration of 10^8 cells/500µl of autoMACS (using the assumption that approximately 40% of cells are labelled). LS columns were placed on the pre-cooled separation magnet (both Miltenyi Biotec Ltd, Surrey, UK) with 50µm cell filters (CellTrics®, Partec UK Limited, Canterbury, UK) placed on each column. LS columns were pre-washed with 3ml of autoMACS and cells were applied at a ratio of 500µl per column. Once the cells passed through, the LS columns and filters were washed three times with 3 ml of autoMACS, the filters discarded following the first wash. To elute the CD10$^+$ cells, LS columns were removed from the magnet, 5ml of autoMACS was added and gentle pressure was applied with a plunger until the cells were eluted. Cells were kept on ice until further use, or pelleted at 10^6 cells/pellet and frozen at -80^{o}C.

2.2.4 CD40L stimulation of GC B cells

Freshly isolated GC B cells were pelleted by centrifugation at 1000rpm, 4°C for 10 minutes and re-suspended in RPMI 1640 medium (supplemented as per section 2.1.1) at a concentration of $2x10^6$ cells/ml. Cells were stimulated with 200ng/ml soluble CD40L (Autogen Bioclear UK Ltd, Wiltshire, UK) or of equivalent volume of sterile 0.1% bovine serum albumin (BSA) solution made using tissue culture grade BSA (Sigma-Aldrich Ltd., Gillingham, UK). Cells were maintained at 37°C with a humidified atmosphere and 5% CO_2 for up to 12h.

2.3 Plasmid preparation

2.3.1 Agar and broth preparation

L-broth agar (LBA) plates were prepared using 2g of L-broth and 1.5g select agar powder (Life Technologies Ltd, Paisley, UK) per 100 ml distilled water. LBA was autoclaved and antibiotic added prior to being poured into petri dishes (Bibby Sterilin Ltd., Stone, UK). Plates were left to dry at room temperature and were sealed and stored at 4°C until use. L-broth (LB) was prepared using 2g L-Broth powder in 100 ml distilled water, autoclaved and stored at room temperature. Antibiotics were added prior to use. Ampicillin (Sigma-Aldrich Company Ltd., Gillingham, UK) was added at a final concentration of 100µg/ml to both LB and LBA. Kanamycin monsulphate (Sigma-Aldrich Company Ltd., Gillingham, UK) was added at a final concentration of 30µg/ml.

2.3.2 Making competent bacteria

TOP10 competent *E. coli* cells (Life Technologies Ltd, Paisley, UK) or XL-1 Blue competent cells (Stratagene; Agilent technologies, Santa Clara, CA, USA) were plated on non-

selective LBA plates and incubated overnight at 37°C. XL1-blue cells are tetracycline resistant and can be grown under 10µg/ml tetracycline (Sigma-Aldrich Company Ltd., Gillingham, UK) selection for this process, while TOP10 bacteria need to be grown without antibiotics. Individual colonies were picked into 2ml LB and shaken at 37°C until reaching OD_{600} of 0.6-0.8. Cells were pelleted by centrifugation at 1560g at 4°C for 10 minutes. Pellets were resuspended in 5mM$CaCL_2$/10MTris-HCL and incubated on ice for 15 minutes. Cells were then pelleted as before and resuspended in 10ml of 5mM$CaCL_2$/15% Glycerol (Life Technologies Ltd, Paisley, UK) aliquoted and frozen at -80°C.

2.3.3 Transformation

Competent bacteria were thawed on ice. Plasmid DNA was added to 50µl of competent bacteria at a ratio of 1:50, incubated on ice for 30 minutes, heat shocked at 42°C on a heat block for 1 minute and immediately returned to ice for 2 minutes. Bacteria were then grown in 250µl of LB without antibiotics at 37°C for one hour before being transferred onto pre-warmed LBA plates and incubated at 37°C overnight. For long-term storage, transformed bacteria were grown in 2ml LB under antibiotic selection overnight, following which 850µl of bacteria were mixed with 150µl Glycerol and frozen at -80°C.

2.3.4 Plasmid purification

A single colony from a freshly streaked LBA plate was incubated in a starter culture of 2ml of LB under antibiotic selection for 6 hours at 37°C with shaking. The starter culture was then added to 100 ml of LB and further incubated at 37°C overnight under antibiotic

selection. Following the incubation, bacteria were harvested by centrifugation at 6000rcf for 15 minutes at 4°C. Cell pellets were lysed and plasmid purified using the Nucleobond Xtra Midi Plus EF kit and as per manufacturer's instructions (MACHEREY-NAGEL, Düren, Germany). Details of the plasmids used are listed in Table 2.2.

Table 2.2: Plasmid details

Plasmid	*Antibiotic resistance*	*Company/source*
pFR-zsGreen	Ampicillin	Based on pFR-LUC, Agilent technologies, Santa Clara, CA, USA. GFP coding region was cloned into plasmid to replace the luciferase gene by Dr Vockerodt.
pFC-MEKK	Ampicillin	Agilent technologies, Santa Clara, CA, USA
pFC-MEK3	Ampicillin	Agilent technologies, Santa Clara, CA, USA
pFA-CHOP	Kanamycin	Agilent technologies, Santa Clara, CA, USA
pFA-ATF2	Kanamycin	Agilent technologies, Santa Clara, CA, USA
pNF-κB hr-GFP	Ampicilin	Agilent technologies, Santa Clara, CA, USA
pSG5	Ampicillin	Agilent technologies, Santa Clara, CA, USA
pSG5 LMP1	Ampicillin	Provided by Prof. Elliott D. Kieff (Brigham and Women's Hospital and Harvard Medical School, Boston, MA).
pcDNA3.1+	Ampicillin	Life Technologies Ltd, Paisley, UK
pcDNA3.1 S1PR2-HA	Ampicillin	UMR cDNA Resource Center, University of Missouri, Rolla, MO, USA
pMACS 4.1	Ampicillin	Miltenyi Biotec Ltd, Surrey, UK
pMACS LNGFR-IRES	Ampicillin	Miltenyi Biotec Ltd, Surrey, UK
pMACS LNGFR-IRES LMP1	Ampicillin	Cloned based on pSG5 LMP1 by Dr Vockerodt

2.4 Transfection and enrichment of cell lines and primary GC B cells

2.4.1 Transfection of BL2 and DG75 cell lines by electroporation

Cells were seeded at a concentration of 5 x 10^5 cells/ml 24 hours prior to transfection. Cells were centrifuged at 173g at 4^{o}C for 10 minutes and resuspended at a concentration of 10^7cells/250µl of ice cold cell media per transfection reaction. The cell suspensions were then supplemented with 25mM 4-(2-hydroxyethyl)-1-piperazineethanesulfonic acid (HEPES; Gibco®, Life Technologies Ltd, Paisley, UK) and up to a total of 20µg of

plasmid, as detailed below. The supplemented cell suspensions were transferred into ice cold 4mm electroporation cuvettes (Geneflow Limited, Lichfield, UK). Cells were electroporated at 250V, and high capacity of 950µF using a Bio-Rad Gene Pulser® II electroporator (Bio-Rad Laboratories Ltd., Hemel Hempstead, UK), following which they were immediately transferred into 10ml of pre-warmed media and incubated at 37°C in 5% CO_2 for 24h before analysis.

For S1PR2 expression, DG75 cells were transfected with 20µg of pcDNA3.1 or pcDNA3.1 S1PR2-HA. For the optimization of the PathDetect system, BL2 cells were transfected with 3µg of either positive control (pFC-MEKK or pFC-MEK3) or pSG5 plasmid as well as a combination of trans-activator (pFA-ATF2 or pFA-CHOP) and pFR-zsGreen reporter plasmids detailed in Table 2.3.

Table 2.3: PathDetect plasmid titration

Plasmid	***Amount (µg)***		
Trans-activator	1	2	4
pFR-zsGreen	11	10	8
Plasmid of interest	3	3	3

2.4.2 Transfection of L428 and GC B cells by nucleofection

Nucleofection of L428 cells was carried out at room temperature, using Cell Line Nucleofector® Kit L and Nucleofector (1st generation) device (Lonza, Slough, UK). L428 cells were seeded at a concentration of 5 x 10^5 cells/ml 24 hours prior to transfection. Cells were centrifuged at 90g at room temperature for 10 minutes and resuspended at a concentration of 3x10^6cells/100µl of nucleofection solution per reaction, with 4µg of pcDNA3.1+ or pcDNA3.1 S1PR2 plasmid per reaction. Cells were transferred into

nucleofection cuvettes supplied with the kit and electroporated using the X-01 setting on the Nucleofector device. Cells were incubated in cuvettes at room temperature for 10 minutes post electroporation following which they were transferred into 2ml of pre-warmed media and incubated at 37°C in 5% CO_2 for 24h before analysis.

Nucleofection of GC B cells was carried out within 1 hour of isolation, at room temperature, using Human B Cell Nucleofector® Kit and Nucleofector (1st generation) device (Lonza, Slough, UK). GC B cells were centrifuged at 90g at room temperature for 10 minutes and resuspended at a concentration of 5x10^{6}cells/100µl of nucleofection solution per reaction, with 10µg of plasmid per reaction, as detailed below. Cells were transferred into nucleofection cuvettes supplied with the kit and electroporated using the U-15 setting on the Nucleofector device following which they were immediately transferred into 2ml of pre-warmed media and incubated at 37°C in 5% CO_2 for 12-16h before analysis.

For array validation, GC B cells were transfected with 7µg of pSG5 or pSG5LMP1 and 3µg of pMACS LNGFR-IRES. For the NF-κB reporter assay GC B cells were transfected with 3.5µg of pSG5 or pSG5LMP1, 1.5µg of pMACS LNGFR-IRES and 5µg of pNF-κBhrGFP reporter plasmid. For the PathDetect assay GC B cells were transfected with 2µg of trans-activator (pFA-ATF2 or pFA-CHOP) and 4µg of pFR-zsGreen reporter plasmid and 1.5µg of pMACS LNGFR-IRES, pMACS LNGFR-IRES LMP1 or positive control (pFC-MEKK or pFC-MEK3). A further 1.5µg of pMACS LNGFR-IRES was added to the positive control samples to allow for selection transfected cells in later analysis. To control for plasmid amount, 1.5µg of pSG5 was added to the rest of the samples.

2.4.3 MoFlo enrichment of transfected GC B cells

Following incubation, transfected GC B cells were washed twice with 10x volume of autoMACS, using centrifuge at 173g at 4^{o}C for 10 minutes. Pellets were resuspended in 250µl of autoMACS with anti-LNGFR-Allophycocyanin (APC) antibody (Miltenyi Biotec Ltd, Surrey, UK) at a 1/10 dilution. Cells were incubated for 10 minutes at 4^{o}C in the dark, following which they were washed with 40x volume of autoMACS. Cells were resuspended in 250µl of autoMACS and passed through a pre-washed 50µl filter into 5ml Polypropylene Round Bottom Falcon tubes (BD Biosciences, USA). The same volume of autoMACS was applied onto the filter to wash all the cells through and cells were kept at 4^{o}C in the dark until cell sorting. Immediately prior to cell sorting, propidium iodide (PI; Sigma-Aldrich Ltd., Gillingham, UK) was added at a 1/10 dilution, to identify viable cells (PI negative). LNGFR-APC and CD10-PE positive, PI negative cells were collected by fluorescence-activated cell sorting (FACS) on a MoFlo sorter (Dako UK Ltd., Cambridgeshire, UK). Cells were collected into RNase free tubes with 750µl of RNase free phosphate buffered saline (PBS) solution (Gibco®, Life Technologies Ltd, Paisley, UK). Cells were pelleted by centrifugation at 3000rpm, 4^{o}C for 10 min using a Heraeus Pico 17 Microcentrifuge (Thermo Fisher Scientific Inc, Waltham, MA, USA). Pellets were immediately stored at -80^{o}C.

2.5 RNA analysis

All procedures were carried out on ice, with RNase free equipment. Work surfaces were decontaminated using RNaseZap® Decontamination Solution (Ambion®, Life Technologies Ltd, Paisley, UK).

2.5.1 RNA extraction from cultured cells and stimulated GC B cells

Cells were washed once with ice cold PBS prior to pelleting at a concentration of $3x10^6$ cells/pellet (cell lines) and $2x10^6$ cells/pellet (stimulated GC B cells). RNA was extracted from cell lines and stimulated GC B cells using the QIAGEN RNeasy® mini kit according to the manufacturer's protocol (QIAGEN Ltd, Manchester, UK). RLT buffer was supplemented with 14.3M β-mercaptoethanol (β-ME; Sigma-Aldrich Company Ltd., Gillingham, UK) as per kit instruction. On-column DNase digestion was performed as per manufacturer's instructions using the RNase-Free DNase Set (QIAGEN Ltd., Manchester, UK). RNA was eluted from the columns provided with the kit using 30µl of DEPC-treated water (supplied in kit) pipetted directly onto the membrane. The concentration of RNA was determined using a NanoDrop ND-1000 spectrophotometer (Thermo Fisher Scientific Inc, Waltham, MA, USA).

2.5.2 RNA extraction and amplification from nucleofected GC B cells

Cell pellets from sorted, nucleofected GC B cells (approximately 10000 cells) were lysed in 100µl RLT buffer supplemented with 1µl of 14.3M β-ME and 1µl N-carrier (AmpTec, supplied by AMS Biotechnology (Europe) Ltd, Abingdon, UK). RNA was extracted using the QIAGEN RNeasy® micro kit according to the manufacturer's protocol (QIAGEN Ltd, Manchester, UK). The quality of the isolated RNA was determined using a NanoDrop ND 1000 (Thermo Fisher Scientific Inc, Waltham, MA, USA) and a Bioanalyzer 2100 (Agilent, Waldbronn, Germany). Only those samples with a 260/280 nm ratio between 1.8-2.1 and a 28S/18S ratio within 1.5-2.0 were processed for RNA amplification. RNA amplification was carried out using the ExpressArt® mRNA Amplification Kit Nano

version as per manufacturer's instructions for two rounds of amplification (AmpTec, supplied by AMS Biotechnology (Europe) Ltd, Abingdon, UK).

2.5.3 Reverse transcription (RT) of RNA to cDNA

For reverse transcription of RNA to copy DNA (cDNA), 500ng of RNA was used from cell lines and stimulated GC B cells, while only 300ng was used from 2nd round of GC B cell RNA amplification. RNA was made up to 11µl volume in sterile 0.2ml PCR tubes using sterile DEPC treated water (Invitrogen®, Life Technologies Ltd, Paisley, UK). To this, 2µl of a 1:1 mix of 100µg/ml random hexamer primers (Promega UK Ltd, Hampshire, UK) and 10mM deoxyribonucleotide triphosphates (dNTP; Roche Diagnostics Limited, UK) was added. Samples were incubated at 65^{o}C for 5 minutes using the Veriti® Thermal Cycler (Applied Biosystems®; Life Technologies Ltd, Paisley, UK). Samples were then cooled on ice for 1 minute, before the addition of 7µl of the following master mix (made up to the ratio of 4:1:1:1): 5x First Strand buffer, 0.1 M dithiothreitol (DTT), RNaseOUT™ and SuperScript® III reverse transcriptase (Invitrogen ™; Life Technologies Ltd, Paisley, UK). The sample was mixed and incubated using the Veriti® Thermal Cycler with the following protocol: 5 minutes at 25^{o}C, 1 hour at 50^{o}C, 15 minutes at 70^{o}C and hold at 4^{o}C. The cDNA samples were stored at -20^{o}C until required.

2.5.4 Quantitative polymerase chain reaction (qPCR)

The qPCR reaction was set up as a multiplex reaction in a 20µl volume in a 96-well optical reaction plate (Applied Biosystems®; Life Technologies Ltd, Paisley, UK). Each reaction contained 5 µl of diluted cDNA (typically 1:20 with DEPC treated water), 10 µl of FastStart Universal Probe Master mix (Roche Diagnostics Limited, UK), 1 µl of 20x

primer/probe of gene of interest (FAM labelled) and 1 µl of 20x primer/probe of GAPDH endogenous control (VIC TAMRA labelled) (Taqman® Life Technologies Ltd, Paisley, UK) and 3 µl of DEPC treated water. All primers and probes are listed in Table 2.4. All samples were set up in triplicate and a non-target (water) control was included. The plate was sealed with optically clear adhesive film (Applied Biosystems; Life Technologies Ltd, Paisley, UK).

Table 2.4: Taqman primer/probes from Applied Biosystems (ABI)

Gene	*ABI probe ID*	*Dye label*
ATM	Hs01112355	FAM
TNFAIP3	Hs00234713	FAM
HSPA1A	Hs00359163	FAM
CCL5	Hs00174575	FAM
STAT5A	Hs00234181	FAM
ID2	Hs00747379	FAM
PTEN	Hs02621230	FAM
RASSF6	Hs00698249	FAM
CD72	Hs00233564	FAM
VPREB3	Hs00353682	FAM
GAPDH	Hs02758991	VIC TAMRA
RGS13	Hs00243182	FAM
S1PR2	Custom ABI assay containing: 5' primer: GTGCTAGGCGTCTTTATCGTC 3' primer: GTAGTGGGCTTTGTAGAGGATC Probe: AGGAGTGGACGGGACAGGCATA	FAM

The reaction for the detection of LMP1 transcripts was set up in a final volume of 25µl, with 12.5µl of FastStart Universal Probe Master mix, 2.5µl of the 5' and 3' primers, 1µl of probe, 1µl of 20x primer/probe of endogenous control and 1.5µl of DEPC treated water. The sequences of the LMP1 primers and probe have been previously described (Bell et al., 2006) and were ordered accordingly (Sigma-Aldrich Company Ltd., Gillingham, UK).

Samples were amplified using the standard relative quantification method of the 7500 Fast Real-Time PCR System (Applied Biosystems®; Life Technologies Ltd, Paisley, UK). Briefly, samples were subjected to enzyme activation (50°C for 2 minutes) and denaturation (95°C for 10 minutes) followed by 40 cycles of amplification (denaturation at 95°C for 15 seconds and extension at 60°C for 1 minute).

The delta-delta (ΔΔ) Ct method was used to determine relative gene expression of the samples. This is a two-step method, first normalising the sample values against an endogenous control (e.g. GAPDH), second relative gene expression is determined based on the selection of a reference sample to act as a baseline for gene expression, resulting in an absolute value of fold change (Livak and Schmittgen, 2001).

2.6 Protein analysis

2.6.1 Western blotting

2.6.1.1 Protein extraction from GC B cells

GC B cell pellets were lysed in 20µl RIPA lysis buffer (140mM NaCl, 10mM Tris-HCl pH8, 1mM EDTA, 1% triton, 0.1% SDS, 0.1% Sodium deoxycholate (Deoxycholic acid)) supplemented with 1mM of activated sodium vanadate and 4% v/v protease inhibitor (cOmplete Tablets, EDTA-free; Roche Diagnostics Limited, UK). Cells were vortexed with lysis buffer, left on ice for 30 minutes and centrifuged at maximum speed, 4°C for 15 minutes on a Heraeus Pico 17 Microcentrifuge (Thermo Fisher Scientific Inc, Waltham, MA, USA) to collect cell debris. The supernatant was transferred to a clean 0.5 ml tube and either used immediately or frozen at -20°C.

2.6.1.2 Sodium dodecyl sulphate polyacrylamide gel electrophoresis (SDS-PAGE)

SDS-PAGE gels were made as per Lab FAQs booklet (Roche Diagnostics Limited, UK). Due to the low cell numbers in the sample, the extracted protein was not quantified, instead whole lysate was diluted 1:1 with 2x SDS-PAGE buffer (10%SDS, 1.5M Tris-HCl (pH6.8), 1% Bromophenol blue, 1M dithiothreitol (DTT) in H_2O). Protein was denatured by heating the sample at 95^{o}C for 10 minutes prior to loading samples along with Spectra™ Multicolor Broad Range Protein ladder (Thermo Fisher Scientific Inc, Waltham, MA, USA). Gels were placed in Tris-Glycine-SDS PAGE Buffer (Geneflow Ltd, Lichfield, UK) and the solubilised proteins were separated by electrophoresis in Mini Trans-Blot® Cell tank (Bio-Rad Laboratories Ltd., Hemel Hempstead, UK), at 125 V, (300 mA limit) for 1.5-2 hours depending on protein size.

2.6.1.3 Protein transfer

Six sponges, six pieces of Whatman® chromatography paper (Sigma-Aldrich Company Ltd., Gillingham, UK) and one piece of nitrocellulose membrane (Amersham Hybond-C extra; GE Healthcare Life Science, Buckinghamshire, UK) were pre-soaked in 1x Tris-Glycine Electro-Blotting Buffer (Geneflow Ltd, Lichfield, UK). To set up the protein transfer, the components were stacked in the following order: 3 sponges, 3 pieces of filter paper, gel, 1 nitrocellulose membrane, 3 pieces of filter paper, and 3 sponges in an XCell II Blot Module within the XCell *Surelock* Mini-Cell (Invitrogen; Life Technologies Ltd, Paisley, UK). The tank was topped up with 1x transfer buffer, placed in ice and in a cold room. Transfer was run at 40 V, 400 mA for 2 hours.

2.6.1.4 Immunoblotting and visualisation

Non-specific protein binding was blocked by incubating the membrane for 1 hour at room temperature in 5% non-fat dried milk dissolved in TRIS buffered saline-tween (Milk/TBST). TBST consists of 1.21 g TRIS and 8.77 g NaCl in 1 litre distilled water (pH adjusted to 7.6 using concentrated HCl) with 0.5 ml Tween20 (Fisher Scientific). Membranes were incubated with primary antibody (BCL6 and PARP, Cell Signaling) diluted 1:1000 in 5% BSA/TBST overnight at 4^{o}C on a roller. Membranes were washed 3x in TBST before incubation for 1 hour at room temperature with polyclonal goat anti-Rabbit-HRP secondary antibody (Dako UK Ltd., Cambridgeshire, UK), diluted 1:1000 in 5% BSA/TBST.

The membrane was again washed 3x in TBST, following which antibody-protein complexes were detected using the ECL Western Blotting System (GE Healthcare Life Science, Buckinghamshire, UK). The two ECL reagents were mixed 1:1 immediately prior to use, the membrane was incubated in the ECL mixture for 1 minute and then the excess liquid drained off. The membrane was transferred to an autoradiography cassette and developed in a dark room using a sheet of Hyperfilm™ (GE Healthcare Life Science, Buckinghamshire, UK) and a Kodak X-OMAT 1000 processor (Kodak Limited).

Following the detection of the protein of interest, the membrane was washed in TBST and re-probed for β-actin-HRP (clone AC-15; Sigma-Aldrich Ltd., Gillingham, UK) for 1 hour at room temperature, at a 1:10000 dilution in 5% BSA/TBST. Membrane was developed as described.

2.6.2 Immunohistochemistry and immunofluorescence

2.6.2.1 Cytospin preparation

2 x 10^6 cells were centrifuged, washed in serum-free RPMI 1640 and resuspended in 1 ml serum-free RPMI 1640 with 10% v/v formaldehyde (Sigma-Aldrich Ltd., Gillingham, UK). Cells were attached on X-tra Adhesive micro slides (Surgipath Europe, Peterborough, UK) in Cytospin3 cytocentrifuge (Shandon, Runcorn, UK) using Cytofunnel® disposable sample chambers, filter cards and Cytoclips™ (all Thermo Fisher Scientific Inc, Waltham, MA, USA) and centrifuged at 1000rpm for 5 minutes. Cytospin preparations were air dried and stored at -20°C until required. When required, slides were thawed and the endogenous peroxidase activity was blocked by immersing the slides for 10 minutes in 0.3% hydrogen peroxide (Sigma-Aldrich Ltd., Gillingham, UK), following which slides were rinsed in running tap water.

2.6.2.2 Preparation of tissue sections

Paraffin-embedded blocks of HL and DLBCL patients were obtained from the Queen Elisabeth Hospital, Birmingham, UK.

Paraffin-embedded blocks were cut to 4µm thickness and placed onto X-tra Adhesive micro slides (Surgipath Europe, Peterborough, UK). Sections were then de-waxed by immersing the slides for 10 minutes in Histo-Clear (National Diagnostics, supplied by AGTC Bioproducts t/a National Diagnostics UK, Hessle, UK), and re-hydrated by immersing the slides for 5 minutes in 100% ethanol (Sigma-Aldrich Ltd., Gillingham, UK), followed by tap water. Next, the endogenous peroxidase activity was blocked by

immersing the slides for 10 minutes in 0.3% hydrogen peroxide (Sigma-Aldrich Ltd., Gillingham, UK), following which slides were rinsed in running tap water.

2.6.2.3 Antigen retrieval

Citrate buffer (1.26 g sodium citrate and 0.25 g citric acid in 1l distilled water, pH 6.0) was boiled in a glass beaker for 10 minutes at full power in a microwave before immersing the slides pre-loaded on a rack into the buffer. The beaker was covered with cling film and was returned to the microwave and heated for 10 minutes at moderate power then 10 minutes at low power. The buffer was allowed to cool completely before the slides were removed and rinsed in running water.

2.6.2.4 Detection of antigen by immunohistochemistry

After antigen retrieval, slides were placed in a metal microscope slide staining tray (Richardsons of Leicester Ltd., Leicester, UK) and the tissue section encircled using an ImmEdge Hydrophobic Barrier Pen (Vector Laboratories Ltd., Peterborough, UK). Slides were washed with PBS-Tween-20 (0.1%) (PBST) for 5 minutes and then blocked in 100µl of 5X casein blocking solution (Vector Laboratories Ltd., Peterborough, UK) to reduce non-specific background staining. The sections were incubated with 100µl of diluted primary antibody (Table 2.5), with the slide tray filled a thin layer of water and covered with a lid to minimize evaporation.

Table 2.5: Antibodies used for IHC

Antibody	*Clone*	*Source*	*dilution*	*incubation*	*DAB time*
S1PR2	polyclonal	Sigma	1/400, 1/200 for IF	Overnight at 4	6min
HA	Y-11	Santa Cruz	1/50	1 hour at room temperature	3min
LMP1	cs1-4	Dako	1/50 for cytospin, 1/25 for tissue	Overnight at 4	6min

Following incubation, samples were washed with PBST for 5 minutes and incubated with 2 drops of DAKO Envision secondary antibody (Dako UK Ltd., Cambridgeshire, UK) for 30 minutes at room temperature. Visualization was carried out using the ImmPact DAB substrate system (Vector Laboratories Ltd., Peterborough, UK) which generated a brown product that is insoluble in water and organic solvents. Slides were further rinsed with distilled water and counterstained with Mayer's haematoxylin (Sigma-Aldrich Ltd., Gillingham, UK) for 30-60 seconds and washed under hot running tap water for 2 minutes. Slides were then dehydrated by immersing the slides for 5 minutes in 100% ethanol, followed by 10 minutes in Histoclear and mounted with cover slips using DPX mounting medium (Sigma-Aldrich Ltd., Gillingham, UK).

2.6.2.5 Detection of antigen by immunofluorescence

After antigen retrieval, slides were placed in a metal microscope slide staining tray (Richardsons of Leicester Ltd., Leicester, UK) and the tissue section encircled using an ImmEdge Hydrophobic Barrier Pen (Vector Laboratories Ltd., Peterborough, UK). Slides were washed with PBS-Tween-20 (0.1%) (PBST) for 5 minutes and then blocked in 100µl of 5X casein blocking solution (Vector Laboratories Ltd., Peterborough, UK) to reduce non-specific background staining. The sections were incubated with 100µl of diluted primary antibody (Table 2.5), with the slide tray filled a thin layer of water and covered with a lid to minimize evaporation.

Following incubation, samples were washed with PBST for 5 minutes and incubated with Alexa Fluor® secondary antibody diluted 1:1000 at 37^{o}C for 1 hour. Secondary antibodies used: Alexa Fluor® 594 Goat Anti-Mouse IgG (H+L) and Alexa Fluor® 488 Goat Anti-

Mouse IgG (H+L) (Invitrogen; Life Technologies Ltd, Paisley, UK). Slides were washed with PBST for 5 minutes and mounted with cover slips using VECTASHIELD Mounting Medium with DAPI (Vector Laboratories Ltd., Peterborough, UK). Cells were visualised using a Nikon E600 UV microscope.

2.6.3 Flow cytometry

To detect cell-surface marker expression, cells were washed 2x with autoMACS and resuspended in 50µl of autoMACS containing a 1/10 dilution antibody (antibodies are listed in Table 2.6). Cells were incubated with antibody for 15 minutes in the dark at 4^{o}C, following which they were washed in 10x volume of autoMACS and resuspended in 500µl of autoMACS (or 200µl for GC B cell samples which contained less cells). Cells were kept on ice in the dark and analysed within 1h. Propidium iodide (PI) was added to all stained samples immediately before measurement. Cells were analysed by flow cytometry using the FACSCalibur and the CellQuest software (BD Biosciences, USA). Data was analysed using Flowjo software (TreeStar Inc.). Only the viable cells were considered for analysis based on their light scatter (FSC/SSC) characteristics and PI negativity.

Table 2.6: Fluorescently labelled antibodies used for flow cytometry

Antibody	*Clone*	*Fluorescent label*	*Source*
ICAM1 (CD54)	15.2	FITC	AbDserotec
CD10	eBioCB-CALLA	PE	eBioscience
CD19	LT19	APC	Miltenyi Biotech
CD77	5B5	FITC	BD biosciences
CXCR4 (CD184)	12G5	APC	eBioscience
CD95	DX2	FITC	eBioscience
CD3	UCHT1	FITC	eBioscience
CD24	SN3	FITC	eBioscience
CD38	T16	FITC	Coulter/Immunotech
CD27	O323	FITC	Biolegend
CD83	HB15e	FITC	eBioscience
CD86	B-T7	FITC	abcam
CD271 (NGFR)	ME20.4-1.H4	APC	Miltenyi Biotech

2.7 Migration assay

Migration assay on transfected L428 cells was performed using DiOC16(3) dye (Biotium, supplied by Cambridge BioScience, Cambridge, UK) and 5µM Transwell permeable supports (Corning B.V. Life Sciences, Amsterdam, Netherlands). Transfected cells were pelleted 24h post transfection, washed 2x with autoMACS and re-suspended at a concentration of $5x10^5$cells/ml in autoMACS with DiOC(3) dye at a final concentration of 2.5µM. Cells were incubated at 37°C, 5% CO_2 for 30 minutes, washed 1x with autoMACS and resuspended at a concentration of $5x10^5$cells/200µl in serum-free RPMI 1640. A 24 well plate was prepared with 600µl of supplemented RPMI 1640 (described in section 2.1.1), transwells were inserted and 200µl of labelled cells were added to each insert. At each time point, the inserts were removed onto a separate 24 well plate and fluorescence in the bottom of the wells was read on a Wallac 1420 Victor2 Microplate Reader (PerkinElmer, Cambridge, UK), with excitation/emission filters F485/F510.

Fluorescence measurements across all experiments were averaged, the media only control fluorescence was subtracted and the values from S1PR2 transfected cells were normalised to vector control for each time point.

2.8 Proliferation assay

Proliferation assay on transfected L428 cells was performed using CellTiter-GLO ® Luminescent Cell Viability Assay (Promega UK Ltd, Hampshire, UK). 10^6 transfected cells were pelleted 24h post transfection, washed 1x with supplemented RPMI 1640 and re-suspended at a concentration of $2x10^5$cells/ml and incubated at 37°C, 5% CO_2. At each time point cells were mixed and 2x 50µl were removed into opaque 96 well plates. Cells and CellTiter-GLO reagent were left for 30 minutes to equilibrate to room temperature, prior to adding reagent to cells at a 1:1 ratio. Plates were shaken for 2 minutes and left to stand for 10 minutes prior to reading luminescence on a Wallac 1420 Victor2 Microplate Reader. Luminescence measurements across all experiments were averaged and the media only control fluorescence was subtracted for each time point.

2.9 Statistical analysis

2.9.1 Re-analysis of published microarrays

The three arrays re-analysed in Chapter 4 section 4.2.1 were Affymetrix HG-U133 Plus2 transcriptional arrays. Probe level quantile normalisation (Bolstad et al., 2003) and RMA (robust multi-array analysis) (Irizarry et al., 2003) were performed using the affy package of the Bioconductor project (http://www.bioconductor.org). Differentially expressed probe sets were identified using limma (Smyth, 2004) using criteria of fold change >1.5 and $p < 0.001$.

For the survival analysis of the DLBCL array, GSE10846 was downloaded from GEO. Probe level quantile normalisation (Bolstad et al., 2003) and RMA (Irizarry et al., 2003) were performed using the affy package of the Bioconductor project (http://www.bioconductor.org) and the custom cdf HGU133Plus2_Hs_ENTREZG (version 16). Survival analysis was performed using the R survival package (http://www.r-project.org/). Both of the above analysis were performed by Dr Wenbin Wei, Senior Bioinformatician, School of Cancer Sciences, University of Birmingham.

Analysis of the DLBCL IHC result was performed by Dr Judy Powell, Senior Lecturer, Public Health, Epidemiology and Biostatistics, School of Health and Population Sciences, University of Birmingham. Survival time was analysed using Kaplan-Meier survival analysis, and the results were plotted as survival curves. For overall survival, survival time was defined as the time in months between the disease diagnosis and death. Event-free survival was defined as the time between diagnosis and the first disease event (relapse, progression or death without relapse or progression). Subjects not experiencing death or an event were censored at the last date known to be alive or disease free respectively. The log-rank test was used to determine if observed differences between the survival curves were statistically significant, significance being defined as a p-value less than 0.05. All analysis was done using SPSS Version 21.

Chapter 3

An investigation of the phenotype of germinal centre B cells following their in vitro separation and short term culture

3 An investigation of the phenotype of germinal centre B cells following their in vitro separation and short term culture

3.1 Introduction

The majority of B cell lymphomas, including Burkitt's lymphoma (BL), Hodgkin's lymphoma (HL) and diffuse large B cell lymphoma (DLBCL), are believed to derive from germinal centre (GC) B cells (Kuppers et al., 1999, Klein and Dalla-Favera, 2008). In the absence of animal models and primary cell lines, the manipulation of primary human GC B cells in vitro provides an alternative approach to interrogate the mechanisms of lymphomagenesis.

The isolation of tonsillar GC B cells using CD10 directed MACS separation has already been described (Vockerodt et al., 2008). Following their isolation CD10 positive GC B cells can be transfected and maintained in short term culture (Vockerodt et al., 2008). Subsequent chapters in this thesis explore the transcriptional consequences of virus gene expression and CD40 stimulation in tonsillar GC B cells.

The purpose of the work described in this chapter is to describe the phenotype of CD10 positive tonsillar cells directly after isolation and short-term culture.

3.2 Results

3.2.1 Isolated CD10 positive tonsillar mononuclear cells are viable

I first wanted to measure the viability of isolated CD10 positive GC B cells. Tonsillar mononuclear cells (TMCs) were isolated and CD10 positive cells enriched by magnetic cell sorting as described in Materials and Methods, section 2.2.

Flow cytometry was used to measure the viability of CD10 positive cells (Figure 3.1). I used two methods to do this. In the first method, I measured cell size by forward scatter (FSC) and morphology by side scatter (SSC). Gates were drawn around the dense population of live cells (Figure 3.1a). In this way cell debris (seen at the bottom end of the FSC scale) and dead cells which have a higher granularity (top end of SSC) are gated out from the analysis. In the second method, I stained cells with propidium iodide (PI) which can only enter cells with disrupted cell membranes, leaving healthy cells unstained (Figure 3.1b).

I found that following their isolation the mean viability of CD10 positive cells as measured by forward scatter was 91.7% (range: 88.3-95.6%) and by PI staining was 95.7% (range: 89.2-96.7%). This observation was based on the analysis of tonsillar preparations from 12 patients.

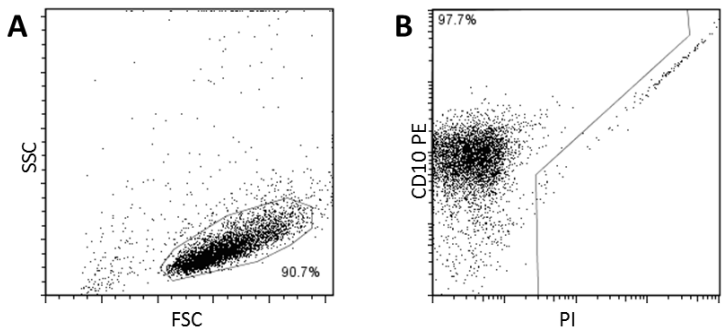

Figure 3.1: Viability and gating strategy for isolated cell populations
Gating is shown for a representative experiment of isolated CD10 positive cells (12 replicates)
A) Viable cells are gated based on size (FSC) and granularity (SSC) Gates were drawn around the dense population of live cells to exclude cell debris (seen at the bottom end of the FSC scale) and dead cells which have a higher granularity (top end of SSC).
B) Viable cells are gated based on PI negativity. Propidium iodide can only enter cells with disrupted cell membranes, leaving healthy cell unstained.

3.2.2 Isolated CD10 positive tonsillar mononuclear cells display a GC B cell phenotype

Having shown that the majority of isolated CD10 positive are viable, I next wanted to investigate the phenotype of these cells. To do this, I repeated the CD10 based isolation above from a further 3 tonsils and assessed cell surface marker expression by flow cytometry (Table 3.1). I first stained tonsillar mononuclear cells (TMCs) to assess the proportion of GC B cells and T cells in the population. I used anti-mouse IgG1 specific fluorescent antibodies (isotype control) to identify non-fluorescent cells and set the gates for further analysis (Figure 3.2a). A large proportion of TMCs express CD10, and nearly all CD10 expressing TMCs are also positive for CD77. Approximately 20% of TMCs are T cells, of which only a minority are CD8 positive T cells.

Table 3.1: Markers used for identifying cellular subsets

Gene	*Cell type*	*References*
CD10	GC B cell (Bm3, Bm4) and GC founder cell (Bm2', Bm3δ-4δ)	(Bohnhorst et al., 2001, Pascual et al., 1994)
CD19	B cell marker	(Bohnhorst et al., 2001)
CD77	Centroblast (Bm3)	(Klein et al., 2003, Pascual et al., 1994)
CXCR4	Centroblast (Bm3)	(Allen et al., 2004, Caron et al., 2009)
CD95 (Fas)	GC B cell (Bm3, Bm4)	(Hao et al., 2008, Lagresle et al., 1995)
CD3	T cells	(McClory et al.)
CD24	Immature B cell and transitional B cells	(Palanichamy et al., 2009, Sims et al., 2005)
CD38	GC B cell, plasma cell	(Jego et al., 1999, Bohnhorst et al., 2001)
CD27	Memory B cell (Bm5)	(Klein et al., 1998)
CD83	Dendritic cell marker. Can identify centrocytes (Bm4) in conjunction with CXCR4	(Victora et al., 2012)
CD86	Dendritic cell marker. Can identify centrocytes (Bm4) in conjunction with CXCR4	(Victora et al., 2012)
BCL6	GC B cell (Bm3, Bm4)	(Cattoretti et al., 1995, Basso and Dalla-Favera, 2010)

Figure 3.2b shows that the majority of the isolated CD10 positive cells express CD19, a known B cell surface antigen. In addition, the majority of CD10 expressing cells also express CD38, a molecule expressed in haematopoietic cells, including GC B cells. A small population of cells display more intense staining for CD38; these could either be GC B cell founder cells or emerging plasmablasts, both of which also express CD10 (Bohnhorst et al., 2001, Jego et al., 1999). CD10 positive cells also express CD95 and BCL6 which is consistent with their GC phenotype. Approximately 15% of CD10 positive cells also express CD27, a molecule found on somatically hypermutated memory B cells (either GC B cells differentiating to memory or memory B cells re-entering the GC reaction) and only a small proportion of T cells (Klein et al., 1998). I have also confirmed the expression of BCL6, a molecule essential for GC formation, in two replicates (Figure 3.2c).

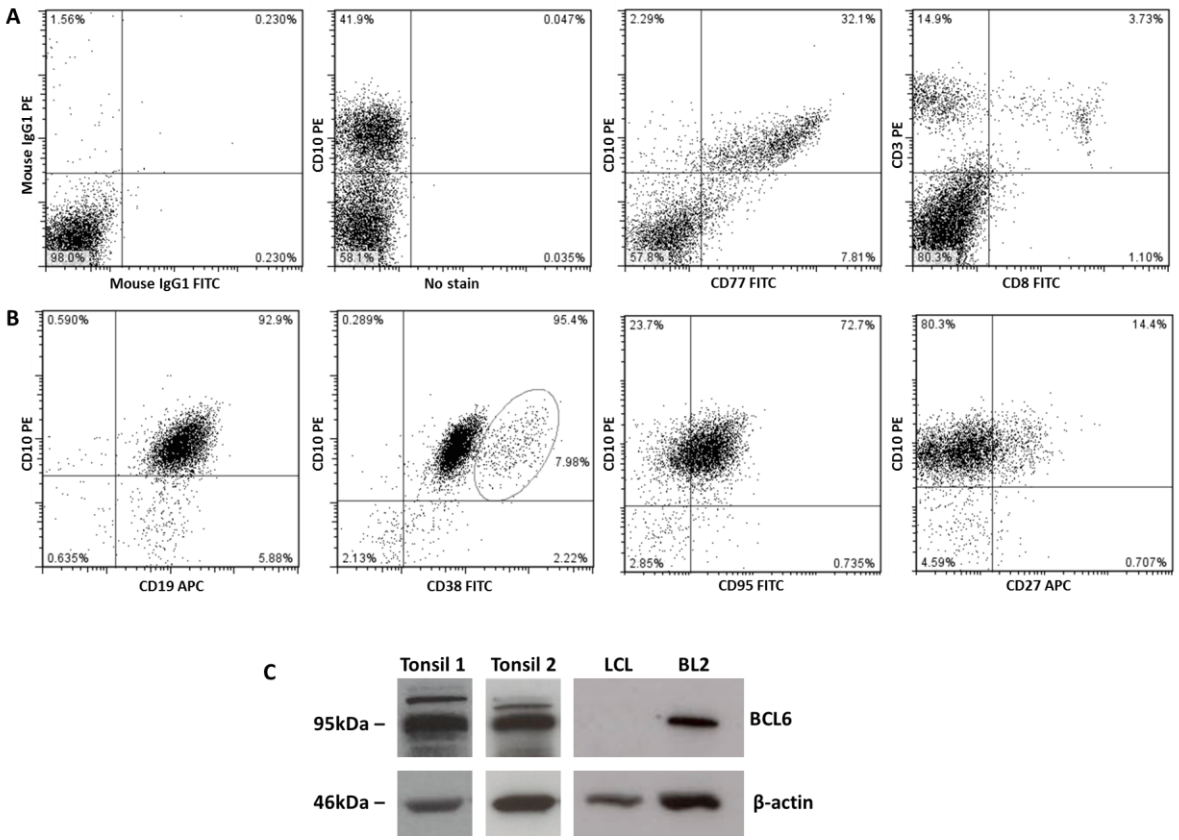

Figure 3.2: Phenotype of isolated CD10 positive cells

Cells have been gated as per Figure 3.1 to identify viable cells and the population of the two gates were combined. The resulting population of viable cells were used for analysis. Cells were not gated for CD10 expression

A) Tonsillar mononuclear cells (TMCs) were stained with isotype control antibody (anti-mouse IgG1) to determine the position of the gates for later analysis. A large proportion of TMCs express CD10, and nearly all CD10 positive TMCs are also positive for CD77 expression. Approximately 20% of TMCs are T cells, of which only a minority are CD8 positive T cells. Data is representative of 3 replicates

B) CD10 sorted cells were stained for either: CD19, CD38, CD95 or CD27 to assess their GC phenotype.

GC B cells are positive for CD10, CD19 and CD38, with most expressing CD95 on their surface. The percentage of CD27 positive cells is low. Data is representative of 3 replicates

C) Western blot of isolated CD10 positive cells from two tonsils showing that BCL6 is expressed in the GC B cells of both tonsils. BL2 Burkitt's lymphoma cell line acts as a positive control and lymphoblastoid cell line (LCL) act as a negative control. β-actin acts as a loading control as expression of this housekeeping molecule should be identical in the samples.

I found that on average 82.1% (range: 77.2-87%) of CD10 positive cells also express CD77 (Figure 3.3a). Although originally believed to be a specific marker of centroblasts, it has recently been reported that $CD77^+$ and $CD77^-$ GC B cells have near identical transcription profiles and that CD77 alone does not discriminate between centroblasts and centrocytes (Hogerkorp and Borrebaeck, 2006, Pascual et al., 1994, Klein et al., 2003). CXCR4 and CXCR5 have been reported to be expressed on human centroblasts and centrocytes, respectively (Allen et al., 2004). Furthermore, a recent study has confirmed expression of CXCR4 on centroblasts (Caron et al., 2009). I analysed the expression of CXCR4 and CD77 on CD10 positive cells. Figure 3a shows that the majority of cells are double positive for CXCR4 and CD77 expression (average 72.9%, range 46-86.5%); with a large proportion of cells that express only CXCR4 (average 12%, range 3.1-25.4%) or CD77 (average 8.8%, range 5.5-11.3%). These observations indicate that the expression of CXCR4 and CD77 do not consistently overlap in GC B cells. As CD77 has been shown to be an inconsistent marker of centroblasts, CXCR4 positivity could provide a more accurate measure of these cells. Taken together, the data indicate that centroblasts comprise the most abundant population in the CD10 isolated cells.

CD83 and CD86 have recently been identified on the surface of centrocytes and when used in conjunction with CXCR4 can distinguish centroblasts ($CXCR4^{high}CD83^{low}$ or $CXCR4^{high}CD86^{low}$) and centrocytes ($CXCR4^{low}CD83^{high}$ or $CXCR4^{low}CD86^{high}$) (Victora et al., 2012). Figure 3.3b shows that of the isolated CD10 positive cells 18.7% were $CXCR4^{low}CD83^{high}$ and 22.8% were $CXCR4^{low}CD86^{high}$ suggesting that only a minority of isolated cells have a centrocyte phenotype.

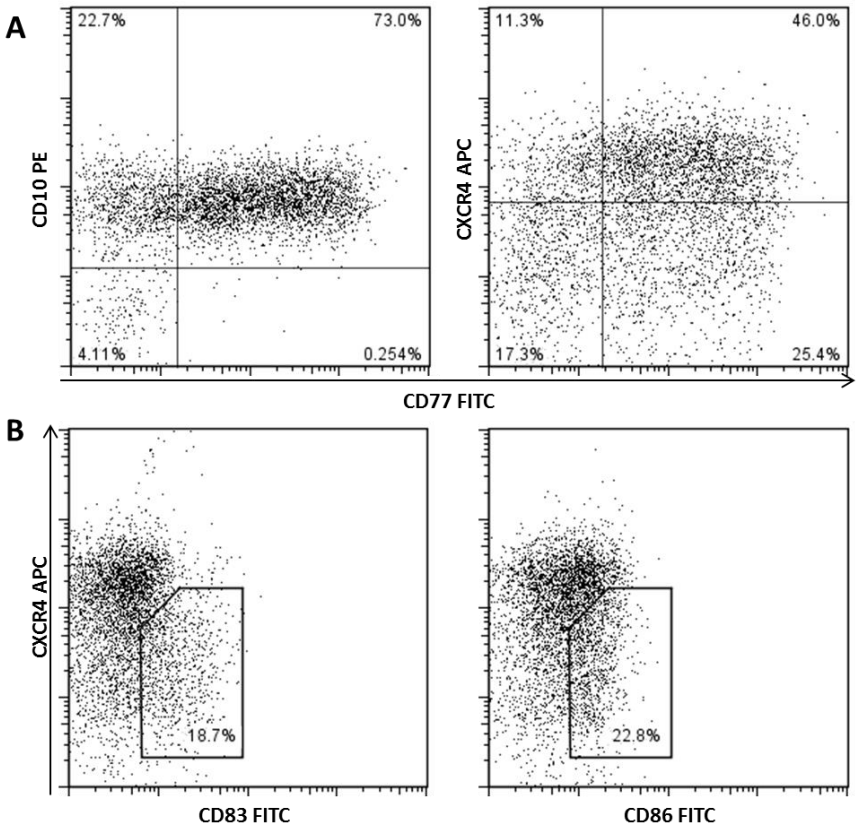

Figure 3.3: Levels of centroblasts and centrocytes

Cells have been gated as per Figure 3.1 to identify viable cells and the population of the two gates were combined. The resulting population of viable cells were used for analysis. Cells were not gated for CD10 expression.

A) CD10 sorted cells were stained for CXCR4 and CD77. Centroblasts are represented in the top right quadrants as CD10/CD77 double positive or CXCR4/CD77 double positive cells. (Representative of 3 replicates).

B) Expression of centrocyte markers CD83 and CD86 and centroblast marker CXCR4 identifying centrocytes ($CXCR4^{low}CD83^{high}$ or $CXCR4^{low}CD86^{high}$) and centroblasts ($CXCR4^{high}$).

I found that a small fraction (less than 5%) of isolated cells were CD10 negative (Figure 3.3a), therefore I wanted to check the purity of the isolated populations. I stained the isolated cells for CD3 (to distinguish T cells) and CD24 (to distinguish transitional B cells). CD24 in conjunction with other markers, such as CD10, can be used to identify transitional B cells in peripheral blood (Palanichamy et al., 2009, Sims et al., 2005). As these cells circulate from the bone marrow to the spleen, some could potentially be in (the blood vessels of) the tonsil and may be isolated during the CD10 magnetic enrichment.

There is a low level, 1.5% of T cells in the sample (Figure 3.4a). Importantly, two thirds of the CD3 positive T cells express CD10, allowing for the selection of these cells during enrichment. However, the overall percentage of these cells in the total population is very low (<1%) and thus unlikely to skew any analysis. The level of CD10/CD24 double positive transitional B cells is very low, representing only 0.57% of the total isolated GC B cell population (Figure 3.4b). There is also a small population of $CD10^{-}CD24^{+}$ cells in the isolated sample. As all CD24 expressing cells are positive for CD19 (Figure 3.4b), this population of $CD10^{-}CD24^{+}$ cells are likely to represent non-GC B cells.

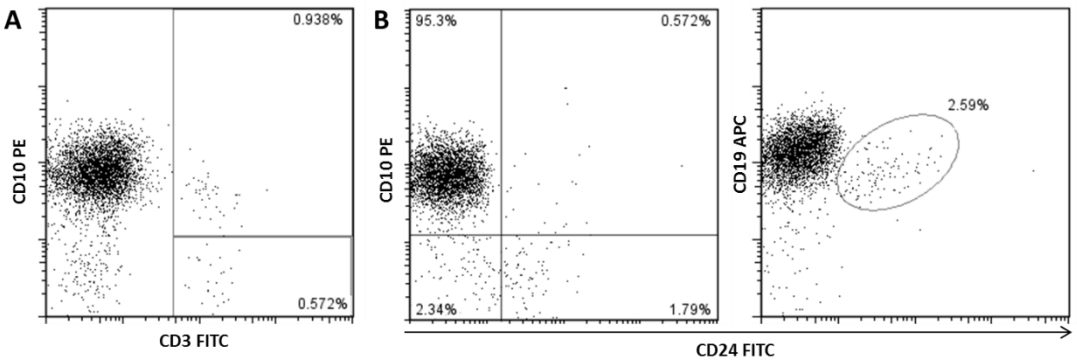

Figure 3.4: Cells of non-GC B cell origin in the isolated cells
Cells have been gated as per Figure 3.1 to identify viable cells and the population of the two gates were combined. The resulting population of viable cells were used for analysis. Cells were not gated for CD10 expression.
A) CD10 sorted cells were stained for CD3 to detect T cells, present as either CD3 positive CD10 negative cells (0.57%) or CD10/CD3 double positive cells (0.94%).
B) CD10 sorted cells were stained for CD24 and CD19 to detect transitional B cell contamination, represented as CD10/CD24 double positive cells. In most CD24 positive cells express CD19, identifying them as B cells.

3.2.3 Isolated GCB cells undergo apoptosis in culture but a proportion remains viable for up to 12 hours

I next investigated if the isolated CD10 positive cells undergo apoptosis in culture. I used both flow cytometry for the detection of viable cells (as described in section 3.2.1) and western blotting for the detection of PARP cleavage. Poly(ADP-ribose) polymerases (PARPs) have various functions, however PARP-1 has been shown to play a key role in the initiation of apoptosis through the release of the apoptosis-inducing factor (AIF) (Ame et al., 2004). PARP-1 cleavage is one of several consequences of apoptosis induction.

Figure 3.5 shows that CD10 positive cells underwent apoptosis in culture which increased with time. As seen previously, the two different flow cytometric estimates of cell viability do not identify the same number of viable cells; however, the decrease in viability observed was similar with both methods. I found that the addition of CD40 ligand (CD40L) partially rescued these cells from apoptosis. These data are consistent with previous reports showing that germinal centre B cells undergo apoptosis in culture, but are partially protected from cell death by CD40L (Hennino et al., 2001, Klein and Dalla-Favera, 2008, Liu et al., 1989).

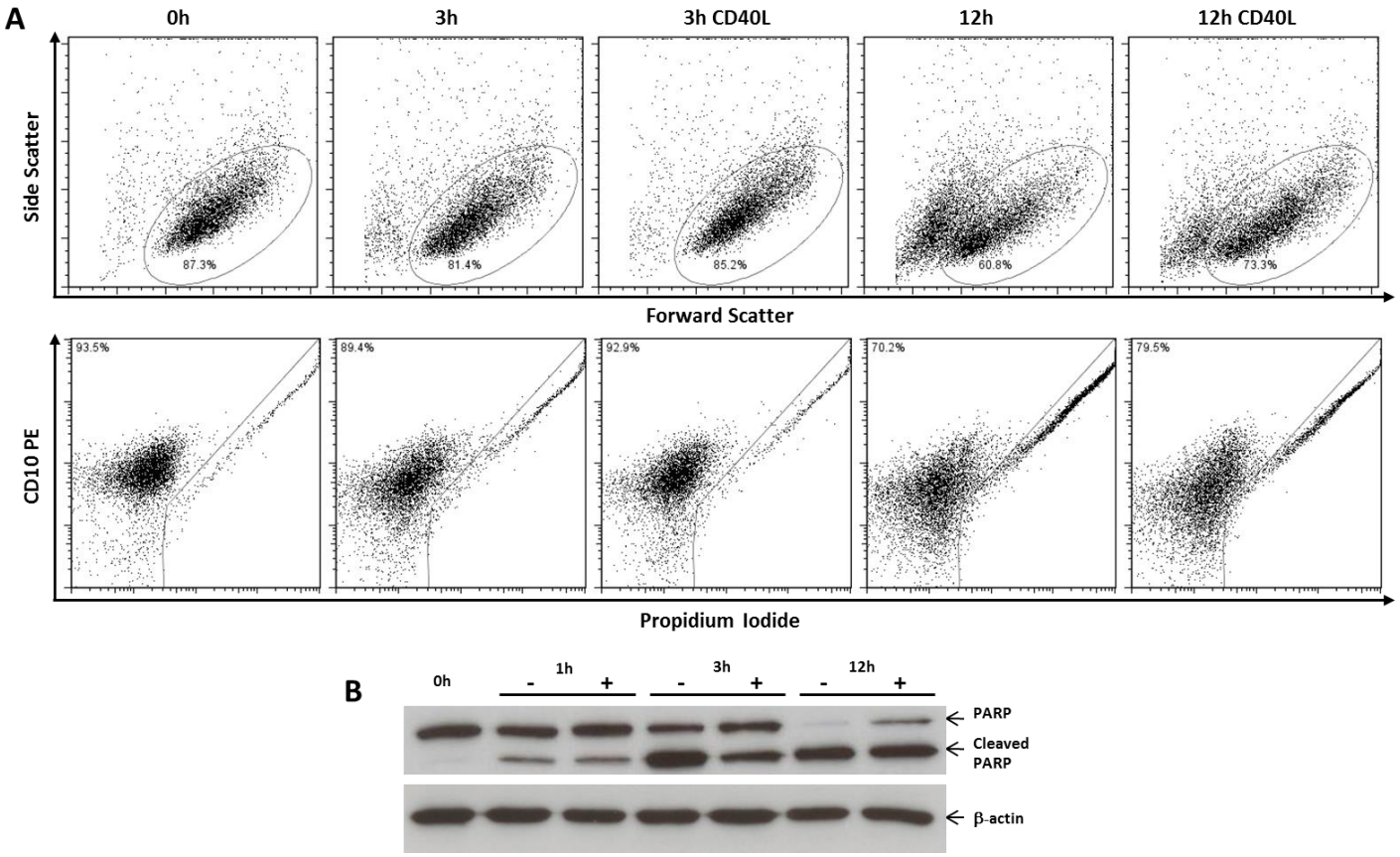

Figure 3.5: CD10 enriched cells display signs of apoptosis in culture

A) Cells were analysed by flow cytometry and Side Scatter: Forward Scatter analysis (top row) as well as inability to take up Propidium Iodide (bottom row) was used to identify viable cells as per Figure 3.1. Live cells are displayed inside the gates.

B) Cells were analysed by western blotting for PARP cleavage at 1, 3 and 12 hours in culture in the presence or absence of CD40L (- or + respectively). Cleaved PARP is represented on the blots at a lower molecular weight. β-actin was used as a loading control.

The data are representative of three experiments on three different donors.

3.2.4 Isolated CD10 positive cells do not retain a germinal centre phenotype in culture

I next wanted to determine if the isolated and viable $CD10^{+}$ cells retain their phenotype during short term culture. Figure 3.6a shows that while CD95 expression was retained, the intensity of CD10 and CD38 staining decreased over time in culture, with the loss of the high intensity ($CD38^{++}$) population seen at the time of extraction. The expression of CD27 decreased by 3 hours in culture, with no further change at the later time point. The addition of CD40L did not affect CD10, CD38 and CD27 expression, whereas the expression of CD95 increased with CD40L stimulation compared to normal culture conditions. Decreased BCL6 expression was first observed after 3 hours in culture and was drastically reduced by 12 hours (Figure 3.6b). The addition of CD40L partially rescued this effect; an effect that was only consistently observed after 12 hours.

I also observed some variation in the expression of centroblast and centrocyte markers during culture. I found that while CXCR4 expression increased over time in culture, CD77 expression decreased (Figure 3.7). Both CXCR4 and CD77 intensity increase in the presence of CD40L. The starting population of $CXCR4^{low}CD83^{high}$ and $CXCR4^{low}CD86^{high}$ centrocytes decrease by 3 hours in culture regardless of the presence of CD40L. However, there is an increase in CD83 and CD86 intensity over time in culture, and this intensity is further increased in the presence of CD40L. This is reflected in the increase of $CXCR4^{high}CD83^{high}$ and $CXCR4^{high}CD86^{high}$ cells.

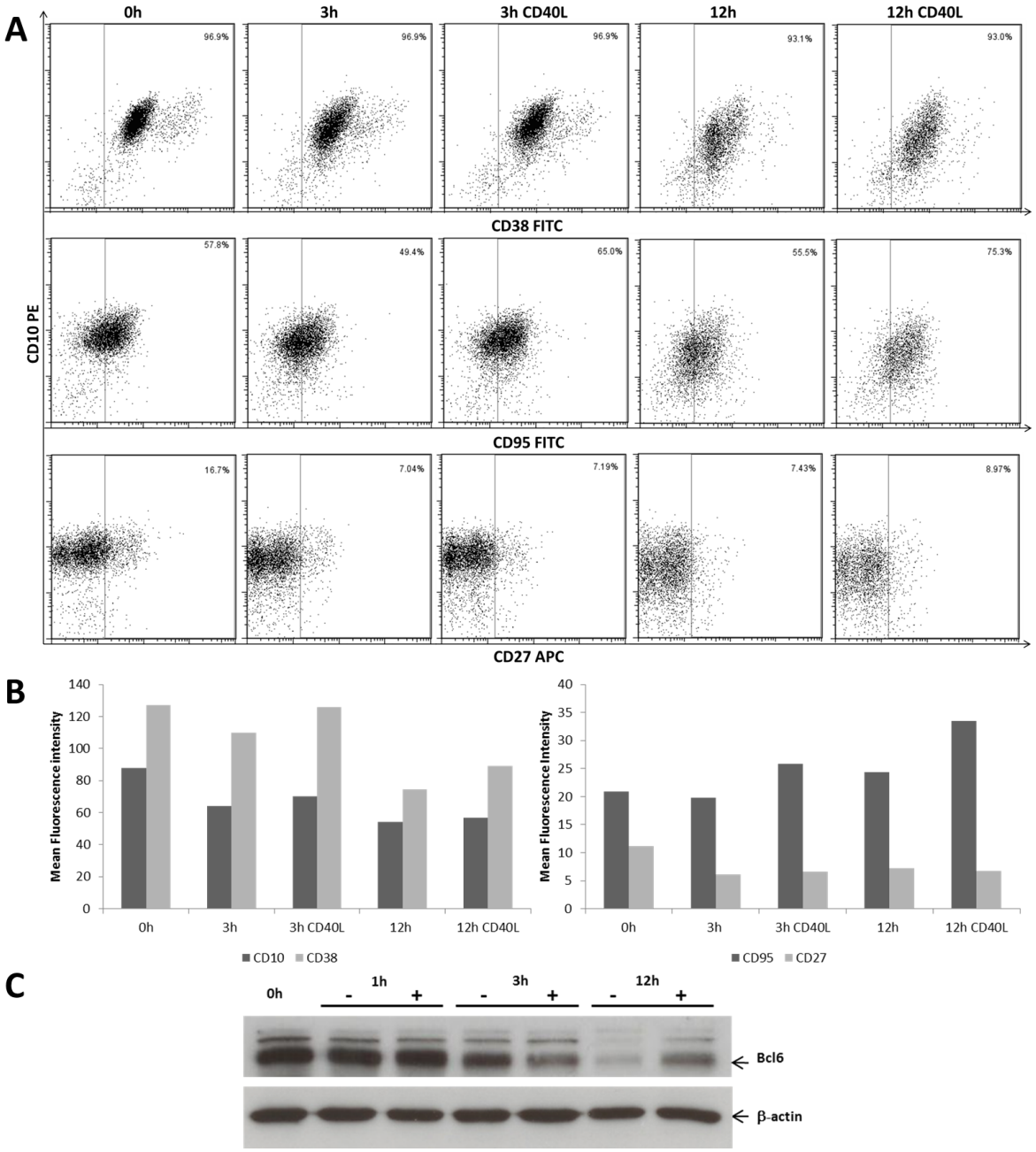

Figure 3.6: CD10 enriched cells do not retain their GC B cell phenotype in culture

A-B) Cells were analysed by flow cytometry for CD10, CD38, CD95 and CD27 expression at time of extraction and 3 and 12 hours in culture in the presence or absence of CD40L. Cells have been gated as per Figure 3.1 to identify viable cells and the population of the two gates were combined. The resulting population of viable cells were used for analysis. Cells were not gated for CD10 expression. The results are displayed as both dot plots **(A)** and Mean Fluorescence Intensity (MFI) **(B)**. There is a reduction in CD10 and CD38 intensity over time in culture. CD95 expression is retained over time; however there is an increase with CD40L stimulation. CD27 expression is reduced after 3h in culture, but is not further changed at 12h.

C) Cells were analysed by western blotting for BCL6 at 1, 3 and 12 hours in culture in the presence or absence of CD40L (- or + respectively). BCL6 expression is drastically reduced by 12 hours in culture. The presence of CD40L partially rescues this phenotype. β-actin was used as a loading control.

Data is representative of 3 replicates.

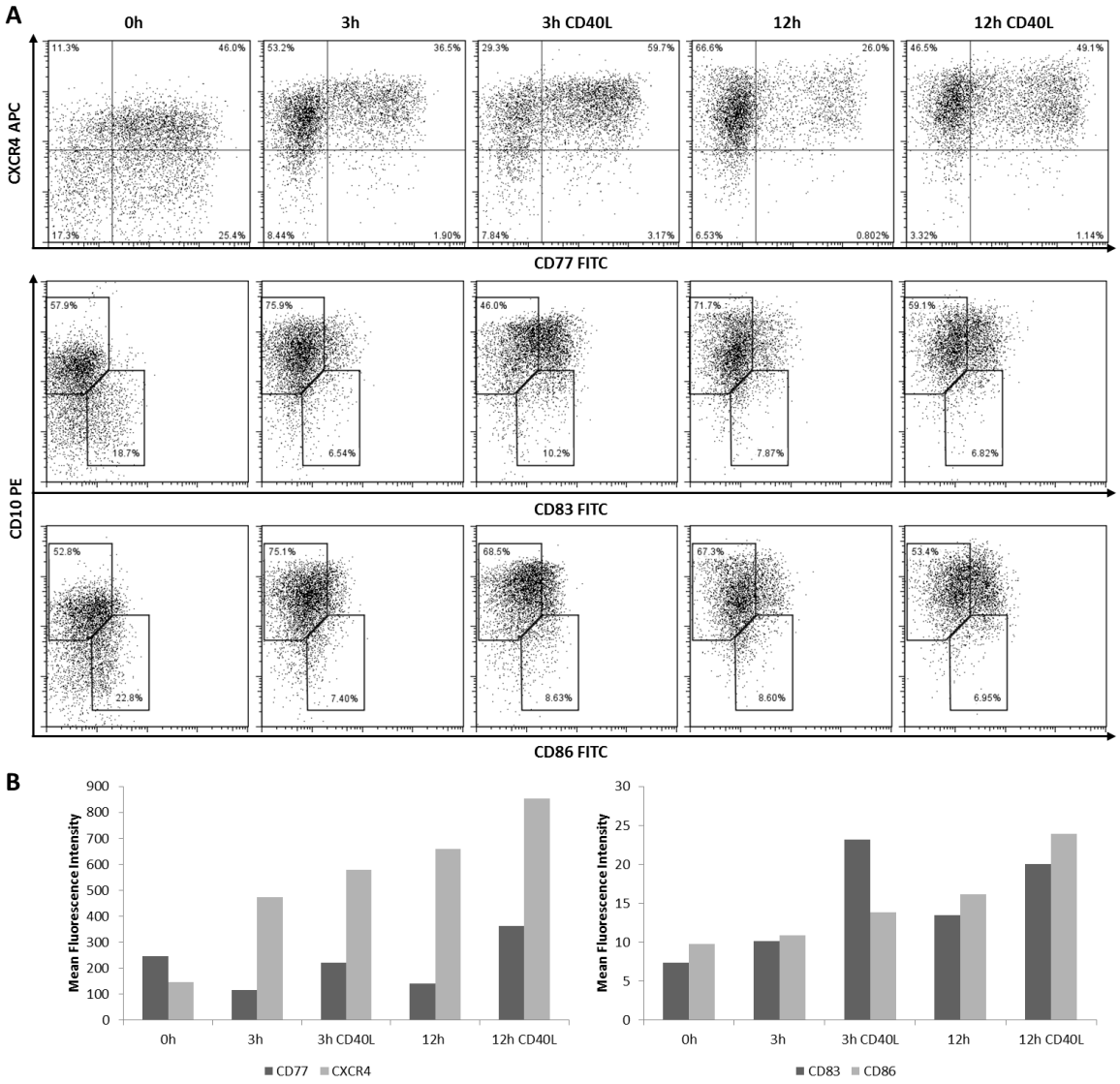

Figure 3.7: Effect of culture on the phenotype of isolated GC B cells

Cells were analysed by flow cytometry for CXCR4, CD77, CD83 and CD86 expression at the time of extraction and after 3 and 12 hours in culture in the presence or absence of CD40L. Cells have been gated as per Figure 3.1 to identify viable cells and the population of the two gates were combined. The resulting population of viable cells were used for analysis. Cells were not gated for CD10 expression. The results are displayed as both dot plots **(A)** and Mean Fluorescence Intensity (MFI) **(B)**.

There is an increase in CXCR4 intensity over time in culture, while CD77 intensity decreases. Both CXCR4 and CD77 intensity increase in the presence of CD40L. The starting population of $CXCR4^{low}CD83^{high}$ and $CXCR4^{low}CD86^{high}$ centrocytes decrease by 3 hours in culture regardless of the presence of CD40L. However, there is an increase in CD83 and CD86 intensity over time in culture, and this intensity is further increased in the presence of CD40L. This is reflected in the increase of $CXCR4^{high}CD83^{high}$ and $CXCR4^{high}CD86^{high}$ cells as seen in the dot plots.

3.3 Discussion

Studies of the pathogenesis of Hodgkin's lymphoma and of other related lymphoid malignancies have been difficult due to the lack of suitable models. When attempting to describe the pathogenic events responsible for the development of these tumours, we have used as models, cell lines. However, these models are unlikely to reveal the mechanisms responsible for the early stages of transformation, since this a process is already complete in cell lines. These cell lines are isolated from relapse patients with advanced disease and who received extensive chemotherapy. Once these cells lines are established in vitro, they are fully immortalised and no longer rely on their microenvironment for survival and growth. In the absence of suitable animal models, the manipulation of primary human GC B cells *in vitro* provides an alternative approach to study the early steps in B cell lymphomagenesis. For several years our group has employed the *in vitro* analysis of primary human GC B cells to this effect (Vockerodt et al., 2008, Vrzalikova et al., 2011, Leonard et al., 2011, Anderton et al., 2011).

Since the initial partial characterisation of isolated GC B cells by our group, several new important observations on the GC B cell phenotype have emerged. For example, although CD77 expression has been used to discriminate between centroblasts and centrocytes, recently it has been reported that $CD77^{+}$ and $CD77^{-}$ GC B cells have near identical transcription profiles and that CD77 alone does not discriminate between centroblasts and centrocytes (Hogerkorp and Borrebaeck, 2006, Klein et al., 2003). CXCR4 is highly expressed on the surface of human centroblasts and is now thought to be a better discriminator of centroblasts and centrocytes (Caron et al., 2009).

Furthermore, CD83 and CD86 have recently been identified on the surface of centrocytes and when used in conjunction with CXCR4 can more effectively distinguish centroblasts ($CXCR4^{high}CD83^{low}$ or $CXCR4^{high}CD86^{low}$) and centrocytes ($CXCR4^{low}CD83^{high}$ or $CXCR4^{low}CD86^{high}$) (Victora et al., 2012).

We have yet to show how the expression of these new GC markers varies during the isolation and culture of primary human tonsillar GC B cells. In this chapter, I set out to rectify this deficiency by extensively characterising the phenotype of isolated and cultured human GC B cells. I have shown that CD10 positive cells isolated from fresh paediatric tonsils are viable and express typical GC B cell markers including CD10, CD38, CD95 and BCL6. The majority of these cells have a centroblast phenotype ($CXCR4^{high}CD83^{low}$ or $CXCR4^{high}CD86^{low}$), while a minor population are centrocytes ($CXCR4^{low}CD83^{high}$ or $CXCR4^{low}CD86^{high}$). There is only a minor contamination of T cells (<1%) and $CD10^{+}CD24^{+}$ transitional B cells (0.57%) in the isolated population.

I also observed the expected induction of apoptosis in isolated GC B cells upon culture. Over 50% of these cells appear viable at 12 hours as measured by flow cytometry. However, while flow cytometric analysis can identify late apoptotic and necrotic cells (disrupted cell membranes allowing PI uptake, highly granular morphology and cell debris) it does not identify cells undergoing the initial stages of apoptosis. Western blot analysis revealed high levels of PARP cleavage in GC B cells as early as 3h in culture, with majority of PARP cleaved by 12h. This indicates that a large proportion of cells identified as viable by flow cytometry have initiated apoptosis. Performing annexin staining by

flow cytometry would give a more informative analysis of the proportion of apoptotic GC B cells.

Analysis for PARP cleavage revealed that the addition of soluble CD40L can partially rescue GC B cells from apoptosis. This is consistent with previous reports showing that germinal centre B cells are partially protected from cell death by CD40L in culture (Hennino et al., 2001, Klein and Dalla-Favera, 2008, Liu et al., 1989). This indicated that the soluble CD40L used is functional.

The use of the trimeric soluble CD40 ligand used in these experiments was originally optimised by Dr Martina Vockerodt in our group. Soluble CD40L was titrated with concentrations ranging from 1ng/µl to 2µg/µl and the re-gain of CD77 expression was used as a functional readout. Cells showed a dose-dependent re-expression of CD77. The concentration of 200ng/µl of CD40L was found to be saturating, resulting in the highest increase in CD77 expression. Additionally, up-regulation of ICAM1 following CD40L stimulation, as shown in the subsequent chapter, also indicates that soluble CD40L is functional.

I observed that the expression of the majority of typical GC B cell associated molecules do not remain stable over time in culture. The GC B cell markers CD10, CD38 and CD77 decreased in culture, while there is an increase in CXCR4, CD83 and CD86 expression in culture. This increase is reflected in the decrease of $CXCR4^{low}CD83^{high}$ or $CXCR4^{low}CD86^{high}$ centrocytes and in the increase of a population of cells displaying an 'intermediate' phenotype, expressing high levels of both CXCR4 and CD83/CD86 ($CXCR4^{high}CD83^{high}$ or $CXCR4^{high}CD86^{high}$) and thus cannot be classed as centroblasts or

centrocytes. These 'intermediate' cells could be GC B cells cycling between centroblastic and centrocytic states; however one would expect only low numbers of cells to cycle. Therefore a more likely explanation is that the cells are becoming activated.

The serum activation of GC B cells in culture is supported by the finding that there is a slight increase in cell size as measured by forward scatter and the increase in CD83 and CD86 expression, which is especially marked upon CD40L stimulation. Both CD83 and CD86 have been shown to be up-regulated following serum activation, a process which can also result in increased cell size. These observations, coupled together with the fact that the cells are cultured in the presence of serum, indicate that the cells are becoming activated. It is unlikely that cells are undergoing differentiation into plasma cells as there is no increase in $CD38^{high}$ and $CD27^{high}$ cells.

The expression of BCL6 shows a marked decrease following 12 hours in culture. However, whereas following 3h of CD40L stimulation leads to a decrease in BCL6 expression, at 12h CD40L stimulation appears to rescue BCL6 expression in GC B cells. This is unexpected as CD40 activation leads to the down-regulation of BCL6 expression. Most likely, the presence of BCL6 expression with CD40L stimulation is a result of the apoptosis protection mediated by CD40L. This would explain the loss of BCL6 expression in un-stimulated GC B cells, which would be highly apoptotic. One caveat is that β-actin (house keeping control) levels remain stable throughout the culture. However, β-actin is a highly stable molecule and is therefore likely to remain intact for longer during apoptosis.

Taking all the observations together, isolation and culture of CD10 positive tonsillar mononuclear cells for up to 3 hours can yield sufficient numbers of viable cells with a phenotype representative of GC B cells for experiments. However, a short coming of this model is that longer culture, of 12 hours, leads to marked cell death and serum activation of the cells, making the model less representative. This needs to be taken into account in the design of experiments based on the model.

Chapter 4

Comparison of the transcriptional programmes of LMP1 and CD40 in primary human GC B cells with a focus on the effects of the expression of lipid signalling genes

4 Comparison of the transcriptional programmes of LMP1 and CD40 in primary human GC B cells with a focus on the effects of the expression of lipid signalling genes

4.1 Introduction

Although LMP1 has been shown to be an oncogene that is expressed in germinal centre (GC)-derived lymphomas such as Hodgkin's lymphoma, it is also believed to be expressed in the GC B cells of the healthy, where together with LMP2 it is thought to drive antigen independent GC reactions (Thorley-Lawson and Gross, 2004). Indeed LMP1 is thought to promote the differentiation of EBV infected GC B cells by acting as a mimic of the CD40 receptor (Gires et al., 1997).

However, it is not entirely clear how LMP1 can exert its oncogenic effects while at the same time promoting a physiological CD40-like signal. Previous studies suggest that it is the constitutive nature of the LMP1 signal that is oncogenic (Homig-Holzel et al., 2008, Rastelli et al., 2008). In order to gain more insight into potential differences between LMP1 and CD40 that may explain LMP1's oncogenic effects I compared the global gene expression programme of these proteins in normal GC B cells.

4.2 Results

4.2.1 Validation of the overlapping transcriptional programme of CD40 and LMP1 in primary human GC B cells

The starting point for this study was three existing arrays:

1. An array that identified the transcriptional consequences of CD40L stimulation in GC B cells. This array consisted of nine biological replicates with matched un-stimulated controls, harvested 3h after stimulation with 200ng/ml CD40L. (Experiments were performed in our laboratory by Dr Schrader)
2. A previously published array which identified LMP1 mediated transcriptional effects in GC B cells (Vockerodt et al., 2008). This array consisted of three GC B cell replicates transfected either with LMP1 or with appropriate vector control.
3. Re-analysis of a previously published dataset which compared the transcriptional profile of HRS cells with that of normal centrocytes (Brune et al., 2008). This array consisted of twelve HRS cell samples and five centrocyte samples.

All three arrays were performed using the Affymetrix HG-U133 Plus2 platform and all the data sets were re-analysed using limma analysis with a fold change cut off of 1.5 and $p < 0.001$.

Stimulation of GC B cells with CD40L identified 194 up-regulated probe sets, representing 147 unique genes and 268 down-regulated probe sets, representing 233 unique genes. Transfection of GC B cells with LMP1 revealed 420 up-regulated probe sets, representing 327 unique genes and 628 down-regulated probe sets, representing 532 unique genes. Comparison of the two arrays showed that 60 genes were up-

regulated and 43 genes were down-regulated by both CD40 and LMP1 (Figure 4.1, appendix Table 7.1). This significant overlap between LMP1 and CD40 transcriptional profiles confirms the well described overlapping functions of these receptors (hypergeometric probability, $p<1.317e-111$).

It is worth noting that some genes may appear to be regulated in opposite direction when using alternative probe sets. There are various possibilities why this might be the case. The Affymetrix HG-U133 Plus2 array mostly contains probe sets measuring the 3' end of genes, but has redundant probe sets, which measure different regions of the same gene and thus may identify alternative splice forms. Not all probe sets identify unique genes, instead they may measure multiple genes, and thus it is not clear which transcript is differentially regulated. Additionally, with some probe sets the full extent of gene recognition is unknown, and thus they could potentially measure transcripts other than the one named. These three probe set variants are all marked in the probe label thus can be examined when looking at gene expression.

I repeated the LMP1 transfection and CD40 stimulation in GC B cells derived from different tonsils. LMP1 expression in these tonsils was confirmed by qPCR (Figure 4.2). I next went on to examine ICAM1 protein expression following LMP1 transfection and 12h CD40L stimulation of four GC B cell replicates. I chose the 12h time point to allow for ICAM1 protein expression following the increase in transcription observed at 3h. ICAM1 protein expression was significantly up-regulated by LMP1 transfection, and by CD40 stimulation (Figure 4.3a-b).

As ICAM1 is an NF-κB target gene, I decided to use an NF-κB reporter system, to show that LMP1 expression in GC B cells leads to a functional readout. For this I transfected isolated GC B cells with the appropriate vector and an NF-κB reporter plasmid which expresses GFP upon NF-κB activation. Cells were left in culture for 12h before analysis. There is a low level of NF-κB activation in the system (2.16%), as seen in the vector control; however LMP1 activated NF-κB in GC B cells (4.54%) (Figure 4.3c).

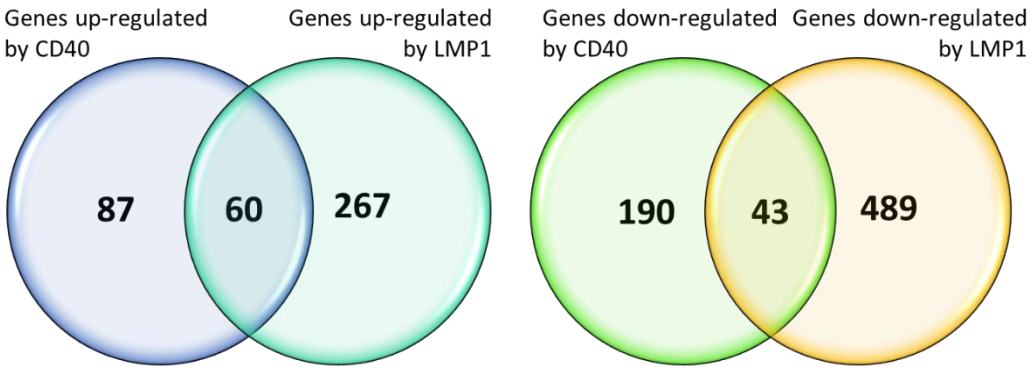

Figure 4.1: Summary of array comparison
Comparison of the transcriptional programmes of CD40 and LMP1 in GC B cells.
Venn diagrams showing numbers or genes up- or down-regulated by CD40 and LMP1 in GC B cells. Genes identified as differentially regulated in LMP1 and CD40 arrays with a fold change cut off of 1.5 and p<0.001

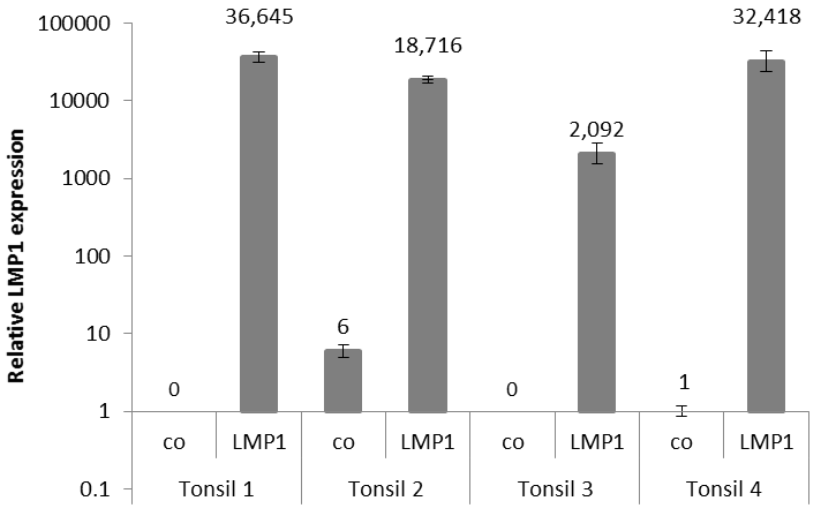

Figure 4.2: LMP1 is strongly expressed following transfection in all for GC B cell samples
LMP1 mRNA expression in transfected GC B cells relative to vector control transfected GC B cell from Tonsil 4. RNA isolated form transfected GC B cells was subjected to two rounds of amplification prior to RT-PCR analysis. LMP1 CT values were normalised to GAPDH expression, following which LMP1 expression was calculated as relative gene expression compared to vector control transfected Tonsil 4. Relative expression values were then plotted. Expression value of zero indicates that LMP1 transcript was not detected in the sample.

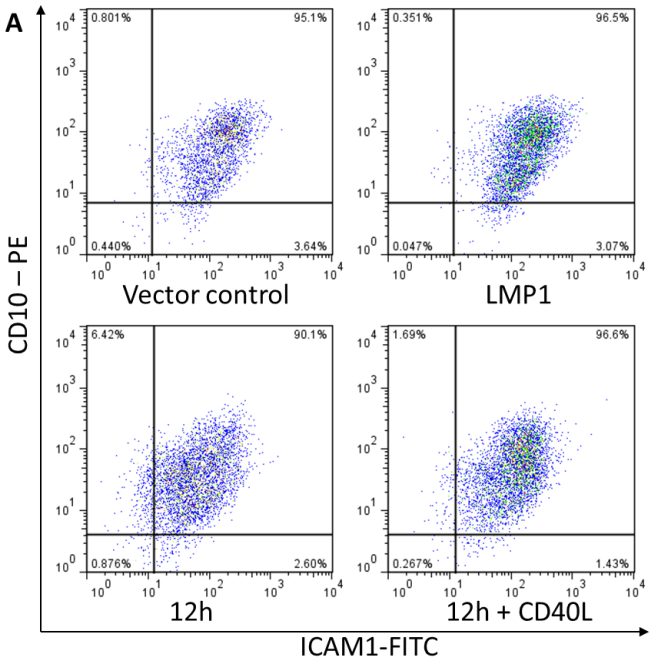

B

Tonsil	*LMP1 Transfection*		*CD40L Stimulation*	
	Control	LMP1	12h	12h + CD40L
T98	165	212	86.5	141
T103	173	246	71.3	139
T104	193	231	79.4	123
P value	**0.04**		**0.02**	

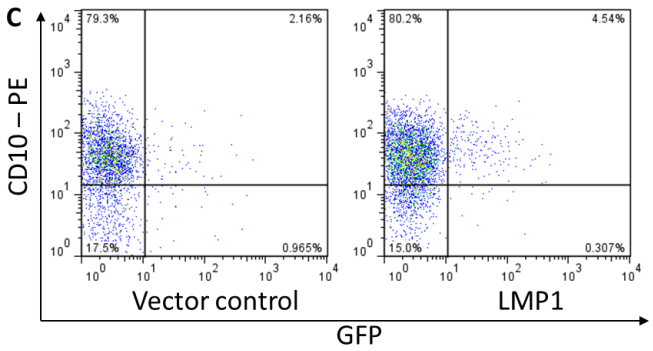

Figure 4.3: Up-regulation of ICAM1 and NF-κB following LMP1 transfection of GC B cells
For all flow cytometric analysis, live cells have been identified based on morphology and PI negativity and gated as per Figure 3.1. The population of the two gates were combined, with the resulting population of viable cells used for analysis. Cells were not gated for NGFR or CD10 expression therefore changes in ICAM1 and GFP expression are small.
a) ICAM1 up-regulation by LMP1 transfection as observed by flow cytometry, shown for T98. ICAM1 expression is shown on x-axis, CD10 expression (used to identify GC B cells) is shown on the y-axis. There is a high expression of ICAM1 in GC B cells. Expression levels shift higher following LMP1 transfection.
b) Mean fluorescence intensity of ICAM1 in GC B cells (isolated from four tonsils) following LMP1 transfection and CD40L stimulation.
c) GFP expression (x-axis) as a result of the successful activation of NF- κB following transfection.

4.2.2 Validation of LMP1 target genes not regulated by CD40 in primary human GC B cells and relevant to the pathogenesis of HL

Next, I wanted to identify LMP1 target genes that are potentially relevant to the pathogenesis of EBV positive Hodgkin's lymphoma. First, genes whose expression was altered by LMP1 but not by CD40L stimulation were identified. I found that LMP1 up-regulated 267 and down-regulated 489 genes that were not differentially expressed following CD40 stimulation (Figure 4.4, appendix Table 7.2). This set of LMP1 target genes were compared to those genes differentially expressed in HRS cells compared to centrocytes Figure 4.4. This yielded a list of 62 up-regulated and 145 down-regulated genes which were concordantly regulated by LMP1 and in HRS cells (appendix Table 7.3).

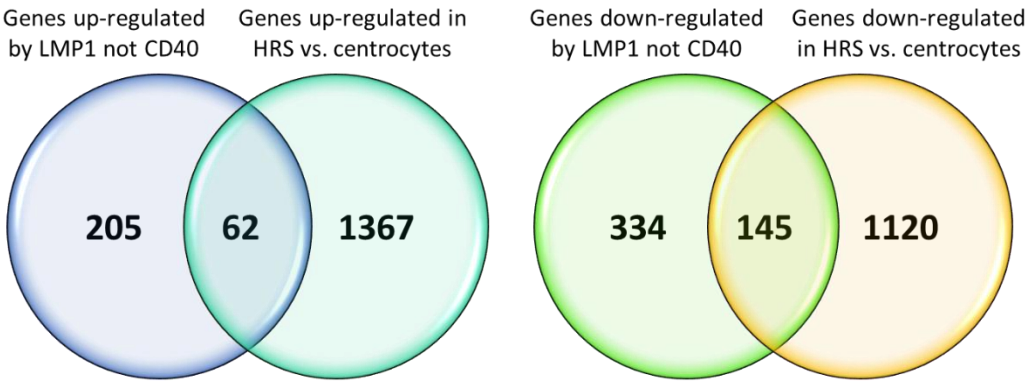

Figure 4.4: Summary of array comparisons showing genes concordantly regulated by LMP1 and in HL
Venn diagrams showing overlap between genes identified as regulated by LMP1 but not CD40, with those genes differentially expressed in HRS cells compared to centrocytes (fold change cut off of 1.5 and $p<0.001$).

Gene ontology analysis of the genes concordantly regulated by LMP1 and in HRS cells revealed that the majority of the genes transcriptionally altered belonged to five major biological groups: cellular process, metabolic process, cell communication, immune system process and developmental (Table 4.1). The cellular process category covers genes involved in cell growth and motility while the cell communication category covers components of cellular signalling pathways. Interestingly the immune system process category not only covers immune response genes, but also genes involved in macrophage activation. Differential regulation of these genes may be important for the recruitment of macrophages to the HL microenvironment.

Table 4.1: Gene ontology analysis of LMP1 and HRS cell target genes

Up-regulated by LMP1 and in HRS cells		*Down-regulated by LMP1 and in HRS cells*	
Biological Processes	**Number of genes**	**Biological Processes**	**Number of genes**
metabolic process	27	cellular process	67
cellular process	22	cell communication	48
immune system process	22	metabolic process	47
response to stimulus	15	developmental process	27
developmental process	15	immune system process	23
cell communication	14	system process	21
transport	8	transport	19
apoptosis	6	cell cycle	18
system process	6	response to stimulus	16
cell cycle	6	apoptosis	13
cellular component organization	5	cell adhesion	12
cell adhesion	5	cellular component organization	11
reproduction	2	reproduction	6
generation of precursor metabolites and energy	1	localization	2
		regulation of biological process	2

Twelve genes concordantly regulated by LMP1 (but not CD40) and in HRS cells were selected for qPCR analysis. I selected these genes on the basis that they were previously reported to be differentially expressed in HL or are known LMP1 target genes or that they had a potentially lymphomagenic function (Table 4.2).

Table 4.2: LMP1 target genes selected for validation

Gene	*Function*	*Direction of regulation*	*Known LMP1 target*	*Altered in HL*	*References*
ATM	DNA damage	Down	Yes	Yes	(Ma et al., 2011, Dutton et al., 2007, Bose et al., 2007)
TNFAIP3	TNFR signaling and apoptosis	Up	Yes	Yes	(Schmitz et al., 2009a, Dirmeier et al., 2005)
HSPA1A	Apoptosis	Up	Yes	Yes	(Vrzalikova et al., 2011, Vockerodt et al., 2008)
CCL5	Chemokine	Up	Yes	Yes	(Fischer et al., 2003, Buettner et al., 2007)
STAT5A	Transcription factor	Up		Yes	(Hinz et al., 2002)
ID2	Transcription factor	Up	Yes	Yes	(Vockerodt et al., 2008, Renne et al., 2006)
PTEN	Tumour suppressor	Down	Yes		(Chen et al., 2013)
RASSF6	Tumour suppressor	Down			
CD72	B cell associated	Down			
VPREB3	B cell associated	Down	Yes		(Vockerodt et al., 2008)
S1PR2	Germinal centre regulation	Down			
RGS13	Germinal centre regulation	Down			

I chose to include a set of genes that have been well described to be altered by LMP1 and in HRS cells, including ATM, TNFAIP3, HSPA1A, CCL5, STAT5A and ID2. I expected these genes to validate as LMP1 target genes, thus confirming that my GC B cell transfections with a LMP1-expression vector were successful. Furthermore, confirming that these genes are not regulated by CD40 stimulation, a physiological signal required for GC B cell survival, could imply that aberrant regulation of these genes by LMP1 plays a role in LMP1 mediated lymphomagenesis.

I was also interested in those B cell associated and tumour suppressor genes that were down-regulated by LMP1 and in HRS cells. Any such genes down-regulated by LMP1 but not CD40 could have a role in LMP1 mediated lymphomagenesis. In particular I was interested in the down-regulation of S1PR2 and RGS13, two molecules involved in the regulation of GC size and morphology.

For this analysis, I used the same samples shown in Figure 4.2 as well as three repeats of CD40L stimulation. Genes were defined as differentially expressed if they showed significant difference in 3 out of 4 LMP1 transfected GC B cells or 2 out of 3 CD40L stimulated GC B cells at either time point (1-tailed T-test, $p<0.05$). I failed to confirm the observed changes in PTEN (Figure 4.5a). I found a further 5 genes which were regulated by LMP1 and CD40; VPREB3, TNFAIP3, HSPA1A, STAT5a and ID2 (Figures 4.5b-f). Three genes, ATM, RASSF6 and RGS13 were regulated by CD40 alone (Figures 4.5g-i) and three genes, CCL5, CD72 and S1PR2 were regulated by LMP1 alone (Figures 4.5j-l).

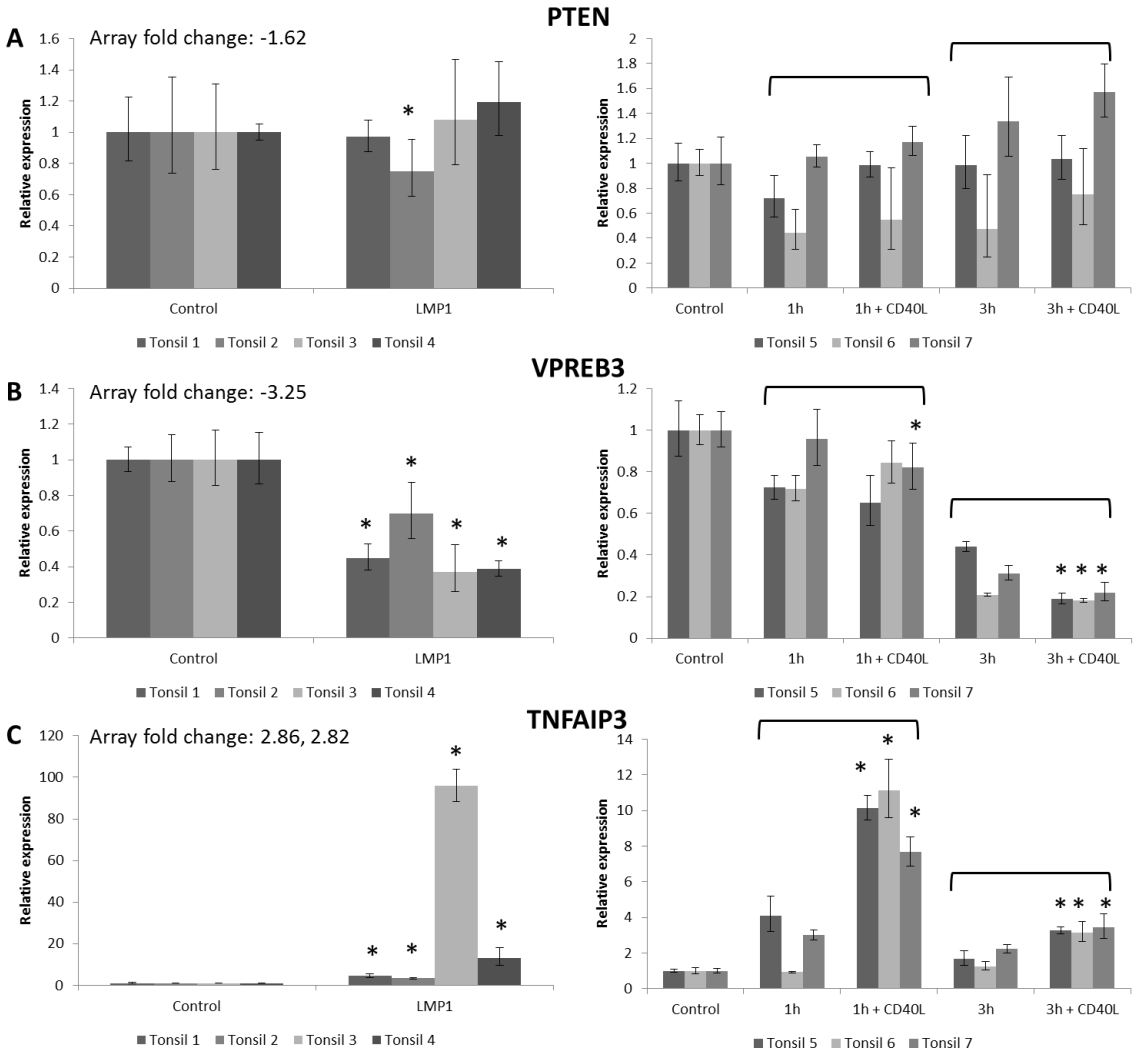

Figure 4.5: Validation of genes concurrently regulated by LMP1 and in HRS cells

Gene expression in LMP1 transfected GC B cells relative to vector control and in CD40L stimulated GC B cells, relative to 0h isolated control. RT-PCR analysed by ddCT method with resulting relative gene expression plotted on the y-axis. The LMP1 mediated fold change from the array analysis is indicated for each gene. Where multiple probe-sets were identified both fold change values are included.

For the comparison of vector control and LMP1 transfected GC B cells, the cells were cultured for 12h post transfection followed by sorting based on CD10 and NGFR positivity and PI negativity prior to RNA isolation. For the CD40L stimulated samples the brackets indicate the samples that were compared, namely non-stimulated versus CD40L stimulated GC B cells at 3h and at 12h time points.

***** Denotes gene significantly altered ($p<0.05$)

Denotes gene significantly altered, but opposite direction to array result ($p<0.05$).

The analysis shows that VPREB3, TNFAIP3, HSPA1A, STAT5a and ID2 were LMP1 and CD40 targets, ATM, RASSF6 and RGS13 were CD40 targets and CCL5, CD72 and S1PR2 were LMP1 targets.

Validation shown for PTEN, VPREB3 and TNFAIP3 **(A-C)**

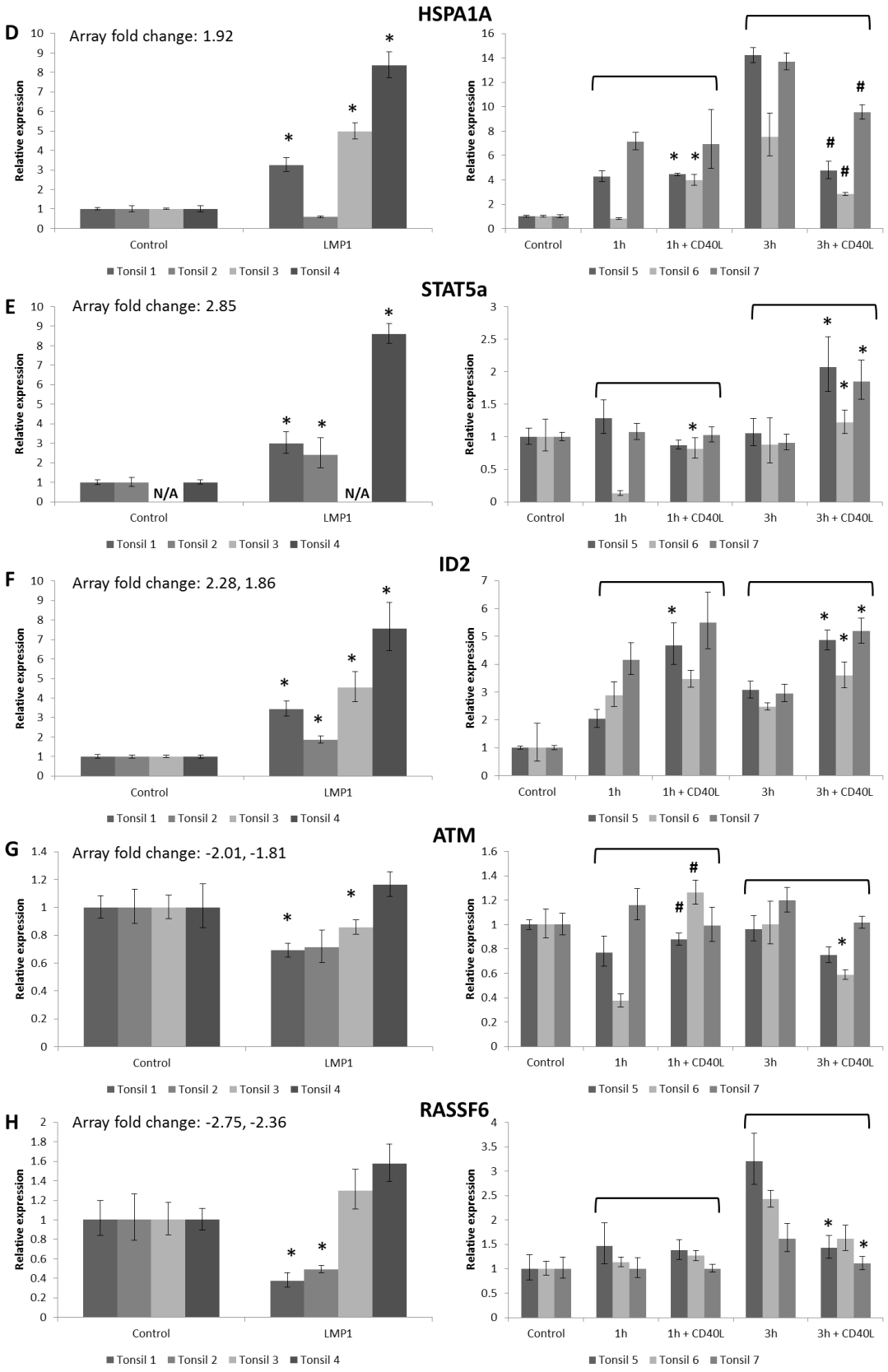

Validation shown for HSPA1A, STAT5a, ID2, ATM and RASSF6 **(D-H).** In STAT5A N/A, there was no STAT5 expression in vector control, but there was expression in the LMP1 transfected sample.

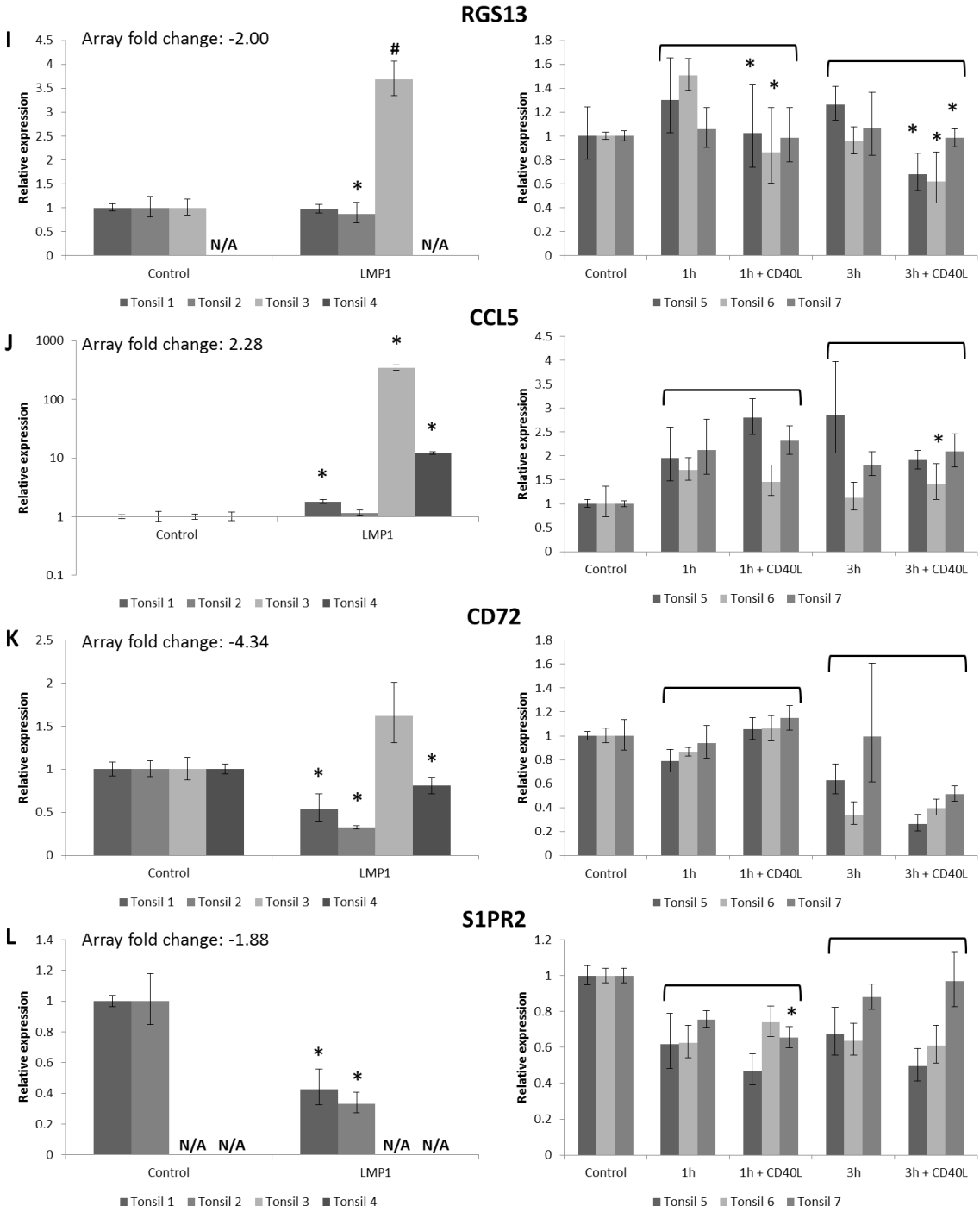

Validation shown for RGS13, CCL5, CD72 and S1PR2 **(I-L)**. In RGS13 N/A, sample was exhausted. In S1PR2 N/A, there was no S1PR2 expression in Tonsil 3, and sample was exhausted for Tonsil 4.

4.2.3 S1PR2 mRNA expression predicts survival in DLBCL and its over-expression reduces tumour cell migration in a HL cell line model

S1PR2 is a receptor for sphingosine 1 phosphate (S1P), a bioactive lipid signalling molecule that has been implicated in cancer (Pyne and Pyne, 2010). There are indications that S1PR2 functions as a tumour suppressor. S1PR2 has been shown to reduce the migration of melanoma cells in response to S1P (Arikawa et al., 2003), somatic mutations in S1PR2 have been found in around a quarter of DLBCL cases tested in a study and S1PR2 null mice have been shown to develop DLBCL with age (Cattoretti et al., 2009).

Having shown that S1PR2 transcription is down-regulated by LMP1 expression in GC B cells, I next wanted to look at S1PR2 expression in primary HL and DLCBL cases. I first optimised the S1PR2 antibody. I transfected DG75 cells, a Burkitt's lymphoma cell line, with vector control and an S1PR2 expression plasmid which contained a haemagglutinin (HA) tag. I failed to validate the antibody in western blot or flow cytometry. I validated the antibody for immunohistochemistry (IHC), showing specific S1PR2 staining in the transfected cells, similar to that seen when staining for the HA tag (Figure 4.6). The faint S1PR2 staining seen in vector control cells is localised to the membrane and most likely represents endogenous S1PR2 expression.

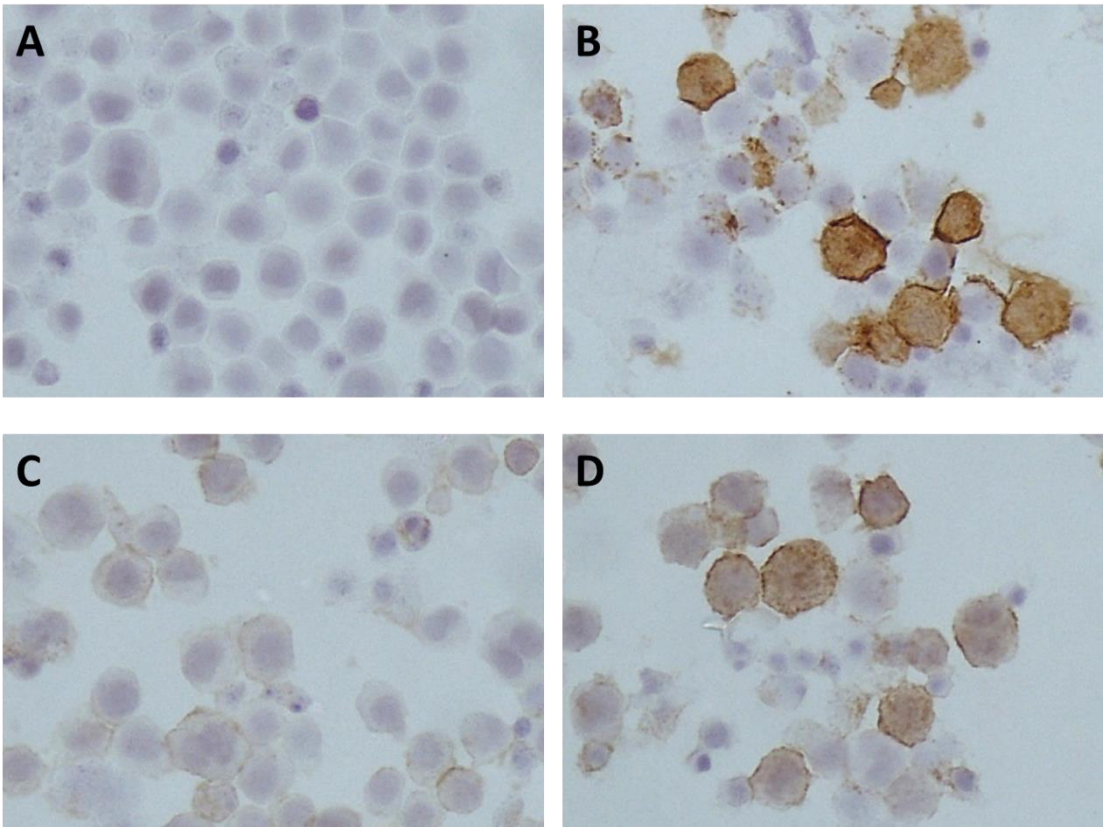

Figure 4.6: Validation of the S1PR2 antibody in IHC
DG75 cells were transfected with vector control or S1PR2-expression plasmid. Cells were stained for HA tag, showing no staining in vector control **(A)** and positive staining (in brown) in a proportion of S1PR2 transfected cells **(B)**. S1PR2 staining shows faint staining in vector control cells **(C)** and similar level of positive staining as HA, in S1PR2 transfected cells **(D)**.

I then used immunohistochemistry to look at S1PR2 expression in 155 HL and 169 DLBCL cases that were available to me. Staining for S1PR2 revealed that only 13/155 HL and 53/169 DLBCL cases had S1PR2 expression. Examples of S1PR2 and LMP1 staining in HL (Figure 4.7) and DLBCL (Figure 4.8) are shown. I then set out to examine LMP1 expression in these cases. I stained the HL cases for LMP1, while the DLBCL cases were subjected to EBER in situ hybridisation by Dr Gary Reynolds, Immunity and Infection, University of Birmingham. EBER positive cases were then stained for LMP1 expression. The results of the LMP1 and S1PR2 staining are summarised in Table 4.3 for the HL and Table 4.4 for the DLBCL cases. The correlation between LMP1 expression and S1PR2 status was significant in the DLCBL cases (Fisher's exact test, $p=0.0318$), but not the HL cases (Fisher's exact test, $p=0.0635$).

I also examined the correlation between S1PR2 protein expression in DLBCL and patient survival in a cohort of 300 patients of which S1PR2 expression was measured in 167 patients (53 positive and 114 negative cases). There was no significant correlation between S1PR2 expression and survival in these cases (Figure 4.9a-b). Furthermore, there was no significant difference between DLBCL subtype and survival in the cohort (Figure 4.9c-d).

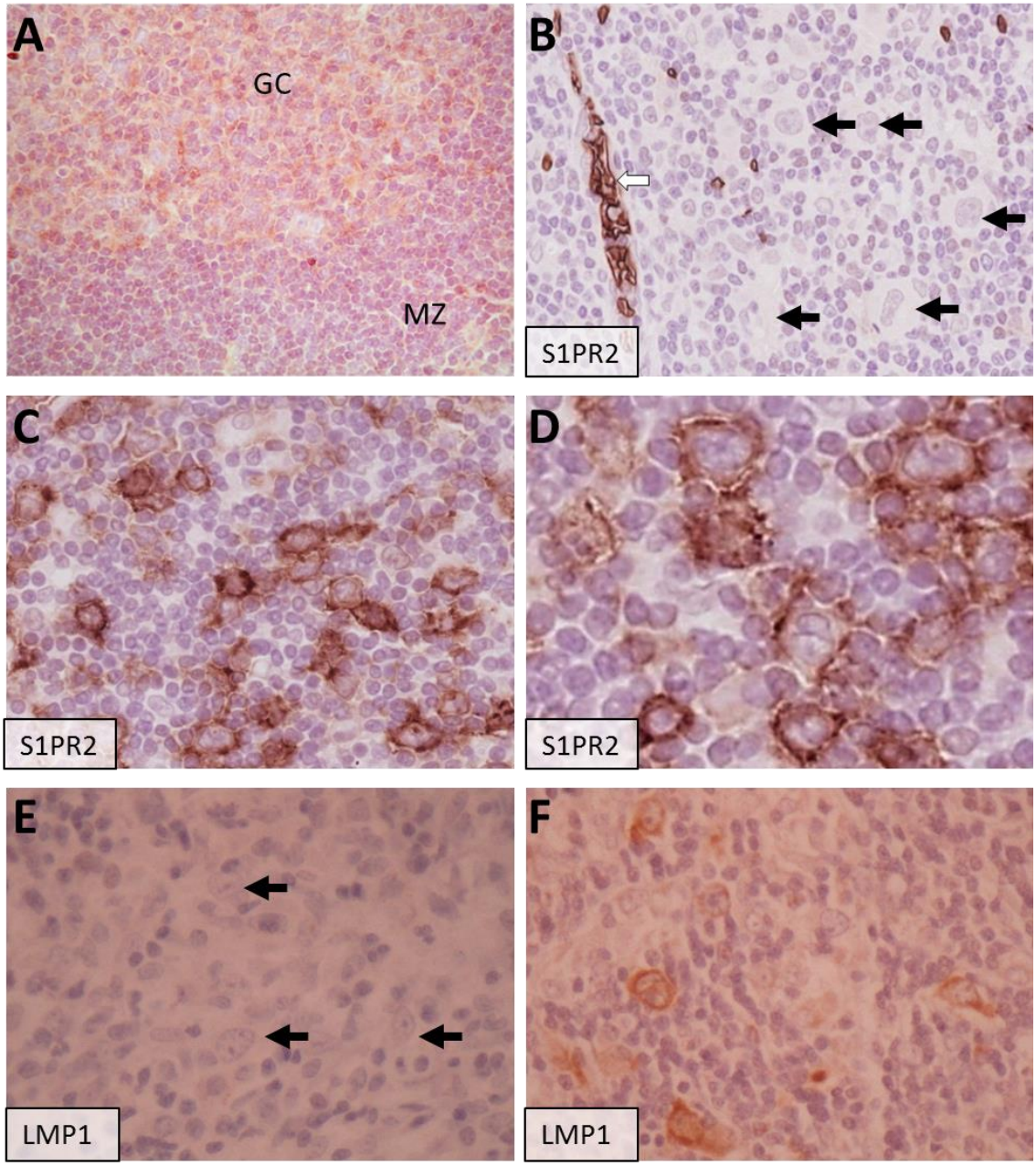

Figure 4.7: S1PR2 and LMP1 expression in HL
Immunohistochemistry staining of tonsil **(A)** and HL **(B-D)** tissue for S1PR2 expression, and HL tissue for LMP1 expression **(E-F).** Examples of both negative **(B, E)** and positive **(C-D, F)** staining shown. Black arrows indicate negative tumour cells **(B, E)** while positive tumour cells are stained in brown **(C-D, F)**. White arrows indicate the internal control (staining of erythrocytes in HL).
The GC of tonsil are positive for S1PR2, with the surrounding mantle zone (MZ) negative. Higher magnification of S1PR2 positive tumour cells shows membrane specific staining **(D)**.
LMP1 negative tumour cells are indicated by the black arrows **(E)** while positive tumour cells are stained in brown **(F)**.

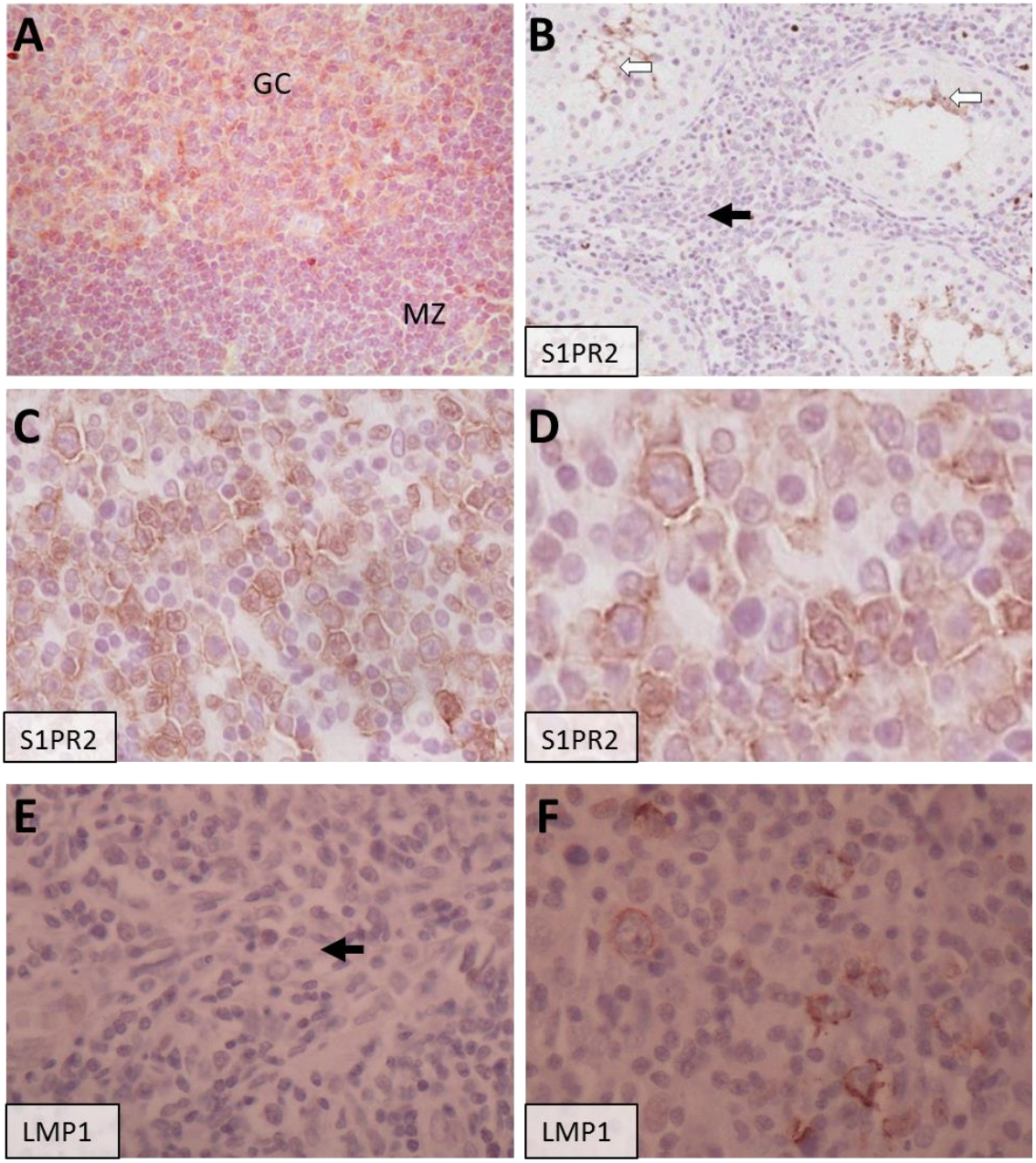

Figure 4.8: S1PR2 and LMP1 expression in DLBCL
Immunohistochemistry staining of tonsil **(A)** and DLBCL **(B-D)** tissue for S1PR2 expression, and DLBCL tissue for LMP1 expression **(E-F).** Examples of both negative **(B, E)** and positive **(C-D, F)** staining shown. Black arrows indicate negative tumour cells **(B, E)** while positive tumour cells are stained in brown **(C-D, F)**. White arrows indicate the internal control (staining of seminiferous tubules of the testis in DLBCL).
The GC of tonsil are positive for S1PR2, with the surrounding mantle zone (MZ) negative. Higher magnification of S1PR2 positive tumour cells shows membrane specific staining **(D)**.
LMP1 negative tumour cells are indicated by the black arrows **(E)** while positive tumour cells are stained in brown **(F)**.

Table 4.3: LMP1 and S1PR2 expression in 155 Hodgkin's lymphoma cases *

	S1PR2 +	*S1PR2 -*	***Total***
LMP1 +	8	46	**54**
LMP1 -	5	96	**101**
Total	**13**	**142**	**155**

* Cases were reviewed by two independent pathologists and scored as positive when over 10% of tumour cells displayed positive staining.

Table 4.4: LMP1 and S1PR2 expression in 169 Diffuse large B cell lymphoma cases *

	S1PR2 +	*S1PR2 -*	***Total***
LMP1 +	0	10	**10**
EBER -	53	106	**159**
Total	**53**	**116**	**169**

* Cases were reviewed by two independent pathologists and scored as positive when over 10% of tumour cells displayed positive staining.

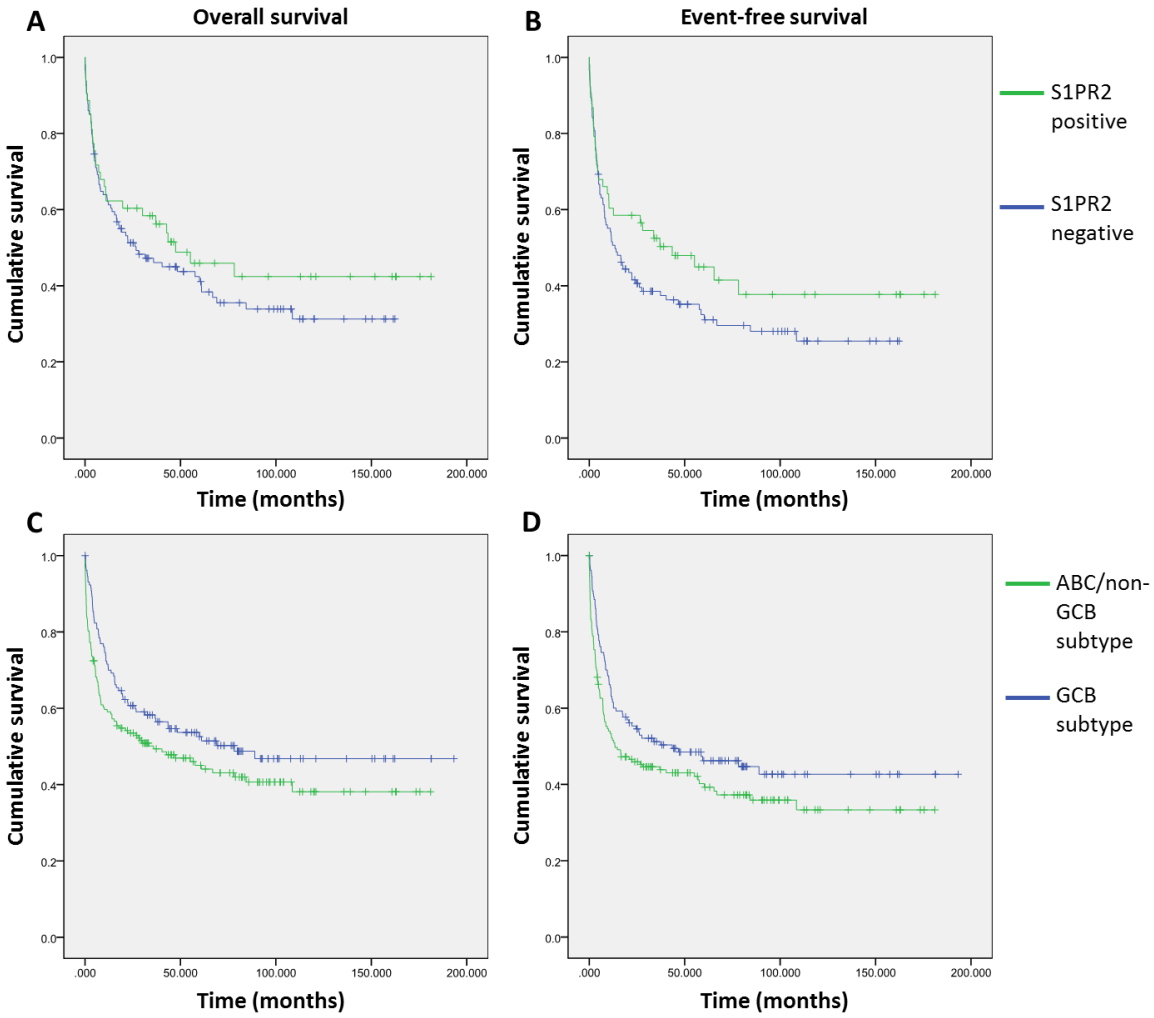

Figure 4.9: S1PR2 protein expression and DLBCL survival
Kaplan-Meier curve showing the correlation between survival and S1PR2 status or disease subtype. For event-free survival, an event is defined as relapse/progression or death without relapse/progression.
S1PR2 expression does not correlate with overall survival (p=0.328) **(A)** or event-free survival (p=0.156) **(B)**.
DLBCL subtype does not correlate with overall survival (p=0.073) **(C)** or event-free survival (p=0.056) **(D)**.

I also had access to a re-analysis of a published array of pre-treatment tumour gene expression profiles of 414 DLBCL patients (Lenz et al., 2008b) of which 181 patients received CHOP (cyclophosphamide, doxorubicin, vincristine and prednisolone) and 233 received R-CHOP (CHOP with addition of rituximab) therapy. Analysis revealed that low S1PR2 expression correlates with decreased survival in these patients in both treatment groups (Figure 4.10a-b). However, S1PR2 level was significantly higher in GCB DLBCL compared to ABC DLBCL in both treatment groups (Figure 4.10c), and GCB DLBCL has a significantly better survival then ABC DLBCL (Figure 4.10d-e). S1PR2 expression was not significantly correlated with survival in the ABC or GCB subtypes separated by the treatment groups (Figure 4.11).

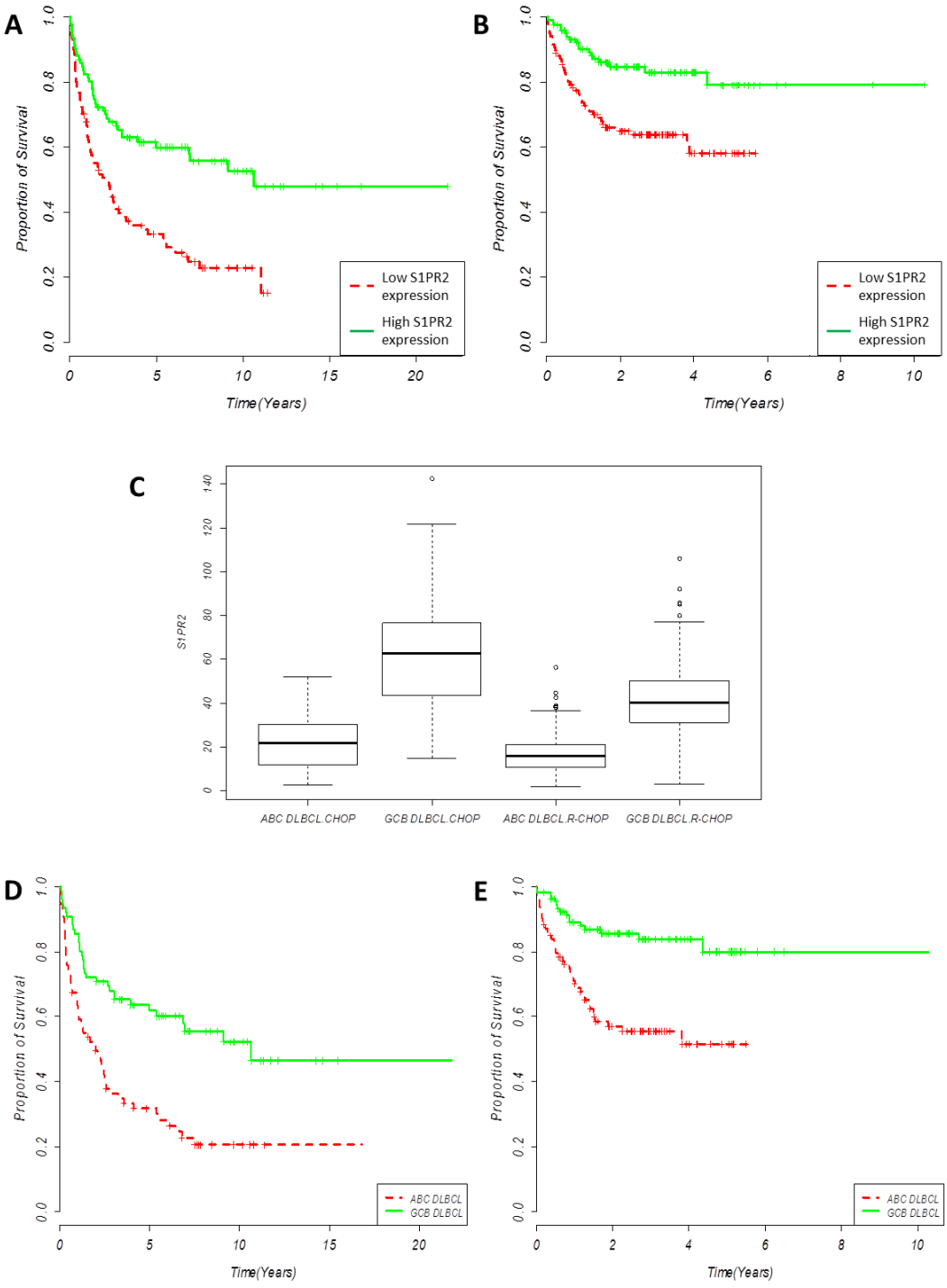

Figure 4.10: S1PR2 expression in pre-treatment tumour predicts survival
a-b) Survival analysis showing that low S1PR2 expression (red line) correlates with reduced survival in the cohort of patients receiving CHOP **(A)** and R-CHOP **(B)** therapy (p=0.0000355 and p=0.000414 respectively).
c) Boxplot showing S1PR2 expression is lower in the ABC compared to the GCB subtype of DLBCL for both the CHOP and R-CHOP treatment cohorts (Mann-Whitney p values: CHOP p=3.70e-20, R-CHOP p=3.48e-21)
d-e) Survival analysis showing that ABC DLBCL (red line) correlates with reduced survival in the cohort of patients receiving CHOP **(D)** and R-CHOP **(E)** therapy (p=0.0000345 and p=0.0000152 respectively).

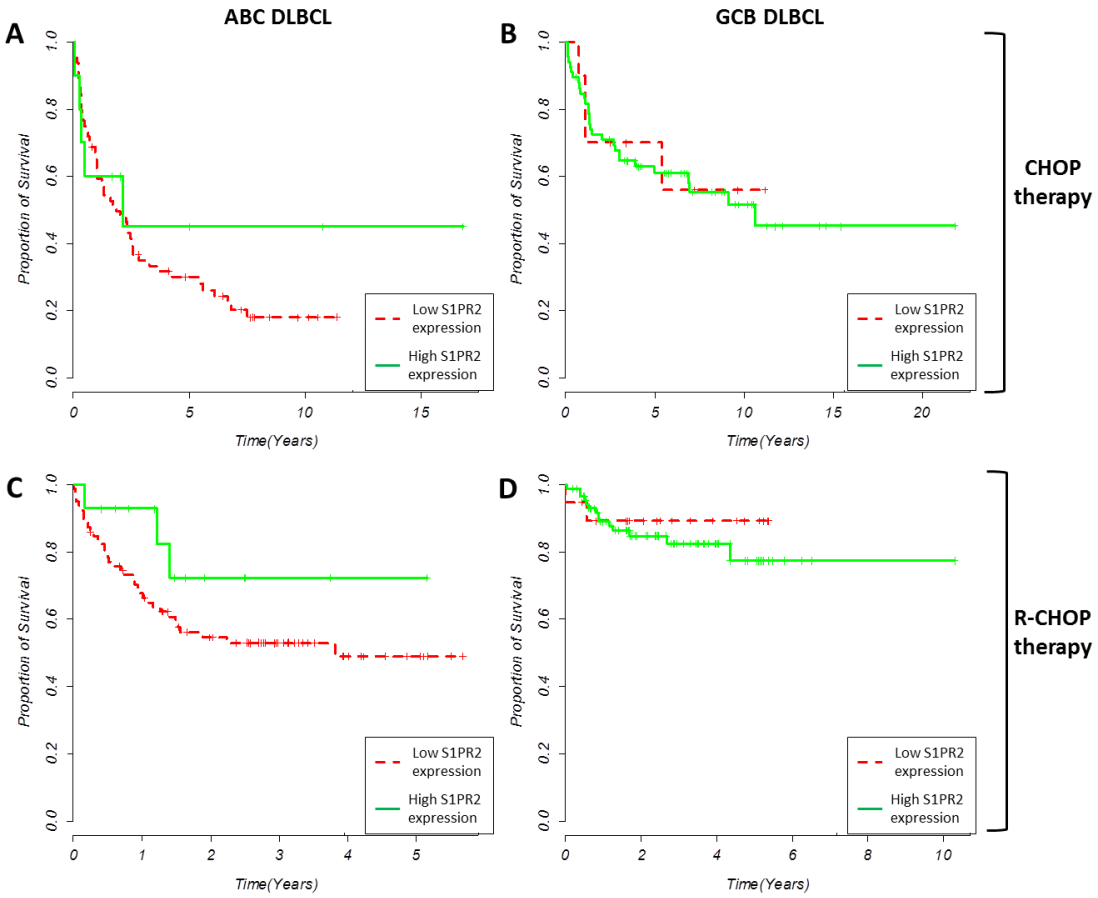

Figure 4.11: S1PR2 expression does not predict survival in ABC and GCB DLBCL stratified by treatment
Kaplan-Meier curve showing the correlation between survival and S1PR2 status in four cohorts defined based on disease subtype and therapy received. These are patients with: ABC subtype DLBCL receiving CHOP therapy **(A)** GCB subtype DLBCL receiving CHOP therapy **(B)** ABC subtype DLBCL receiving R-CHOP therapy **(C)** GCB subtype DLBCL receiving R-CHOP therapy **(D)**
The survival analysis showed no significant correlation between S1PR2 status and survival in the four patients cohorts (p=0.425 **(A)**, p=0.864 **(B)**, p=0.182 **(C)**, p=0.536 **(D)**).

Having found that S1PR2 is low in most primary HL and DLCBL cases, I next set out to investigate which HL and DLBCL cell lines re-capitulate this phenotype, as this will be an important factor. I found that compared to normal isolated GC B cells, S1PR2 expression varies among the cell lines, with most having a lower expression than GC B cells (Figures 4.12-4.13). Of the HL cell lines, L591 expresses the highest level of S1PR2 (Figure 4.12). This is unexpected as this cell line expresses high levels of LMP1. However, this cell line is highly heterogeneous for S1PR2 expression levels and it is possible that those cells with high S1PR2 expression do not express LMP1 or have low level of expression. In fact, when L591 cells are stained for LMP1 and S1PR2 expression by immunofluorescence the S1PR2 expressing cells appear to be either negative for LMP1 expression or have low LMP1 expression compared to cells expressing LMP1 alone, as shown in Figure 4.12b. However, this result is not conclusive. S1PR2 staining by immunofluorescence is weaker than staining by immunohistochemistry, thus cells with low S1PR2 expression may not be visible using this method.

Of the DLBCL cell lines U2932 and Ocily3 appear to have the lowest S1PR2 expression (Figure 4.13). These cell lines are classed as ABC subtype and thus are expected to have lower S1PR2 expression than GCB subtype cell lines. As with the HL cell lines, the EBV positive DLBCL cell line, Farage, has high expression of S1PR2.

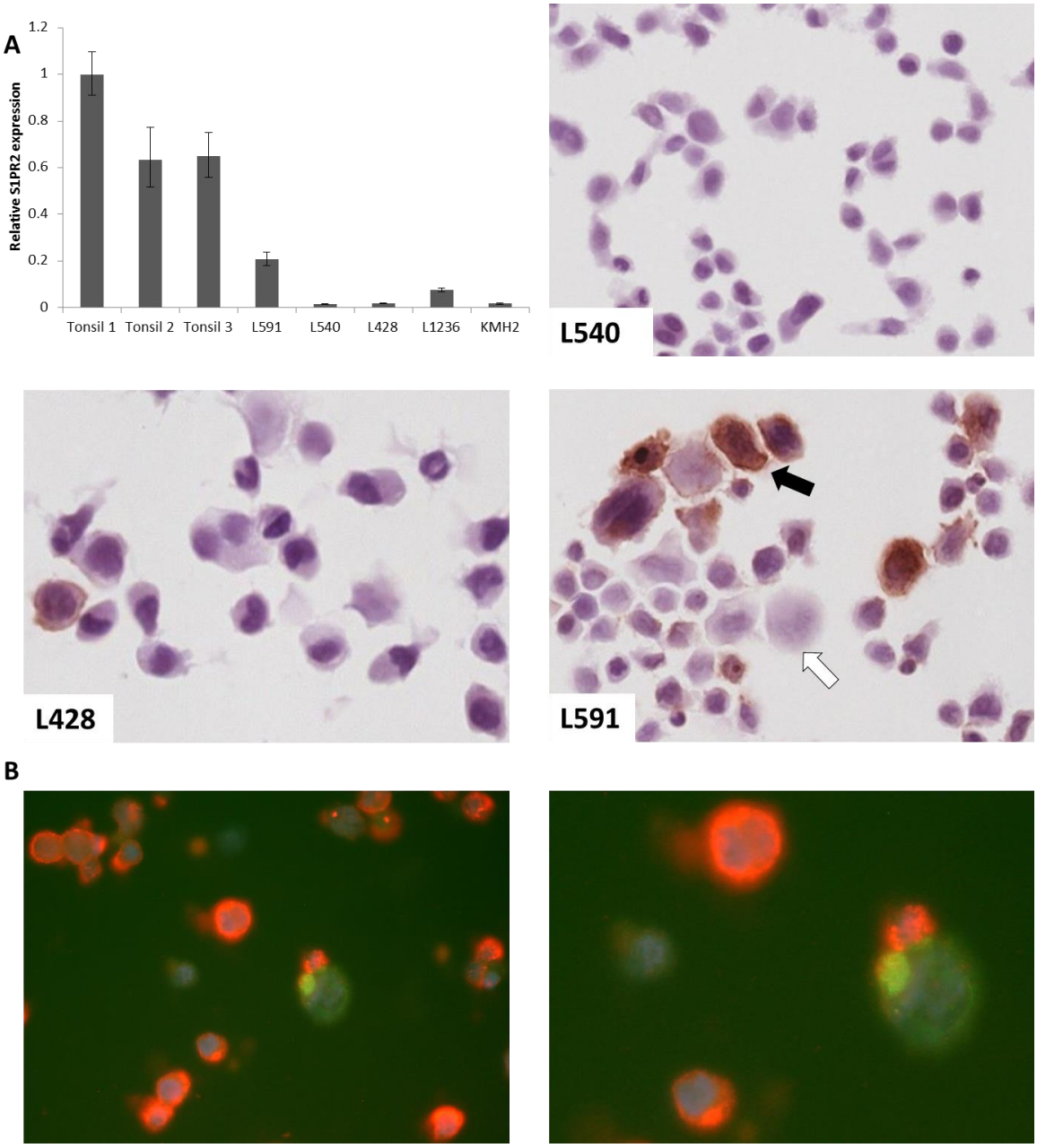

Figure 4.12: S1PR2 expression in HL cell lines

a) S1PR2 mRNA and protein expression HL cell lines. RT-PCR analysed by ddCT method with resulting gene expression relative to Tonsil 1 plotted on the y-axis. L591 is an EBV positive cell line, expressing high levels of LMP1. S1PR2 staining (brown) on two cell lines with low S1PR2 expression (L540 and L428) and one with higher expression (L591, black arrow indicated positive, white arrow negative staining). Cell nucleus is stained in blue. Pictures taken at 40x magnification.

b) S1PR2 (green) and LMP1 (red) expression in L591 cells as shown by immunofluorescence. Pictures taken at 40x (left) and 60x (right) magnification.

.

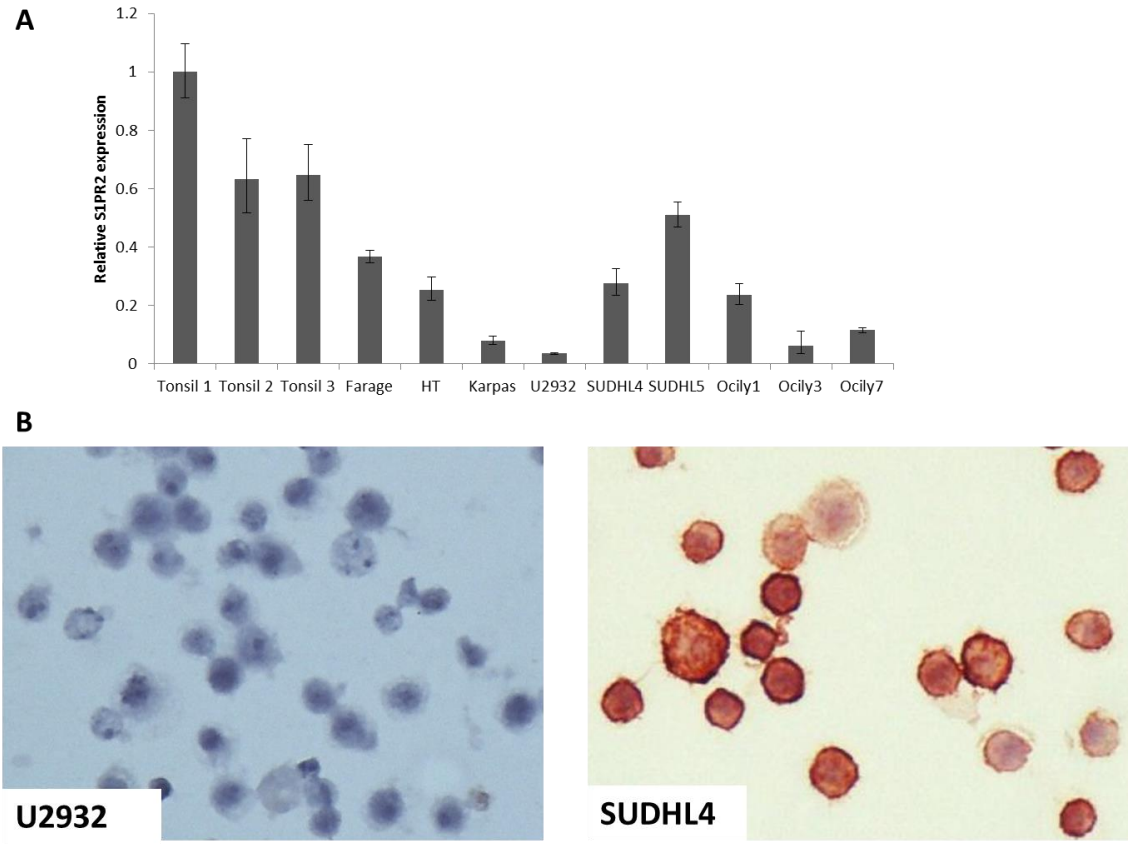

Figure 4.13: S1PR2 expression in DLBCL cell lines
S1PR2 mRNA and protein expression DLBCL cell lines (U2932 and OCILY3 are classed as ABC type, while the rest are GCB type).
a) RT-PCR analysed by ddCT method with resulting gene expression relative to Tonsil 1 plotted on the y-axis. Farage is an EBV positive cell line that expresses LMP1.
b) S1PR2 staining (brown) on one cell line with low S1PR2 expression (U2932) and one with higher expression (SUDHL4). Cell nucleus is stained in blue. Pictures taken at 40x magnification

Finally, I investigated if the over-expression of S1PR2 affected the migration of a HL cell line. I transfected L428 cells (which have low S1PR2 expression) with either vector control or an HA tagged S1PR2 expression plasmid. Before studying migration I first confirmed the expression of S1PR2 in S1PR2 transfected cells by qPCR (Figure 4.14a) and showed that in the five replicates transfection efficiency as observed by IHC for the HA tag was 18% (Figure 4.14b). The low transfection efficiency is consistent with previous observations from our lab that HA IHC underestimates transfection efficiency.

Cell migration was determined using a fluorescent dye (DiOC) which incorporates into the cell membrane. Cells were stained and resuspended in serum free media prior to the assay, placed into transwells and media with 10% FCS used as a stimulus. Migration was measured by fluorescence at 6h, 24h and 48h. I found that S1PR2 overexpression significantly reduced the migration of L428 cells in all replicates (Figure 4.14c). I also measured cell proliferation using a luminescence based assay and found that S1PR2 over-expression does not alter L428 cell proliferation (Figure 4.14d).

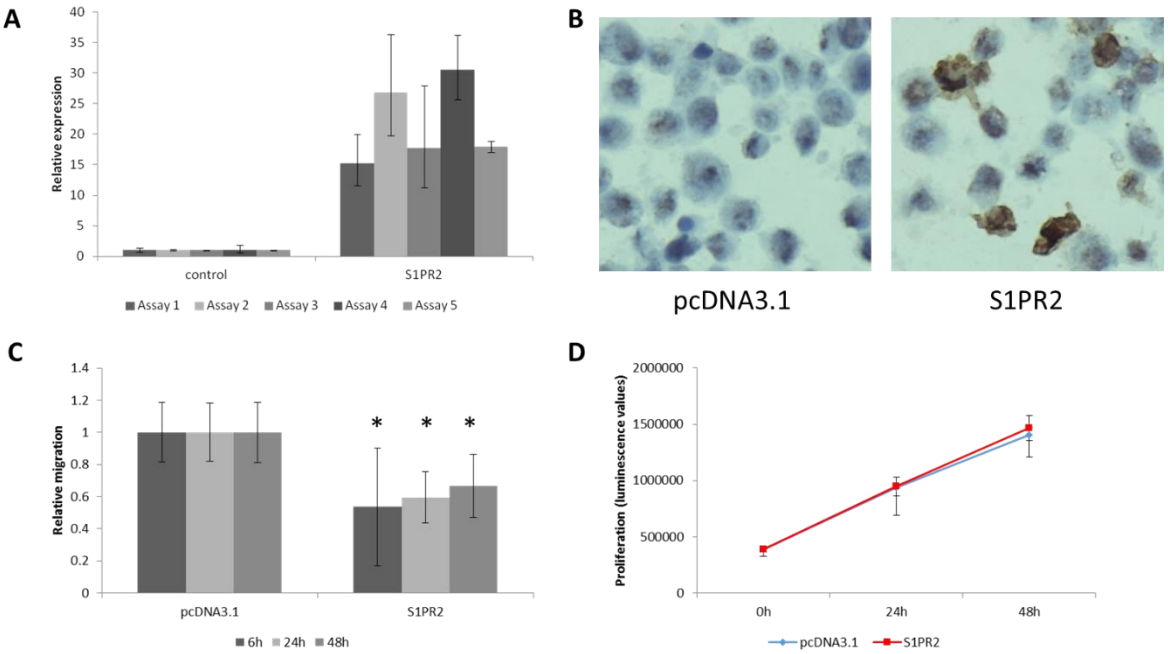

Figure 4.14: Over-expression of S1PR2 in L428 cells leads a reduction in migration

a) S1PR2 mRNA expression in S1PR2 transfected samples showing S1PR2 up-regulation in transfected samples. RT-PCR analysed by ddCT method with resulting relative gene expression to vector control (pcDNA3.1) plotted on the y-axis.

b) Immunohistochemistry for HA tag (brown) in transfected L428 cells, used to obtain transfection efficiency. Cell nucleus is dyed in blue. Pictures taken at 40x magnification. Overall 5 transfections with transfection efficiency ranging from 10-28% (mean 18%).

c) Migration assay on cells from transfections. Cells were dyed with DiOC dye, resuspended in serum free media and placed into the top of the transwell chambers. The bottom of each well contained media with 10% FCS. At the indicated time points fluorescence in the bottom well was measured. Presence of S1PR2 lead to a significant reduction in migration at all of the time points ($p<0.05$).

d) Proliferation assay on cells from transfections showing no significant difference in proliferation between vector control (pcDNA3.1) and S1PR2 transfected cells.

4.3 Discussion

Having established that the isolation and short-term culture of GC B cells can provide a representative *in vitro* model, I set out to address an important question in the lymphoma field, that of the difference between the apparently similar signalling molecules; LMP1, a viral oncogene, and its physiological homologue CD40. I showed that while there is considerable overlap between the transcriptional programmes of LMP1 and CD40 in GC B cells, there are a subset of genes which were regulated by LMP1, but not by CD40, in these cells and which were also concordantly differentially expressed when primary HRS cells were compared to normal centrocytes. These genes have the potential to be involved in the oncogenic functions of LMP1, at least in the context of Hodgkin's lymphoma.

It is important to note that the microarray analysis of HRS cell transcriptional profile has limitations. Namely, as I have shown in the previous chapter, the majority of isolated GC B cells are centroblasts, and thus they are more representative of the GC B cell population, the non-pathogenic counterpart of HRS cells. By contrast, the analysis used centrocytes as the representative GC B cell population. Furthermore, the original paper used CD77 status to differentiate between centrocytes and centroblasts. Although originally believed to be a specific marker of centroblasts, it has recently been reported that $CD77^+$ and $CD77^-$ GC B cells have near identical transcription profiles and that CD77 alone does not discriminate between centroblasts and centrocytes (Hogerkorp and Borrebaeck, 2006, Pascual et al., 1994, Klein et al., 2003). Thus a new analysis comparing HRS cell transcriptional profile to that of centroblasts and centrocytes combines is in

progress. This analysis will provide a more accurate description of pathogenic transcriptional changes in HRS cells.

I next repeated the LMP1 transfection and CD40 stimulation using GC B cells derived from different donors, following which I validated the samples. I used qPCR analysis to confirm LMP1 expression in the LMP1 transfected GC B cells. I chose this method as there are very low numbers of cells obtained following transfection and sorting of GC B cells, typically around 10^4 cells per treatment. As an alternative method, some of the sorted cells could be spotted onto microscope slides and analysed for LMP1 expression by immunohistochemistry, however, extremely low numbers of cells could be used for this.

I showed LMP1 expression in all four replicates. However, there are limitations to this experiment. First, there are no controls, and the use of RNA from an LMP1 positive and a negative cell line would have been informative. Using an LCL control would in particular be valuable as LCLs express high levels of LMP1 and thus can give an estimation of the level of LMP1 expression following transfection. However, due to the nature of the RNA sample used, doing these comparisons was not possible. As the level of RNA obtained from the sorted GC B cells is extremely low, the RNA was subjected to two rounds of RNA amplification. As this process was not done with cell line RNA, direct comparison by qPCR is not informative. The amplification process itself is a limitation, as it cannot rule out the possibility of DNA amplification from the plasmid itself.

I next showed ICAM1 up-regulation following both LMP1 transfection and CD40L stimulation of GC B cells. Although statistically significant, the changes in ICAM1

expression were marginal. This is a consequence of the flow cytometric analysis in which the total cell population was used for measuring ICAM1 expression. Sorting the GC B cells based on NGFR expression prior to analysis to select for transfected cells would result in a clearer measurement of ICAM1 expression following LMP1 transfection.

I next selected 12 LMP1 but not CD40 target genes that were also concordantly regulated in HRS cells for validation. The majority of the selected genes (8 in total) were identified as CD40 targets using qPCR analysis. This can be in part explained by qPCR analysis being more sensitive than microarray. While the LMP1 and HRS cells microarray analysis showed robust fold changes in gene expression, the CD40 microarray analysis showed only small fold changes in transcription, rarely reaching 2 fold, and thus using the threshold of 1.5 fold change may exclude many CD40 target genes. Also, the probes for the qPCR validation were specifically selected for best overall coverage of each gene. Another explanation is that in the validation a shorter time point of 1h stimulation was also looked at. This allows for the identification of even shorter-term transcriptional changes induced by CD40L stimulation, then the 3h time point used for the array.

I confirmed using qPCR, that three of these genes, CCL5, CD72 and S1PR2, were regulated by LMP1 but not CD40 in GC B cells. CCL5 is a known LMP1 target gene and its expression is believed to contribute to the microenvironment of HRS cells (Fischer et al., 2003). CD72 is a B cell receptor (BCR) co-receptor that down-regulates BCR signalling (Li et al., 2006). S1PR2 is a receptor for sphingosine 1 phosphate (S1P), a bioactive lipid signalling molecule that has been implicated in cancer (Pyne and Pyne, 2010). Given its

emerging role in normal GC B cell physiology and lymphoma development I decided to focus on S1PR2.

S1PR2 is a G protein coupled receptor that signals mainly through $G_{12/13}$, and can regulate GC B cell survival and migration in response to sphingosine 1 phosphate (S1P) (Green and Cyster, 2012). In mice, S1PR2-null GC B cells display unlimited growth following chronic antigen stimulation *in vivo* resulting in enlarged and less well defined GCs (Green et al., 2011). Furthermore, S1PR2 deficiency in mice leads to the development of DLBCL, while in humans over one-quarter of patients with DLBCL have multiple somatic mutations in the 5' sequences of the S1PR2 gene (Cattoretti et al., 2009). These observations suggest that LMP1 down-regulation of S1PR2 in GC B cells might promote lymphomagenesis by permitting the unlimited growth of these cells.

In further support of the notion that LMP1 could disrupt normal GC development and promote lymphoma development, it has previously been shown that LMP1 expression in the B cells of transgenic mice leads to a block in GC development (Uchida et al., 1999). Immunisation of these transgenic mice with an antigen led to the secretion of high-affinity IgG that could be detected in the serum and the follicular structures in the spleen were intact. This could imply that the block in GC formation observed in LMP1 expressing transgenic mice could in part be due to LMP1 mediated down-regulation of S1PR2 leading to the disruption of GC architecture.

I have made several observations which suggest that the loss of S1PR2 expression might contribute to lymphomagenesis. First, I showed that S1PR2 expression was absent in the tumour cells of the majority of cases of Hodgkin's lymphoma and diffuse large B cell

lymphoma. Second, a re-analysis of a published microarray data set revealed that lower levels of S1PR2 mRNA expression were associated with adverse outcome in DLBCL; an observation that could be explained by the significantly lower expression of S1PR2 in the ABC subtype of DLCBL, the subtype associated with poorer outcome. In this context it is also important to note that EBV is associated with ABC-, but not GC-type, DLBCL (Oyama et al., 2007, Montes-Moreno et al., 2012).

As I have shown that LMP1 leads to down-regulation of S1PR2 transcription in GC B cells, I was interested in examining if LMP1 is likely to mediate the loss of S1PR2 in primary HL and DLBCL cases. Using the immunohistochemistry data (summarised in Tables 4.2 and 4.3), I performed statistical analysis and showed that LMP1 positive cases of DLBCL but not HL were significantly more likely to lack S1PR2 expression then their LMP1 negative counterparts. However, there are limitations to this analysis. Although I showed that the majority of LMP1 positive cases of HL and DLBCL are negative for S1PR2 expression, the staining was performed on separate sections, and thus it cannot be ruled out that a proportion of LMP1 expressing cells do in fact also express S1PR2.

Ideally double-staining for LMP1 and S1PR2 expression on the same section would give a more accurate description of S1PR2 expression on the LMP1 positive tumour cells. Double staining by immunohistochemistry is challenging but possible when the proteins of interest are expressed in separate compartments of the cell. In this process the section would be stained first for one protein, then for the other, using different detection substrates that result in the formation of different coloured products. However, when both antigens of interest are expressed in the same location, such as

LMP1 and S1PR2 which are both membrane proteins, using double staining would not allow for differentiation between the two detection colours. Double-immunofluorescence is a useful technique in visualising multiple proteins in cells. I am currently in the process of optimising this technique for the detection of LMP1 and S1PR2 on tissue sections.

There is a further limitation to the analysis of LMP1 and S1PR2 expression in HL and DLBCL cases, namely that there are several LMP1 negative cases that also lack S1PR2 expression. In these cases it is clearly not LMP1 that drives the loss of S1PR2 expression. As mentioned previously, over one-quarter of patients with DLBCL have multiple somatic mutations in the 5' sequences of the S1PR2 gene, thus it is highly likely that other factors are involved in the down-regulation of S1PR2 expression in the EBV negative cases of HL and DLBCL. This indicates that while LMP1 may play a role in the loss of S1PR2 in EBV positive disease, it is not the only contributing factor in this loss and other processes, such as mutations, may also contribute to S1PR2 loss in HL and DLBCL.

In this chapter I have shown that there is a loss of S1PR2 expression in primary HL and DLBCL cases, and that in DLBCL the loss of S1PR2 at the RNA level can predict for worse disease outcome. The link between the loss of S1PR2 expression and adverse outcome in DLBCL can be explained in different ways. First, as the S1PR2 negative GC B cells in mice display increased growth, it is probable that loss of S1PR2 can contribute to the expansion of tumour cells in DLBCL. Furthermore, uncontrolled cell growth can increase the likelihood of cells acquiring and surviving secondary oncogenic hits. However, I observed no change in cell proliferation following S1PR2 over-expression in an HL cell

line. Second, loss of S1PR2 expression could result in increased tumour angiogenesis. The loss of S1PR2 has been shown to contribute to solid tumour growth and angiogenesis in mice (Du et al., 2010) while several studies have reported adverse outcomes for HL and DLBCL patients displaying increased tumour micro-vessel density (Korkolopoulou et al., 2005, Cardesa-Salzmann et al., 2011, Ribatti et al., 2013). Third, the loss of S1PR2 can increase cell survival. Mice with S1PR2 deficient GC B cells showed reduced apoptosis as compared to their wild type counterparts (Green et al., 2011). Finally, the loss of S1PR2 expression could contribute to the spread of lymphoma. S1PR2 has been shown to reduce the migration of glioblastoma and melanoma cells in response to S1P (Arikawa et al., 2003, Lepley et al., 2005). In support of this latter possibility I showed that S1PR2 over-expression in an HL cell line inhibited migration toward serum. As serum is known to contain S1P, it is likely that the inhibition of cell migration was in response to S1P.

Chapter 5

Optimisation of the PathDetect system for detection of LMP1 and CD40 induced signalling pathways in GC B cells

5 Optimisation of the PathDetect system for detection of LMP1 and CD40 induced signalling pathways in GC B cells

5.1 Introduction

In the previous chapter, I showed that while there was a considerable overlap between the transcriptional programmes of LMP1 and CD40 in GC B cells, a large group of genes were differentially regulated only by LMP1. However, I wanted to also examine the differences in signalling pathway activation between LMP1 and CD40 in GC B cells. Quantification of signalling pathway activation can be difficult in this cell system due to the very low numbers of cells available for analysis. Thus, in this chapter I set out to establish a method that allows for the detection of signalling pathway activation by LMP1 and CD40 in GC B cells with high sensitivity.

The PathDetect trans-reporting system works through the transfection of the gene of interest, a trans-activator (such as ATF2) and a reporter gene into cells, whereby phosphorylation of the trans-activator can be measured by luciferase activity (Figure 5.1). The reporter plasmid has been modified by Dr Vockerodt to express GFP upon activation. This allows direct detection of positive cells by flow cytometry allowing for the measurement of transcription factor activation in low numbers of cells. This is crucial when looking at GC B cells, where only low numbers of cells are available.

There are six PathDetect trans-reporting systems available. Of these, I chose to analyse the C/EBP homologous protein (CHOP) and activating transcription factor 2 (ATF2)

PathDetect systems, which are available to measure p38 MAPK and JNK activity, respectively. I chose these two systems as aberrant activation of both the p38 MAPK and JNK pathways are implicated in the pathogenesis of Hodgkin's lymphoma. Furthermore, these pathways are activated by numerous stimuli, including LMP1 and CD40 (Figure 5.2). Thus these two PathDetect systems provide strong read-outs for LMP1 and CD40 signalling making them ideal for the establishment of the system in GC B cells.

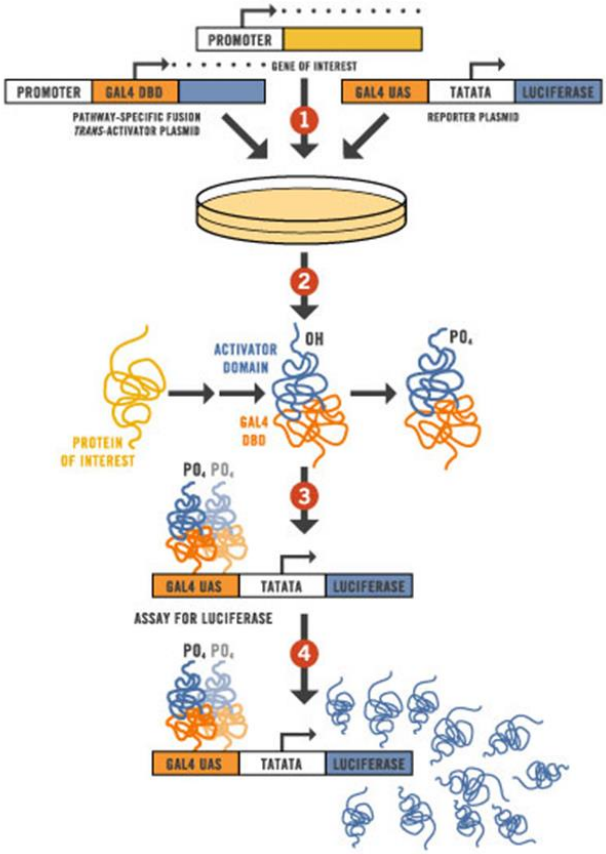

Figure 5.1: The PathDetect trans-system
The PathDetect trans-system works through the transfection of the gene of interest, a trans-activator (such as ATF2) and a reporter plasmid into the cells, whereby activation of specific pathways can be measured. The trans-activator is a fusion protein of GAL4 and a specific transcription factor, and upon phosphorylation by the protein of interest, the trans-activator forms dimers allowing the GAL4 fragment to bind to the GAL4 UAS site on the reporter plasmid, thus initiating transcription. In the modified reporter plasmid the luciferase gene is replaced by GFP, therefore reporter activation results in GFP production which can be measured by flow cytometry. Diagram taken from the manufacturer's website (http://www.genomics.agilent.com/article.jsp?pageId=1360&_requestid=13018).

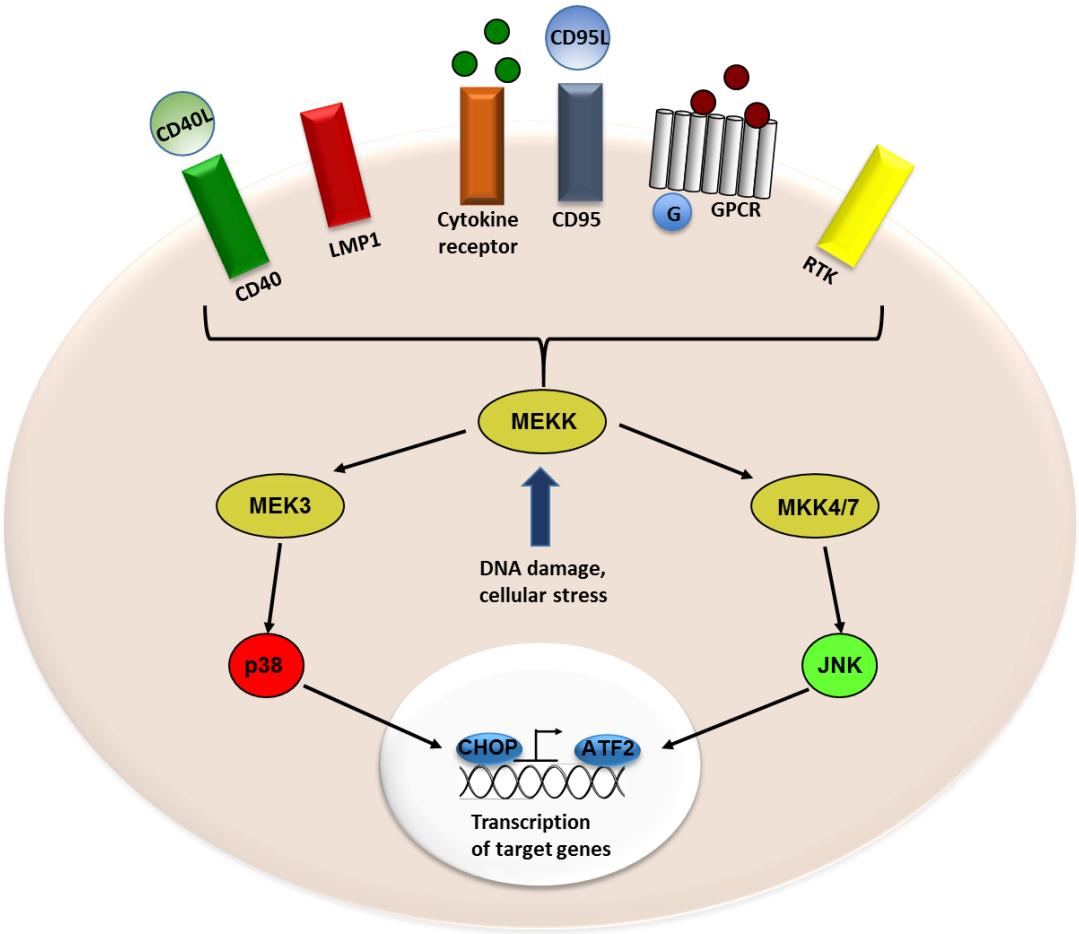

Figure 5.2: The p38 MAPK and JNK signalling pathways
Several internal and external stimuli activate the p38 MAPK and JNK pathways, through the action of a variety of cell surface receptors. Activation of MEKK (MAP3K) results in the activation of MKK4 and MKK7 (MAP2K4 and MAP2K7) which in turn phosphorylate JNK, leading to JNK dimerization and phosphorylation of ATF2. Activation of MEK3 (MAP2K3) results in the activation of p38 MAPK and phosphorylation of CHOP.

5.2 Results

5.2.1 Optimisation of the CHOP and ATF2 PathDetect systems in BL2 cells

I first tested if I could activate the CHOP and ATF2 PathDetect systems in a Burkitt's lymphoma cell line, BL2. I chose this cell line because transgene expression is efficient and cell death low after transfection. I transfected BL2 cells with the CHOP and ATF2 PathDetect systems, consisting of the CHOP or ATF2 trans-activator plasmids, the GFP reporter plasmid and either a positive control plasmid or an empty vector control. The positive control for the CHOP system is MEK3, a known activator of p38 MAPK, while the positive control for the ATF2 system is MEKK, a known activator of JNK. Transfection with the empty plasmid should not lead to pathway activation.

I used increasing amounts of trans-activator plasmid to test pathway activation in these systems. Figure 5.3 shows that both the CHOP and ATF2 systems can be activated by their respective positive control plasmids in BL2 cells, and that activation does not increase with increased concentrations of trans-activator. However, BL2 cells display a basal level of CHOP activation, as seen in the empty vector transfected cells.

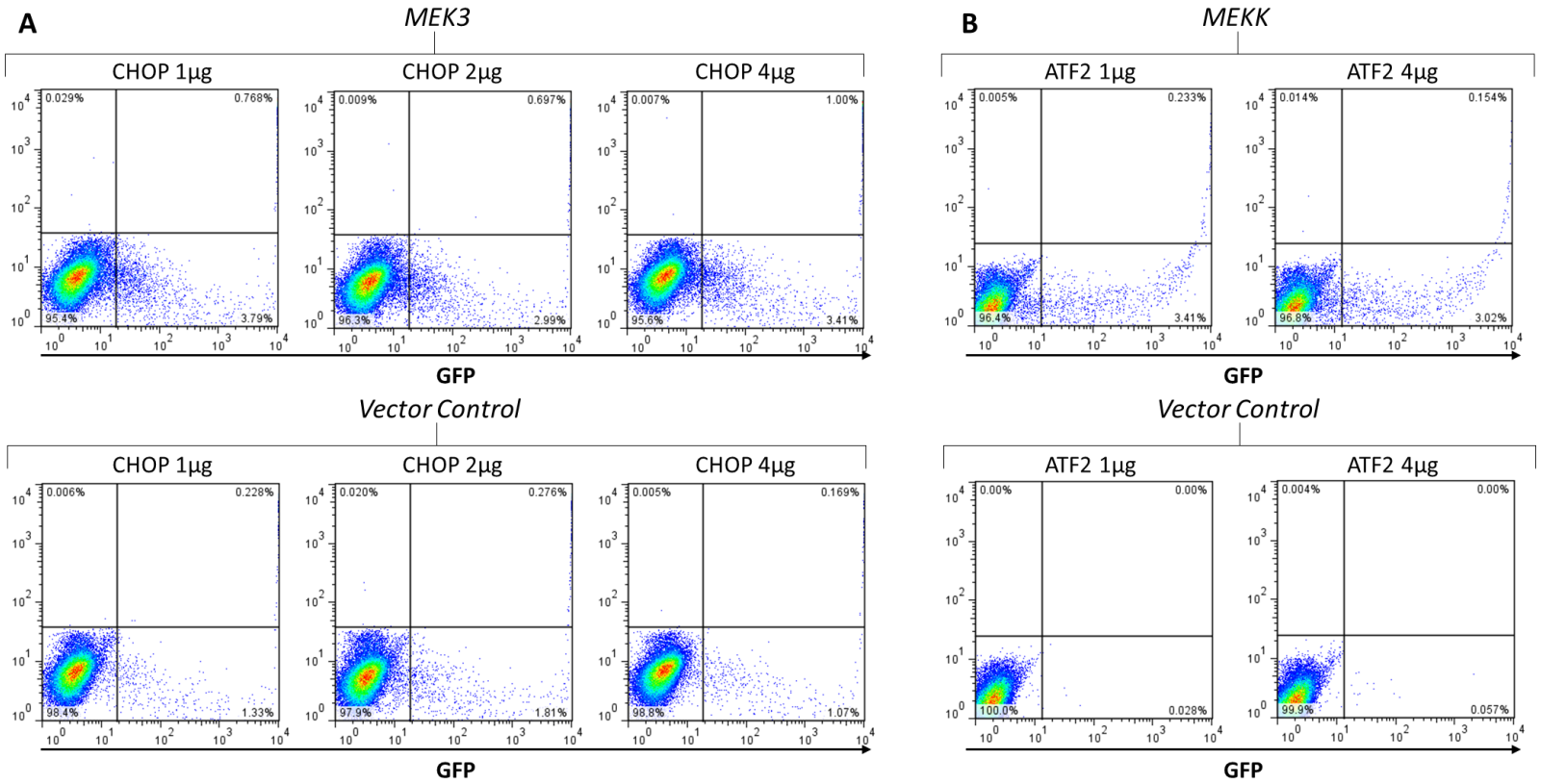

Figure 5.3: Optimisation of the PathDetect system in BL2 cells

GFP expression (x-axis) as a result of the successful activation of the trans-activator (CHOP or ATF2) is plotted against an empty fluorescence channel.

A) MEK3 positive control (top row) and vector control (bottom row) transfected BL2 cells with increasing amount of CHOP trans-activator (1, 2 and 4µg). Increasing the concentration of the CHOP trans-activator did not result in increased GFP production. There is a basal level of CHOP activation in these cells, as shown by low level GFP production in vector control cells.

B) MEKK positive control (top row) and vector control (bottom row) transfected BL2 cells with 1µg and 4µg of ATF2 trans-activator. Increasing the concentration of the ATF2 trans-activator did not result in increased GFP production.

5.2.2 Optimisation of the CHOP and ATF2 PathDetect systems in GC B cells

I next tested the CHOP and ATF2 systems in primary GC B cells. I transfected GC B cells with the CHOP and ATF2 systems, using the positive control and control vector. I also transfected these cells with an LMP1 expression vector, to test if LMP1 signalling can activate ATF2 in GC B cells. The control and LMP1 expression vectors both express a truncated form of the low-affinity nerve growth factor receptor (ΔLNGFR). This molecule is expressed on the cell surface, but has no signalling capability, allowing transfected cells to be identified by flow cytometry. Figure 5.4a shows that only viable transfected (ΔLNGFR) expressing cells were selected for the analysis. For the purpose of the analysis, cells were visualised on CD10 positivity and GFP expression.

Figure 5.4b shows that the positive control plasmid activated the ATF2 trans-activator. However, the positive control plasmid failed to activate the CHOP trans-activator above baseline. In contrast, LMP1 activated both the CHOP and ATF2 trans-activators in GC B cells.

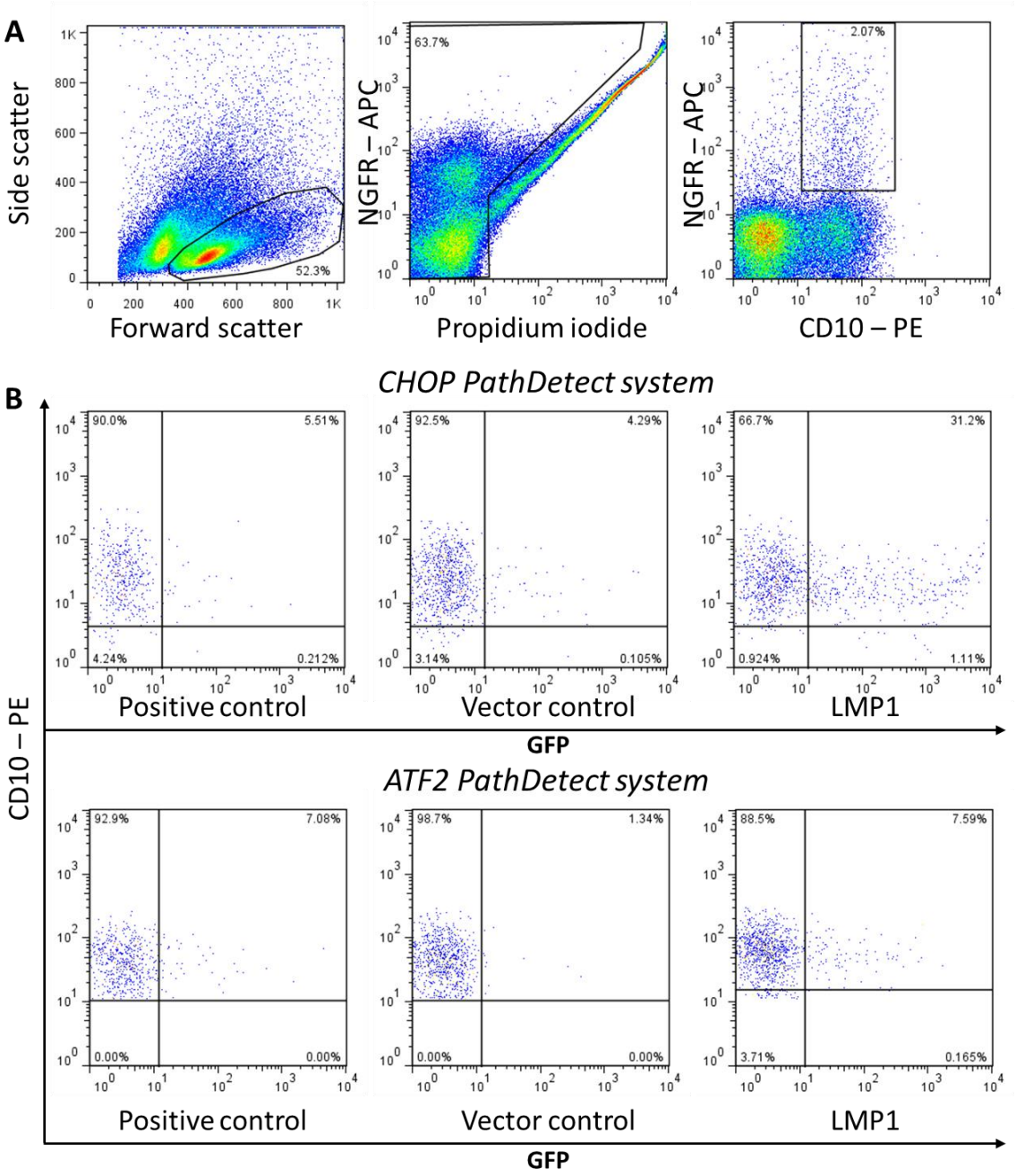

Figure 5.4: Optimisation of the PathDetect system in GC B cells

A) Gating strategy showing gating for viable cells based on morphology (Forward scatter/side scatter) and propidium iodide negativity. Viable cells were further selected for CD10 and NGFR co-expression to identify transfected GC B cells. As the cells were not re-stained with CD10-PE prior to analysis, the large population of CD10 negative cells is most likely due to the loss of CD10-PE antibody from the cell surface during time spent in culture.

B) GFP expression in viable CD10 positive GC B cells as a result of the successful activation of the trans-activator. MEK3 positive control fails to activate the CHOP trans-activator, while LMP1 expression results in activation, as shown by increased GFP production (top row). Both the MEKK positive control and LMP1 activate ATF2 (bottom row).

5.3 CD40L stimulation of the ATF2 PathDetect system in GC B cells

I next wanted to use the PathDetect system to measure the effects of short-term CD40L stimulation on pathway activation in GC B cells. I chose the ATF2 system as it could be activated by the MEKK positive control plasmid and showed minimal basal activation in GC B cells.

I transfected GC B cells with empty vector and with the components of the ATF2 PathDetect system (including one sample with MEKK positive control). Six hours post transfection, half of the vector control cells were stimulated with 200ng/µl CD40L for 6 hours (cells in culture for a total of 12 hours). Figure 5.5, shows that short-term CD40L stimulation did not induce ATF2 activation in this system.

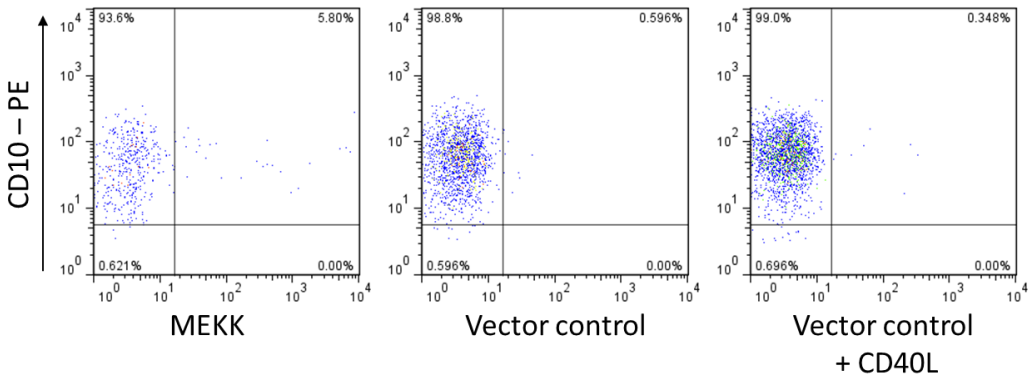

Figure 5.5: Combination of the PathDetect system with CD40L stimulation
GFP expression in viable CD10 positive GC B cells as a result of the successful activation of the trans-activator. MEKK positive control activates the ATF2 trans-activator. CD40L stimulation fails to activate ATF2.

5.4 Summary

One of the greatest challenges with working with GC B cells is the low cell numbers isolated. The use of the PathDetect system can overcome this limitation by providing information on pathway activation in less than 10^5 cells. I have shown that the CHOP and ATF2 PathDetect systems can be activated in BL2 cells and that the ATF2 system can also be activated in GC B cells. In contrast, both systems are activated by LMP1 in GC B cells.

Combining the ATF2 PathDetect system with CD40L stimulation did not result in pathway activation. Six hours of CD40L stimulation provides only a momentary snapshot of pathway activation, and is most likely too long. It is highly likely that pathway activation induced by CD40 ligation is oscillating, resulting in varying levels of down-stream pathway activation over-time. Therefore, a time course of CD40L stimulation ranging from 1-12 hours would provide a more comprehensive picture of CD40 mediated ATF2 activation, from which the time point with the greatest activation can be selected. Additionally, 6 hours may not be long enough for the expression of the system component in the cells, and a longer time point may be required. Alternatively, GC B cells could be transfected with a constitutively active CD40 construct. Although signal provided by such construct may not be physiological, it may provide some insight into CD40 signalling.

These results indicate that while the PathDetect system might be a useful method to detect LMP1 induced signalling pathway activation in GC B cells, it may not be good for

detecting short-term CD40 induced pathway activation. An alternative method would be to perform western blotting on the LMP1 transfected and CD40L stimulated GC B cells and examine the phosphorylation status of various pathway components. While this method works well with cell lines, using it with GC B cells, where only low numbers of cells are available, remains difficult. One way to overcome this limitation would be to pool cells from different experiments, thus increasing cell numbers. Alternatively, enzyme-linked immunosorbent assay (ELISA) could be performed to look for phosphorylation status of various pathway components. The advantage of performing an ELISA is that this assay is more sensitive than traditional western blotting, thus lower cell numbers could be used.

Chapter 6

Future work

6 Future Work

The work presented in this thesis identified a number of areas of future study.

During the investigation of the transcriptional changes induced by LMP1 and CD40 in GC B cells, I have showed that LMP1 but not CD40 can down-regulate the expression of S1PR2 in GC B cells. It has previously been shown that the knock-down of S1PR2 expression in the B cells of mice leads to unlimited growth following chronic antigen stimulation, the disruption of GC architecture and to the development of diffuse large B cell lymphoma. Exploring how LMP1 regulates S1PR2 expression might provide insights into the regulation of S1PR2 in normal tissue as well as in other cancers.

I also showed that over-expression of S1PR2 in L428 cells can reduce cell migration in response to serum. The oncogenic lipid, S1P, is abundant in serum, and its binding to S1PR2 could contribute to the reduced migration of L428 cells. L428 cells express S1PR1 on their cell surface and S1PR1 has been shown to be involved in lymphocyte migration from tissue to plasma in response to S1P (Matloubian et al., 2004). It will therefore be important to establish if the migration of L428 cells is dependent on S1P mediated activation of S1PR1, and whether this can be inhibited by the over-expression of S1PR2.

Having shown that S1PR2 expression in tumour cells is absent in the majority of cases of HL and DLBCL, it will be important to establish if loss of S1PR2 expression contributes to the earlier stages of B cell lymphomagenesis. To do this I might employ the GC B cell system I have used in my project to investigate the effects of S1PR2 inhibition (using the specific antagonist, JTE-013 (Osada et al., 2002)) on the transcriptional programme (using microarrays) and on the activation of cell signalling pathways (using the

PathDetect system) in normal human GC B cells. These experiments might be extended to include a study of the effects of S1PR2 inhibition during the EBV-induced immortalisation of B cells *in vitro*; which a model which has been employed to study the transformation of B cells.

Like S1PR2, RGS13 is also highly expressed in GC B cells. RGS13 is a negative regulator of G_{α}, a G protein involved in CXCR4 and CXCR5 chemotactic signalling in response to ligand, leading to reduced cell motility (Shi et al., 2002, Han et al., 2006). Furthermore, the loss of RGS13 expression leads to increased GC B cell growth compared to wild type in response to antigen stimulation (Hwang et al., 2013). This indicates that the down-regulation of this molecule has the potential to contribute to lymphomagenesis.

Although I failed to confirm RGS13 as an LMP1 target in GC B cells, RGS13 is down-regulated in HL and DLBCL cell lines. The expression of RGS13 in primary HL and DLBCL cases should be examined. If RGS13 expression is lost at the protein level in primary tumour samples, the effect of RGS13 over-expression in a cell line, in terms of growth, survival and migration, could be investigated. Furthermore the impact of the simultaneous over-expression of S1PR2 and RGS13 on S1P signalling and the phenotype of HL cell lines could be examined.

The PathDetect system described in this work has the potential to identify those signalling pathways activated by LMP1 but not by CD40 in GC B cells. Therefore, it will be important to optimise this system for the analysis of the short-term effects of CD40L stimulation in primary GC B cells.

Chapter 7

Appendix

7 Appendix

Table 7.1: Genes concurrently regulated by LMP1 and CD40 in GC B cells

Genes up-regulated by LMP1 and CD40				*Genes down-regulated by LMP1 and CD40*			
Probe Set ID	*NCBI Gene Symbol*	*Fold Change*		*Probe Set ID*	*NCBI Gene Symbol*	*Fold Change*	
		LMP1	**CD40**			**LMP1**	**CD40**
202897_at	SIRPA	10.35	2.72	237137_at	SCARNA2	-5.18	-1.79
225897_at	MARCKS	7.11	2.09	201416_at	SOX4	-4.36	-1.74
213002_at	MARCKS	6.76	1.83	214516_at	HIST1H4B	-3.91	-1.50
231978_at	TPCN2	6.12	2.35	228707_at	CLDN23	-3.86	-1.56
219424_at	EBI3	5.20	2.02	213931_at	ID2 /// ID2B	-3.80	-1.98
231303_at	LINC00158	5.16	1.76	210138_at	RGS20	-3.68	-2.24
207861_at	CCL22	5.02	1.92	210387_at	HIST1H2BG	-3.36	-2.00
239031_at	SSTR2	4.81	1.53	239697_x_at	C3orf67	-3.31	-1.54
201670_s_at	MARCKS	4.55	2.15	204689_at	HHEX	-3.23	-1.56
214597_at	SSTR2	4.31	1.58	230252_at	LPAR5	-3.20	-1.52
211269_s_at	IL2RA	4.10	2.71	225548_at	SHROOM3	-3.20	-1.59
206341_at	IL2RA	4.05	2.50	222958_s_at	DEPDC1	-3.03	-1.75
202896_s_at	SIRPA	4.04	1.70	212915_at	PDZRN3	-3.03	-1.90
209210_s_at	FERMT2	3.98	1.92	219371_s_at	KLF2	-3.01	-1.71
205599_at	TRAF1	3.90	2.43	225762_x_at	LOC284801	-2.84	-1.59
237559_at	GPR55	3.88	1.92	236295_s_at	NLRC3	-2.63	-1.55
201669_s_at	MARCKS	3.85	1.82	227478_at	SETBP1	-2.60	-1.86
209695_at	PTP4A3	3.85	1.56	206115_at	EGR3	-2.57	-1.56
1555573_at	C10orf93	3.81	1.77	235410_at	NPHP3	-2.51	-1.65
204849_at	TCFL5	3.75	2.13	227404_s_at	EGR1	-2.44	-1.53
220230_s_at	CYB5R2	3.63	1.69	204162_at	NDC80	-2.38	-1.54
219045_at	RHOF	3.57	1.92	202499_s_at	SLC2A3	-2.38	-1.73
202638_s_at	ICAM1	3.54	2.07	223624_at	ANUBL1	-2.29	-1.52
211026_s_at	MGLL	3.44	1.64	225767_at	LOC284801	-2.28	-2.00
201502_s_at	NFKBIA	3.36	1.83	206060_s_at	PTPN22	-2.18	-1.87
212761_at	TCF7L2	3.22	2.16	229584_at	LRRK2	-2.17	-1.53
217455_s_at	SSTR2	3.20	1.57	226301_at	C6orf192	-2.16	-1.62
205103_at	C1orf61	3.20	1.55	208079_s_at	AURKA	-2.16	-1.58
227249_at	NDE1	3.05	1.71	1559584_a_at	C16orf54	-2.15	-2.16
225316_at	MFSD2A	3.00	1.67	222670_s_at	MAFB	-2.13	-2.04
220161_s_at	EPB41L4B	2.95	3.47	223434_at	GBP3	-2.07	-1.54
203835_at	LRRC32	2.79	1.62	228531_at	SAMD9	-2.06	-1.51
212977_at	CXCR7	2.78	1.67	203610_s_at	TRIM38	-2.05	-1.52
214787_at	DENND4A	2.78	1.58	202207_at	ARL4C	-2.02	-1.53
211744_s_at	CD58	2.71	1.80	224983_at	SCARB2	-2.02	-1.52
218872_at	TESC	2.70	2.10	238890_at	BRWD1	-1.99	-1.95
202637_s_at	ICAM1	2.68	2.00	228962_at	PDE4D	-1.94	-1.52

212561_at	DENND5A	2.64	1.51	203397_s_at	GALNT3	-1.91	-1.85
213497_at	ABTB2	2.61	2.01	207165_at	HMMR	-1.90	-1.60
205173_x_at	CD58	2.58	1.91	74694_s_at	RABEP2	-1.86	-1.54
1554519_at	CD80	2.57	1.96	236641_at	KIF14	-1.83	-1.66
235116_at	TRAF1	2.51	1.97	239725_at	PGAP1	-1.79	-1.74
226056_at	ARHGAP31	2.48	1.90	202741_at	PRKACB	-1.77	-1.53
218414_s_at	NDE1	2.42	1.60	38241_at	BTN3A3	-1.66	-1.70
210564_x_at	CFLAR	2.35	1.76				
1554352_s_at	DENND4A	2.35	1.58				
204562_at	IRF4	2.32	1.68				
222812_s_at	RHOF	2.30	1.73				
223427_s_at	EPB41L4B	2.28	3.08				
212312_at	BCL2L1	2.28	1.83				
210563_x_at	CFLAR	2.27	1.75				
220002_at	KIF26B	2.27	1.79				
207176_s_at	CD80	2.25	1.79				
209636_at	NFKB2	2.24	1.59				
201625_s_at	INSIG1	2.24	1.58				
212923_s_at	C6orf145	2.23	1.81				
209939_x_at	CFLAR	2.23	1.68				
202431_s_at	MYC	2.19	1.63				
222799_at	WDR91	2.18	1.55				
205965_at	BATF	2.18	1.75				
232682_at	MREG	2.18	1.51				
1554539_a_at	RHOF	2.16	2.01				
239431_at	TICAM2 /// TMED7-TICAM2	2.15	1.61				
238567_at	SGPP2	2.14	2.13				
234284_at	GNG8	2.14	2.04				
211317_s_at	CFLAR	2.12	1.88				
219584_at	PLA1A	2.07	1.87				
228234_at	TICAM2 /// TMED7-TICAM2	2.06	1.75				
230536_at	PBX4	2.06	1.62				
208485_x_at	CFLAR	2.05	1.67				
212019_at	RSL1D1	2.00	1.56				
203045_at	NINJ1	1.99	1.82				
207291_at	PRRG4	1.99	2.20				
211862_x_at	CFLAR	1.99	1.82				
211612_s_at	IL13RA1	1.95	2.39				
216252_x_at	FAS	1.93	2.76				
232746_at	CXCR7	1.91	1.61				
203470_s_at	PLEK	1.91	1.74				
223038_s_at	FAM60A	1.90	1.51				
215346_at	CD40	1.85	1.69				

211316_x_at	CFLAR	1.83	1.61
201888_s_at	IL13RA1	1.76	2.26
205184_at	GNG4	1.73	1.92
205153_s_at	CD40	1.72	1.90
205686_s_at	CD86	1.62	1.59
203879_at	PIK3CD	1.58	1.57

Table 7.2: Genes regulated by LMP1 but not by CD40 in GC B cells

Genes up by LMP1 not CD40			*Genes down by LMP1 not CD40*		
Probe Set ID	*NCBI Gene Symbol*	*Fold Change LMP1*	*Probe Set ID*	*NCBI Gene Symbol*	*Fold Change LMP1*
201564_s_at	FSCN1	17.61	213317_at	CLIC5	-5.12
207900_at	CCL17	8.39	217002_s_at	HTR3A	-4.72
202796_at	SYNPO	8.06	216615_s_at	HTR3A	-4.41
231899_at	ZC3H12C	7.66	215925_s_at	CD72	-4.34
232383_at	TFEC	7.17	205903_s_at	KCNN3	-3.85
204897_at	PTGER4	6.09	223503_at	TMEM163	-3.75
206715_at	TFEC	5.79	206641_at	TNFRSF17	-3.72
201631_s_at	IER3	5.53	226799_at	FGD6	-3.71
202734_at	TRIP10	5.33	238520_at	TRERF1	-3.71
212097_at	CAV1	5.32	227717_at	ARHGEF37	-3.62
235287_at	CDK6	5.30	205902_at	KCNN3	-3.61
236013_at	CACNA1E	5.26	34210_at	CD52	-3.57
232291_at	MIR17HG	5.03	228377_at	KLHL14	-3.40
236831_at	CCDC50	5.01	215933_s_at	HHEX	-3.40
205872_x_at	PDE4DIP	4.96	218935_at	EHD3	-3.39
236289_at	LOC100506563	4.92	207761_s_at	METTL7A	-3.37
214023_x_at	TUBB2B	4.68	219684_at	RTP4	-3.32
235457_at	MAML2	4.61	208046_at	HIST1H4A	-3.28
203196_at	ABCC4	4.58	204967_at	SHROOM2	-3.28
1555935_s_at	HUNK	4.20	220068_at	VPREB3	-3.25
46665_at	SEMA4C	4.17	213906_at	MYBL1	-3.22
201668_x_at	MARCKS	4.12	219396_s_at	NEIL1	-3.17
202510_s_at	TNFAIP2	4.11	203865_s_at	ADARB1	-3.13
206574_s_at	PTP4A3	4.02	215813_s_at	PTGS1	-3.12
202007_at	NID1	3.98	201677_at	C3orf37	-3.10
206176_at	BMP6	3.98	230983_at	FAM129C	-3.08
230188_at	NIPAL4	3.87	235292_at	FLJ32255	-3.06
201170_s_at	BHLHE40	3.79	219577_s_at	ABCA7	-3.05
202421_at	IGSF3	3.78	230560_at	STXBP6	-3.03
225102_at	MGLL	3.77	201678_s_at	C3orf37	-3.01
202341_s_at	TRIM2	3.69	230740_at	EHD3	-2.99
227458_at	CD274	3.67	229021_at	MCTP2	-2.96
236995_x_at	TFEC	3.66	225540_at	MAP2	-2.96
1554242_a_at	COCH	3.64	242525_at	SLC2A5	-2.95
233899_x_at	ZBTB10	3.61	205718_at	ITGB7	-2.93
209835_x_at	CD44	3.47	231254_at	LOC100507635	-2.92
217523_at	CD44	3.45	218692_at	SYBU	-2.91
213113_s_at	SLC43A3	3.42	217853_at	TNS3	-2.91
228218_at	LSAMP	3.42	226809_at	LOC100216479	-2.90
224327_s_at	DGAT2	3.41	204880_at	MGMT	-2.87

243000_at	CDK6	3.40	242794_at	MAML3	-2.87
205229_s_at	COCH	3.38	200765_x_at	CTNNA1	-2.87
1555689_at	CD80	3.36	203144_s_at	KIAA0040	-2.86
206729_at	TNFRSF8	3.24	219190_s_at	EIF2C4	-2.86
205081_at	CRIP1	3.20	214366_s_at	ALOX5	-2.85
201063_at	RCN1	3.20	244467_at	LOC100510485	-2.83
207030_s_at	CSRP2	3.20	216379_x_at	CD24	-2.82
227037_at	PLD6	3.19	218285_s_at	BDH2	-2.82
220658_s_at	ARNTL2	3.16	217983_s_at	RNASET2	-2.79
206825_at	OXTR	3.15	208914_at	GGA2	-2.78
226064_s_at	DGAT2	3.14	242334_at	NLRP4	-2.76
235051_at	CCDC50	3.13	233463_at	RASSF6	-2.75
222301_at	C1orf61	3.13	214290_s_at	HIST2H2AA3 /// HIST2H2AA4	-2.75
219159_s_at	SLAMF7	3.11	203408_s_at	SATB1	-2.73
234306_s_at	SLAMF7	3.05	224482_s_at	RAB11FIP4	-2.73
224851_at	CDK6	3.04	225570_at	SLC41A1	-2.71
220358_at	BATF3	3.00	220528_at	VNN3	-2.71
212014_x_at	CD44	2.96	221908_at	RNFT2	-2.71
218627_at	DRAM1	2.91	205418_at	FES	-2.71
202643_s_at	TNFAIP3	2.86	203283_s_at	HS2ST1	-2.71
202925_s_at	PLAGL2	2.86	235486_at	C11orf41	-2.69
203010_at	STAT5A	2.85	218025_s_at	ECI2	-2.68
231084_at	WDR96	2.83	205128_x_at	PTGS1	-2.68
202644_s_at	TNFAIP3	2.82	220169_at	TMEM156	-2.68
225331_at	CCDC50	2.81	229383_at	MARCH1	-2.66
241871_at	CAMK4	2.81	228258_at	TBC1D10C	-2.66
212397_at	RDX	2.79	222450_at	PMEPA1	-2.65
207169_x_at	DDR1	2.79	1552807_a_at	SIGLEC10	-2.64
202085_at	TJP2	2.79	203143_s_at	KIAA0040	-2.64
222774_s_at	NETO2	2.78	225562_at	RASA3	-2.64
214460_at	LSAMP	2.76	213385_at	CHN2	-2.62
1565868_at	CD44	2.76	219518_s_at	ELL3 /// SERINC4	-2.62
201627_s_at	INSIG1	2.76	214156_at	MYRIP	-2.62
239629_at	CFLAR	2.76	226906_s_at	ARHGAP9	-2.61
210749_x_at	DDR1	2.74	203285_s_at	HS2ST1	-2.60
1554600_s_at	LMNA	2.73	228964_at	PRDM1	-2.60
235444_at	FOXP1	2.70	206100_at	CPM	-2.59
206756_at	CHST7	2.69	231929_at	IKZF2	-2.59
202449_s_at	RXRA	2.68	227184_at	PTAFR	-2.58
230875_s_at	ATP11A	2.68	202742_s_at	PRKACB	-2.58
222838_at	SLAMF7	2.67	204430_s_at	SLC2A5	-2.57
1556308_at	PRRT3	2.67	219313_at	GRAMD1C	-2.56
204489_s_at	CD44	2.66	219667_s_at	BANK1	-2.56
229228_at	CREB5	2.63	211379_x_at	B3GALNT1	-2.56

36711_at	MAFF	2.62	206369_s_at	PIK3CG	-2.56
229910_at	SHE	2.61	228434_at	BTNL9	-2.55
1007_s_at	DDR1	2.61	204164_at	SIPA1	-2.54
208779_x_at	DDR1	2.60	1568751_at	RGS13	-2.54
230093_at	RSPH1	2.59	203281_s_at	UBA7	-2.54
213418_at	HSPA6	2.59	230710_at	LOC100506211	-2.54
210118_s_at	IL1A	2.58	1552323_s_at	FAM122C	-2.53
205920_at	SLC6A6	2.57	204446_s_at	ALOX5	-2.52
204490_s_at	CD44	2.57	212979_s_at	FAM115A	-2.52
202910_s_at	CD97	2.56	204392_at	CAMK1	-2.51
226713_at	CCDC50	2.56	214772_at	C11orf41	-2.50
218868_at	ACTR3B	2.55	201752_s_at	ADD3	-2.50
1558996_at	FOXP1	2.53	203435_s_at	MME	-2.50
220703_at	IDI2-AS1	2.53	226666_at	DAAM1	-2.49
208683_at	CAPN2	2.52	213045_at	MAST3	-2.49
219675_s_at	UXS1	2.52	218729_at	LXN	-2.49
203411_s_at	LMNA	2.51	209771_x_at	CD24	-2.49
216952_s_at	LMNB2	2.49	221643_s_at	RERE	-2.49
202975_s_at	RHOBTB3	2.49	214719_at	SLC46A3	-2.48
209822_s_at	VLDLR	2.48	1554413_s_at	RUNDC2B /// RUNDC2C	-2.47
209949_at	NCF2	2.46	218807_at	VAV3	-2.47
203836_s_at	MAP3K5	2.46	205389_s_at	ANK1	-2.47
200800_s_at	HSPA1A /// HSPA1B	2.44	225739_at	RAB11FIP4	-2.45
227645_at	PIK3R5	2.44	219889_at	FRAT1	-2.45
204435_at	NUPL1	2.44	222449_at	PMEPA1	-2.44
218786_at	NT5DC3	2.44	209276_s_at	GLRX	-2.44
1552671_a_at	SLC9A7	2.43	204961_s_at	NCF1 /// NCF1B /// NCF1C	-2.44
224204_x_at	ARNTL2	2.42	1552626_a_at	TMEM163	-2.43
203837_at	MAP3K5	2.42	210658_s_at	GGA2	-2.43
219279_at	DOCK10	2.39	204220_at	GMFG	-2.41
210407_at	PPM1A	2.39	209570_s_at	D4S234E	-2.40
242905_at	PNO1	2.38	205213_at	ACAP1	-2.40
205681_at	BCL2A1	2.37	236278_at	HIST1H3E	-2.40
205569_at	LAMP3	2.36	218458_at	GMCL1	-2.40
227230_s_at	KIAA1211	2.35	235706_at	CPM	-2.39
224848_at	CDK6	2.35	1569065_s_at	C15orf62	-2.39
202976_s_at	RHOBTB3	2.34	219183_s_at	CYTH4	-2.39
202014_at	PPP1R15A	2.34	203153_at	IFIT1	-2.39
203684_s_at	BCL2	2.34	214369_s_at	RASGRP2	-2.39
1555620_a_at	PTGIR	2.33	1557321_a_at	CAPN14	-2.38
210663_s_at	KYNU	2.32	208087_s_at	ZBP1	-2.38
200704_at	LITAF	2.31	211368_s_at	CASP1	-2.37
209163_at	CYB561	2.31	204429_s_at	SLC2A5	-2.37

238790_at	LOC374443	2.30	229147_at	RASSF6	-2.36
202933_s_at	YES1	2.30	226456_at	RMI2	-2.35
1405_i_at	CCL5	2.28	203418_at	CCNA2	-2.35
201566_x_at	ID2	2.28	218862_at	ASB13	-2.34
1563638_at	FAM18A	2.28	235291_s_at	FLJ32255	-2.34
208920_at	SRI	2.27	221123_x_at	ZNF395	-2.34
214452_at	BCAT1	2.26	219901_at	FGD6	-2.33
201426_s_at	VIM	2.26	213888_s_at	TRAF3IP3	-2.32
229801_at	C10orf47	2.24	226249_at	SNX30	-2.32
201307_at	SEPT11	2.24	206348_s_at	PDK3	-2.32
213138_at	ARID5A	2.23	231837_at	USP28	-2.32
203414_at	MMD	2.23	227100_at	B3GALTL	-2.32
225066_at	PPP2R2D	2.21	1555037_a_at	IDH1	-2.32
212063_at	CD44	2.20	207339_s_at	LTB	-2.31
214662_at	WDR43	2.19	1555137_a_at	FGD6	-2.31
212443_at	NBEAL2	2.19	228622_s_at	DNAJC4	-2.31
219581_at	TSEN2	2.19	218844_at	ACSF2	-2.30
243296_at	NAMPT	2.18	223179_at	YPEL3	-2.30
203023_at	NOP16	2.18	219517_at	ELL3 /// SERINC4	-2.30
211725_s_at	BID	2.18	213772_s_at	GGA2	-2.30
226517_at	BCAT1	2.18	209441_at	RHOBTB2	-2.29
236019_at	RAB12	2.18	205297_s_at	CD79B	-2.29
209900_s_at	SLC16A1	2.17	234987_at	SAMHD1	-2.29
200916_at	TAGLN2	2.17	225637_at	DEF8	-2.29
234411_x_at	CD44	2.17	211685_s_at	NCALD	-2.29
1555392_at	LOC100128868	2.17	235400_at	FCRLA	-2.28
1558292_s_at	PIGW	2.16	201694_s_at	EGR1	-2.28
233409_at	RHBDL3	2.16	1553196_a_at	FCRL3	-2.28
222442_s_at	ARL8B	2.15	217989_at	HSD17B11	-2.28
242586_at	FSD1L	2.15	203758_at	CTSO	-2.28
223182_s_at	AGPAT3	2.15	219691_at	SAMD9	-2.28
225071_at	NUS1	2.14	243109_at	MCTP2	-2.27
212277_at	MTMR4	2.14	217984_at	RNASET2	-2.27
219275_at	PDCD5	2.13	221867_at	N4BP1	-2.27
202016_at	MEST	2.13	209113_s_at	HMG20B	-2.26
218032_at	SNN	2.12	210719_s_at	HMG20B	-2.26
223287_s_at	FOXP1	2.11	215887_at	ZNF277	-2.26
224925_at	PREX1	2.11	219677_at	SPSB1	-2.25
227985_at	LOC100506098	2.11	210844_x_at	CTNNA1	-2.25
237159_x_at	AP1S3	2.11	201315_x_at	IFITM2	-2.25
1553386_at	MFSD2A	2.11	1554240_a_at	ITGAL	-2.24
212089_at	LMNA	2.11	204061_at	PRKX	-2.24
37028_at	PPP1R15A	2.10	209995_s_at	TCL1A	-2.24
201626_at	INSIG1	2.10	221669_s_at	ACAD8	-2.24

1555487_a_at	ACTR3B	2.09	201753_s_at	ADD3	-2.23
244600_at	LOC100506589	2.08	202869_at	OAS1	-2.23
206173_x_at	GABPB1	2.08	223269_at	POLR3GL	-2.23
216056_at	CD44	2.08	1294_at	UBA7	-2.23
219500_at	CLCF1	2.07	218280_x_at	HIST2H2AA3 /// HIST2H2AA4	-2.23
1555384_a_at	LARP4	2.07	206219_s_at	VAV1	-2.22
225341_at	MTERFD3	2.07	39318_at	TCL1A	-2.22
237498_at	NEDD4L	2.07	231455_at	FLJ42418	-2.22
1558569_at	LOC100131541	2.06	219505_at	CECR1	-2.22
218984_at	PUS7	2.05	1553055_a_at	SLFN5	-2.22
203622_s_at	PNO1	2.04	235173_at	LOC401093	-2.21
226998_at	NAA15	2.03	219863_at	HERC5	-2.21
224282_s_at	AGPAT3	2.02	227224_at	RALGPS2	-2.21
228980_at	RFFL	2.02	203434_s_at	MME	-2.21
229029_at	CAMK4	2.00	203198_at	CDK9	-2.21
223376_s_at	BRI3	2.00	205882_x_at	ADD3	-2.21
223183_at	AGPAT3	2.00	208206_s_at	RASGRP2	-2.20
225400_at	TSEN15	1.99	39248_at	AQP3	-2.20
223184_s_at	AGPAT3	1.99	230128_at	IGL@	-2.20
227856_at	C4orf32	1.98	221044_s_at	TRIM34 /// TRIM6-TRIM34	-2.19
206975_at	LTA	1.98	204993_at	GNAZ	-2.19
206181_at	SLAMF1	1.98	217553_at	STEAP1B	-2.19
201952_at	ALCAM	1.98	1554343_a_at	STAP1	-2.19
201951_at	ALCAM	1.97	242785_at	EML6	-2.19
205180_s_at	ADAM8	1.97	228055_at	NAPSB	-2.18
219648_at	MREG	1.97	210176_at	TLR1	-2.18
221563_at	DUSP10	1.97	235353_at	SEL1L3	-2.18
224716_at	SLC35B2	1.96	227189_at	CPNE5	-2.18
209212_s_at	KLF5	1.96	200764_s_at	CTNNA1	-2.17
222666_s_at	RCL1	1.96	220214_at	ZNF215	-2.16
218507_at	C7orf68	1.96	213326_at	VAMP1	-2.16
204385_at	KYNU	1.96	232024_at	GIMAP2	-2.16
244786_at	SNHG10	1.95	1552701_a_at	CARD16	-2.16
218460_at	HEATR2	1.94	218149_s_at	ZNF395	-2.16
200799_at	HSPA1A	1.94	214047_s_at	MBD4	-2.16
203724_s_at	RUFY3	1.94	223849_s_at	MOV10	-2.16
204790_at	SMAD7	1.93	204415_at	IFI6	-2.16
212201_at	ANKLE2	1.93	230036_at	SAMD9L	-2.15
234968_at	DENND4C	1.92	200923_at	LGALS3BP	-2.15
228087_at	CCDC126	1.92	209200_at	MEF2C	-2.14
206035_at	REL	1.92	227168_at	MIAT	-2.14
242807_at	FSD1L	1.91	213174_at	TTC9	-2.14
213746_s_at	FLNA	1.91	218943_s_at	DDX58	-2.14

223172_s_at	MTFP1	1.90	209607_x_at	SULT1A3 /// SULT1A4	-2.14
215207_x_at	NUS1 /// NUS1P3	1.90	214084_x_at	NCF1C	-2.13
226262_at	DHX33	1.89	204867_at	GCHFR	-2.13
212609_s_at	AKT3	1.89	38521_at	CD22	-2.13
201473_at	JUNB	1.89	212981_s_at	FAM115A	-2.13
218886_at	PAK1IP1	1.88	209606_at	CYTIP	-2.13
226117_at	TIFA	1.88	1558827_a_at	ZNF831	-2.12
220118_at	ZBTB32	1.88	213343_s_at	GDPD5	-2.12
205377_s_at	ACHE	1.88	224451_x_at	ARHGAP9	-2.12
213816_s_at	MET	1.87	1552390_a_at	C8orf47	-2.11
33197_at	MYO7A	1.87	203522_at	CCS	-2.11
200859_x_at	FLNA	1.87	223216_x_at	ZNF395	-2.11
200894_s_at	FKBP4	1.87	205352_at	SERPINI1	-2.11
233231_at	MCCC2	1.86	213916_at	ZNF20 /// ZNF625	-2.11
201565_s_at	ID2	1.86	1553102_a_at	CCDC69	-2.11
225615_at	IFFO2	1.86	206039_at	RAB33A	-2.11
209318_x_at	PLAGL1	1.86	239585_at	KAT2B	-2.10
235783_at	MRTO4	1.86	226431_at	FAM117B	-2.10
232504_at	LOC285628	1.85	219911_s_at	SLCO4A1	-2.09
232045_at	PHACTR1	1.85	208913_at	GGA2	-2.09
225023_at	GOPC	1.84	209911_x_at	HIST1H2BD	-2.09
209725_at	UTP20	1.84	204735_at	PDE4A	-2.09
208712_at	CCND1	1.84	214933_at	CACNA1A	-2.09
212200_at	ANKLE2	1.84	225008_at	ASPH	-2.09
48659_at	MIIP	1.84	229005_at	MCTP2	-2.08
203685_at	BCL2	1.83	229656_s_at	EML6	-2.08
227215_at	GOPC	1.83	214059_at	IFI44	-2.08
227214_at	GOPC	1.83	238669_at	PTGS1	-2.08
212563_at	BOP1	1.83	228056_s_at	NAPSB	-2.08
37079_at	NUS1P3	1.83	205922_at	VNN2	-2.08
1554918_a_at	ABCC4	1.83	202203_s_at	AMFR	-2.08
218561_s_at	LYRM4	1.83	243999_at	SLFN5	-2.08
235072_s_at	KIF13A	1.83	228273_at	PRR11	-2.07
217388_s_at	KYNU	1.82	53720_at	C19orf66	-2.07
213320_at	PRMT3	1.80	210033_s_at	SPAG6	-2.07
213327_s_at	USP12	1.80	242624_at	ABLIM2	-2.06
223586_at	ARNTL2	1.80	210279_at	GPR18	-2.06
206380_s_at	CFP	1.80	209580_s_at	MBD4	-2.06
221270_s_at	QTRT1	1.80	211700_s_at	TRO	-2.06
218888_s_at	NETO2	1.79	222589_at	NLK	-2.05
213430_at	RUFY3	1.79	235221_at	CBLN3	-2.05
222592_s_at	ACSL5	1.79	218272_at	TTC38	-2.05
226121_at	DHRS13	1.78	223750_s_at	TLR10	-2.05
223437_at	PPARA	1.76	212886_at	CCDC69	-2.05

33736_at	STOML1	1.76	232543_x_at	ARHGAP9	-2.04
224654_at	DDX21	1.75	201601_x_at	IFITM1	-2.04
214752_x_at	FLNA	1.75	212573_at	ENDOD1	-2.04
218744_s_at	PACSIN3	1.75	213475_s_at	ITGAL	-2.04
223746_at	STK4	1.75	205398_s_at	SMAD3	-2.04
225022_at	GOPC	1.75	209447_at	SYNE1	-2.04
210676_x_at	RGPD5///RGPD8	1.75	203803_at	PCYOX1	-2.03
220688_s_at	MRTO4	1.74	212792_at	DPY19L1	-2.03
225440_at	AGPAT3	1.74	228551_at	DENND5B	-2.03
242727_at	ARL5B	1.73	232693_s_at	FBXO16 /// ZNF395	-2.03
216913_s_at	RRP12	1.73	201193_at	IDH1	-2.03
209366_x_at	CYB5A	1.73	203567_s_at	TRIM38	-2.03
208029_s_at	LAPTM4B	1.72	219211_at	USP18	-2.02
215087_at	C15orf39	1.72	210580_x_at	SULT1A3 /// SULT1A4	-2.02
221987_s_at	TSR1	1.72	209980_s_at	SHMT1	-2.02
226609_at	DCBLD1	1.72	228677_s_at	RASAL3	-2.02
215726_s_at	CYB5A	1.71	225327_at	KIAA1370	-2.02
207760_s_at	NCOR2	1.71	209282_at	PRKD2	-2.02
227804_at	TLCD1	1.71	208442_s_at	ATM	-2.01
204335_at	CCDC94	1.71	227811_at	FGD3	-2.01
215513_at	HYMAI	1.71	225136_at	PLEKHA2	-2.00
220948_s_at	ATP1A1	1.71	235372_at	FCRLA	-2.00
202138_x_at	AIMP2	1.70	242625_at	RSAD2	-2.00
227143_s_at	BID	1.70	204484_at	PIK3C2B	-2.00
219420_s_at	SELRC1	1.70	1552540_s_at	IQCD	-2.00
208836_at	ATP1B3	1.70	1568752_s_at	RGS13	-2.00
218512_at	WDR12	1.69	226158_at	KLHL24	-1.99
238858_at	TIFA	1.69	217825_s_at	UBE2J1	-1.99
207574_s_at	GADD45B	1.69	216684_s_at	SS18	-1.99
201858_s_at	SRGN	1.69	205997_at	ADAM28	-1.99
230272_at	LOC645323	1.69	202455_at	HDAC5	-1.99
219540_at	ZNF267	1.69	208933_s_at	LGALS8	-1.99
232621_at	USP48	1.69	1557915_s_at	GSTO1	-1.99
222292_at	CD40	1.68	203420_at	FAM8A1	-1.98
223028_s_at	SNX9	1.68	218317_x_at	SLX1A /// SLX1B	-1.98
226319_s_at	THOC4	1.68	218217_at	SCPEP1	-1.98
220198_s_at	EIF5A2	1.68	211071_s_at	MLLT11	-1.98
225285_at	BCAT1	1.68	212390_at	PDE4DIP	-1.98
201872_s_at	ABCE1	1.67	232278_s_at	DEPDC1	-1.98
227369_at	SERBP1	1.67	205124_at	MEF2BNB-MEF2B	-1.97
226200_at	VARS2	1.67	205804_s_at	TRAF3IP3	-1.97
232154_at	C19orf76	1.67	38269_at	PRKD2	-1.97
204417_at	GALC	1.67	217824_at	UBE2J1	-1.97
238506_at	LRRC58	1.66	203806_s_at	FANCA	-1.97

209508_x_at	CFLAR	1.66	203140_at	BCL6	-1.97
208754_s_at	NAP1L1	1.66	219352_at	HERC6	-1.97
212846_at	RRP1B	1.66	228252_at	PIF1	-1.97
218982_s_at	MRPS17 /// ZNF713	1.66	210640_s_at	GPER	-1.96
208634_s_at	MACF1	1.65	226372_at	CHST11	-1.96
204700_x_at	DIEXF	1.65	217838_s_at	EVL	-1.96
214011_s_at	NOP16	1.64	225763_at	RCSD1	-1.96
221632_s_at	WDR4	1.64	212311_at	SEL1L3	-1.96
201391_at	TRAP1	1.64	221957_at	PDK3	-1.95
223027_at	SNX9	1.64	203615_x_at	SULT1A1	-1.95
225470_at	NUP35	1.63	205034_at	CCNE2	-1.95
214484_s_at	SIGMAR1	1.63	209682_at	CBLB	-1.95
212074_at	SUN1	1.63	221211_s_at	C21orf7	-1.95
41387_r_at	KDM6B	1.63	213643_s_at	INPP5B	-1.94
208092_s_at	FAM49A	1.63	213674_x_at	IGHD	-1.94
225678_at	POLR3H	1.62	204581_at	CD22	-1.94
212110_at	SLC39A14	1.62	212856_at	GRAMD4	-1.94
1557331_at	POLR1B	1.62	212310_at	MIA3	-1.94
206445_s_at	PRMT1	1.61	204646_at	DPYD	-1.94
226963_at	BTF3L4	1.60	214368_at	RASGRP2	-1.93
220924_s_at	SLC38A2	1.60	1557116_at	APOL6	-1.93
218479_s_at	XPO4	1.59	201853_s_at	CDC25B	-1.93
204015_s_at	DUSP4	1.59	236562_at	ZNF439	-1.93
225585_at	RAP2A	1.58	201688_s_at	TPD52	-1.93
210996_s_at	YWHAE	1.58	219836_at	ZBED2	-1.93
215966_x_at	GK3P	1.57	225144_at	BMPR2	-1.93
203737_s_at	PPRC1	1.57	204336_s_at	RGS19	-1.93
212680_x_at	PPP1R14B	1.57	226860_at	TMEM19	-1.92
225520_at	MTHFD1L	1.57	227053_at	PACSIN1	-1.92
205684_s_at	DENND4C	1.56	208869_s_at	GABARAPL1	-1.92
204123_at	LIG3	1.56	210045_at	IDH2	-1.92
224793_s_at	TGFBR1	1.55	232787_at	PRIC285	-1.92
			213521_at	PTPN18	-1.92
			220059_at	STAP1	-1.92
			225564_at	SPATA13	-1.92
			228868_x_at	CDT1	-1.92
			227122_at	LOC100507237	-1.91
			218031_s_at	FOXN3	-1.91
			225636_at	STAT2	-1.91
			AFFX-HUMISGF3A/M97935_5_at	STAT1	-1.91
			208021_s_at	RFC1	-1.91
			228959_at	PDK3	-1.91
			210347_s_at	BCL11A	-1.90

	217022_s_at	IGHA1 /// IGHA2 /// LOC100126583	-1.90
	209512_at	HSDL2	-1.90
	229538_s_at	IQGAP3	-1.90
	219498_s_at	BCL11A	-1.90
	211385_x_at	SULT1A2	-1.90
	232035_at	LOC100507025	-1.90
	218073_s_at	TMEM48	-1.90
	221893_s_at	ADCK2	-1.90
	227565_at	KLHL5	-1.90
	1552634_a_at	ZNF101	-1.89
	226136_at	GLIPR1	-1.89
	222482_at	SSBP3	-1.89
	218298_s_at	C14orf159	-1.89
	215299_x_at	SULT1A1	-1.89
	1553690_at	SGOL1	-1.89
	217732_s_at	ITM2B	-1.89
	235310_at	GCET2	-1.89
	228230_at	PRIC285	-1.89
	222891_s_at	BCL11A	-1.89
	244008_at	PARP8	-1.89
	201204_s_at	RRBP1	-1.88
	218248_at	FAM111A	-1.88
	206632_s_at	APOBEC3B	-1.88
	225929_s_at	RNF213	-1.88
	202464_s_at	PFKFB3	-1.88
	227606_s_at	STAMBPL1	-1.88
	227684_at	S1PR2	-1.88
	228030_at	RBM6	-1.88
	225558_at	GIT2	-1.87
	220377_at	FAM30A	-1.87
	213988_s_at	SAT1	-1.87
	204396_s_at	GRK5	-1.87
	202759_s_at	AKAP2 /// PALM2-AKAP2	-1.87
	1552532_a_at	ATP6V1C2	-1.87
	206513_at	AIM2	-1.87
	231093_at	FCRL3	-1.87
	1556579_s_at	IGSF10	-1.86
	219676_at	ZSCAN16	-1.86
	235478_at	DCLRE1C	-1.86
	235683_at	SESN3	-1.86
	226630_at	MIS18BP1	-1.86
	32502_at	GDPD5	-1.86
	1552619_a_at	ANLN	-1.86

	213305_s_at	PPP2R5C	-1.86
	223514_at	CARD11	-1.86
	222779_s_at	C17orf85	-1.85
	203823_at	RGS3	-1.85
	215111_s_at	TSC22D1	-1.85
	214022_s_at	IFITM1	-1.84
	223565_at	MZB1	-1.84
	226533_at	HINT3	-1.84
	213596_at	CASP4	-1.84
	205441_at	OCEL1	-1.83
	200632_s_at	NDRG1	-1.83
	230992_at	BTNL9	-1.83
	209085_x_at	RFC1	-1.83
	238861_at	SSBP2	-1.83
	205301_s_at	OGG1	-1.83
	235508_at	PML	-1.83
	225533_at	PHF19	-1.83
	212357_at	FAM168A	-1.83
	1552682_a_at	CASC5	-1.83
	202663_at	WIPF1	-1.82
	207219_at	ZNF643	-1.82
	212665_at	TIPARP	-1.82
	232005_at	DNAH1	-1.82
	225175_s_at	SLC44A2	-1.82
	225045_at	CCDC88A	-1.82
	202524_s_at	SPOCK2	-1.82
	222572_at	PDP1	-1.82
	225618_at	ARHGAP27	-1.82
	202208_s_at	ARL4C	-1.81
	228320_x_at	CCDC64	-1.81
	234974_at	GALM	-1.81
	221104_s_at	NIPSNAP3B	-1.81
	235089_at	FBXL20	-1.81
	232114_at	MED12L	-1.81
	239355_at	GMCL1	-1.81
	202729_s_at	LTBP1	-1.81
	204813_at	MAPK10	-1.81
	202019_s_at	LANCL1	-1.81
	202694_at	STK17A	-1.81
	212672_at	ATM	-1.81
	244687_at	DBT	-1.80
	204774_at	EVI2A	-1.80
	209709_s_at	HMMR	-1.80
	37549_g_at	BBS9	-1.80

	223303_at	FERMT3	-1.80
	234192_s_at	GKAP1	-1.80
	233483_at	TBC1D27	-1.80
	224946_s_at	CCDC115	-1.79
	223339_at	ATPIF1	-1.79
	202388_at	RGS2	-1.79
	210448_s_at	P2RX5	-1.79
	206206_at	CD180	-1.79
	225024_at	RPRD1B	-1.78
	201697_s_at	DNMT1	-1.78
	200940_s_at	RERE	-1.78
	229552_at	LOC283454	-1.78
	222233_s_at	DCLRE1C	-1.78
	227607_at	STAMBPL1	-1.78
	231810_at	BRI3BP	-1.77
	238440_at	CLYBL	-1.77
	214453_s_at	IFI44	-1.77
	225182_at	TMEM50B	-1.77
	227946_at	OSBPL7	-1.77
	221922_at	GPSM2	-1.76
	205550_s_at	BRE	-1.76
	221290_s_at	MUM1	-1.76
	203805_s_at	FANCA	-1.76
	205122_at	TMEFF1	-1.76
	209083_at	CORO1A	-1.75
	238597_at	ANKRD13C	-1.75
	204060_s_at	PRKX /// PRKY	-1.75
	223298_s_at	NT5C3	-1.75
	209876_at	GIT2	-1.75
	204951_at	RHOH	-1.75
	202732_at	PKIG	-1.75
	202645_s_at	MEN1	-1.75
	223220_s_at	PARP9	-1.74
	225630_at	EEPD1	-1.74
	219996_at	ASB7	-1.74
	213659_at	ZNF75D	-1.74
	208731_at	RAB2A	-1.74
	203027_s_at	MVD	-1.74
	213510_x_at	LOC220594	-1.74
	225237_s_at	MSI2	-1.73
	1552334_at	TRIOBP	-1.73
	212399_s_at	VGLL4	-1.73
	224811_at	LPP	-1.73
	225784_s_at	ZC4H2	-1.73

	221572_s_at	SLC26A6	-1.73
	221810_at	RAB15	-1.73
	228787_s_at	BCAS4	-1.72
	213005_s_at	KANK1	-1.72
	224818_at	SORT1	-1.72
	226509_at	ZNF641	-1.72
	223980_s_at	SP110	-1.72
	202213_s_at	CUL4B	-1.72
	221011_s_at	LBH	-1.72
	37577_at	ARHGAP19	-1.72
	227134_at	SYTL1	-1.72
	202548_s_at	ARHGEF7	-1.72
	1554365_a_at	PPP2R5C	-1.71
	226001_at	KLHL5	-1.71
	238647_at	C14orf28	-1.71
	212409_s_at	TOR1AIP1	-1.71
	238025_at	MLKL	-1.71
	218782_s_at	ATAD2	-1.71
	203117_s_at	PAN2	-1.71
	1553227_s_at	BRWD1	-1.71
	221511_x_at	CCPG1	-1.71
	208912_s_at	CNP	-1.71
	217118_s_at	KIAA0930	-1.71
	235139_at	GNGT2	-1.70
	202204_s_at	AMFR	-1.70
	204439_at	IFI44L	-1.70
	215058_at	DENND5B	-1.70
	203564_at	FANCG	-1.70
	212579_at	SMCHD1	-1.70
	231182_at	WIPF1	-1.70
	207124_s_at	GNB5	-1.70
	224756_s_at	ABHD16A /// LY6G6E	-1.70
	214329_x_at	TNFSF10	-1.70
	209827_s_at	IL16	-1.70
	1552275_s_at	PXK	-1.69
	201335_s_at	ARHGEF12	-1.69
	226670_s_at	PABPC1L	-1.69
	213616_at	C18orf10	-1.69
	213082_s_at	SLC35D2	-1.68
	215232_at	ARHGAP44	-1.68
	228524_at	ADCK5	-1.68
	201924_at	AFF1	-1.68
	219914_at	ECEL1	-1.68
	222285_at	IGHD	-1.67

	207122_x_at	SULT1A2	-1.67
	209546_s_at	APOL1	-1.67
	221769_at	SPSB3	-1.67
	214189_s_at	GGA2	-1.67
	209262_s_at	NR2F6	-1.66
	202664_at	WIPF1	-1.66
	230193_at	WDR66	-1.66
	219862_s_at	NARF	-1.66
	226641_at	ANKRD44	-1.66
	204564_at	PCGF3	-1.66
	213827_at	ARHGAP33	-1.66
	219441_s_at	LRRK1	-1.66
	1552623_at	HSH2D	-1.66
	235230_at	PLCXD2	-1.66
	212242_at	TUBA4A	-1.66
	213627_at	MAGED2	-1.66
	225250_at	STIM2	-1.65
	209553_at	VPS8	-1.65
	209479_at	CCDC28A	-1.65
	228532_at	C1orf162	-1.65
	228816_at	ATP6AP1L	-1.65
	202808_at	C10orf26	-1.65
	240159_at	SLC15A2	-1.65
	204820_s_at	BTN3A2 /// BTN3A3	-1.65
	233334_x_at	SLX1A /// SLX1B /// SULT1A3 /// SULT1A4	-1.64
	204674_at	LRMP	-1.64
	235964_x_at	SAMHD1	-1.64
	215184_at	DAPK2	-1.64
	228139_at	RIPK3	-1.64
	209460_at	ABAT	-1.64
	202529_at	PRPSAP1	-1.64
	218429_s_at	C19orf66	-1.64
	212276_at	LPIN1	-1.64
	235061_at	PPM1K	-1.64
	202793_at	LPCAT3	-1.64
	209271_at	BPTF	-1.63
	232914_s_at	SYTL2	-1.63
	228777_at	KBTBD3	-1.63
	211711_s_at	PTEN	-1.62
	244406_at	ZNF20 /// ZNF625	-1.62
	206118_at	STAT4	-1.62
	232112_at	RALGPS2	-1.62
	227352_at	C19orf39	-1.62
	218487_at	ALAD	-1.62

	228298_at	FAM113B	-1.61
	36030_at	IFFO1	-1.61
	211430_s_at	IGHG1 /// IGHG2 /// IGHM /// IGHV4-31	-1.60
	235432_at	NPHP3	-1.60
	235529_x_at	SAMHD1	-1.60
	1557943_at	CNP	-1.60
	205631_at	KIAA0586	-1.60
	202239_at	PARP4	-1.60
	226700_at	U2AF1L4	-1.59
	229937_x_at	LILRB1	-1.59
	220933_s_at	ZCCHC6	-1.59
	223443_s_at	AMZ2P1	-1.59
	212274_at	LPIN1	-1.58
	226763_at	SESTD1	-1.58
	210044_s_at	LYL1	-1.58
	201009_s_at	TXNIP	-1.58
	221778_at	JHDM1D	-1.58
	209141_at	UBE2G1	-1.57
	221080_s_at	DENND1C	-1.56
	225864_at	FAM84B	-1.56

Table 7.3: Genes regulated by LMP1, not CD40 in GC B cells, which are also concurrently altered in HRS cells

Genes up by LMP1 and in HL, not by CD40			*Genes down by LMP1 and in HL, not by CD40*		
Probe Set ID	*Gene name*	*Fold change LMP1*	*Probe Set ID*	*Gene name*	*Fold change LMP1*
201564_s_at	FSCN1	17.61	216615_s_at	HTR3A	-4.41
207900_at	CCL17	8.39	215925_s_at	CD72	-4.34
204897_at	PTGER4	6.09	206641_at	TNFRSF17	-3.72
201631_s_at	IER3	5.53	226799_at	FGD6	-3.71
202734_at	TRIP10	5.33	228377_at	KLHL14	-3.40
214023_x_at	TUBB2B	4.68	215933_s_at	HHEX	-3.40
46665_at	SEMA4C	4.17	207761_s_at	METTL7A	-3.37
202510_s_at	TNFAIP2	4.11	204967_at	SHROOM2	-3.28
201170_s_at	BHLHE40	3.79	220068_at	VPREB3	-3.25
202421_at	IGSF3	3.78	213906_at	MYBL1	-3.22
225102_at	MGLL	3.77	219396_s_at	NEIL1	-3.17
227458_at	CD274	3.67	203865_s_at	ADARB1	-3.13
209835_x_at	CD44	3.47	201677_at	C3orf37	-3.10
213113_s_at	SLC43A3	3.42	230983_at	FAM129C	-3.08
224327_s_at	DGAT2	3.41	230560_at	STXBP6	-3.03
206729_at	TNFRSF8	3.24	201678_s_at	C3orf37	-3.01
201063_at	RCN1	3.20	229021_at	MCTP2	-2.96
207030_s_at	CSRP2	3.20	225540_at	MAP2	-2.96
226064_s_at	DGAT2	3.14	231254_at	LOC100507635	-2.92
219159_s_at	SLAMF7	3.11	218692_at	SYBU	-2.91
220358_at	BATF3	3.00	226809_at	LOC100216479	-2.90
218627_at	DRAM1	2.91	242794_at	MAML3	-2.87
202643_s_at	TNFAIP3	2.86	214366_s_at	ALOX5	-2.85
203010_at	STAT5A	2.85	244467_at	SHISA8	-2.83
202644_s_at	TNFAIP3	2.82	208914_at	GGA2	-2.78
206756_at	CHST7	2.69	242334_at	NLRP4	-2.76
222838_at	SLAMF7	2.67	233463_at	RASSF6	-2.75
1556308_at	PRRT3	2.67	225570_at	SLC41A1	-2.71
204489_s_at	CD44	2.66	221908_at	RNFT2	-2.71
36711_at	MAFF	2.62	203283_s_at	HS2ST1	-2.71
204490_s_at	CD44	2.57	220169_at	TMEM156	-2.68
202910_s_at	CD97	2.56	219518_s_at	ELL3	-2.62
208683_at	CAPN2	2.52	214156_at	MYRIP	-2.62
203411_s_at	LMNA	2.51	226906_s_at	ARHGAP9	-2.61
209949_at	NCF2	2.46	203285_s_at	HS2ST1	-2.60
227645_at	PIK3R5	2.44	206100_at	CPM	-2.59
205569_at	LAMP3	2.36	219667_s_at	BANK1	-2.56
200704_at	LITAF	2.31	211379_x_at	B3GALNT1	-2.56
1405_i_at	CCL5	2.28	206369_s_at	PIK3CG	-2.56
201566_x_at	ID2	2.28	1552323_s_at	FAM122C	-2.53

201426_s_at	VIM	2.26	204446_s_at	ALOX5	-2.52
229801_at	C10orf47	2.24	201752_s_at	ADD3	-2.50
213138_at	ARID5A	2.23	203435_s_at	MME	-2.50
200916_at	TAGLN2	2.17	226666_at	DAAM1	-2.49
223182_s_at	AGPAT3	2.15	1554413_s_at	SNX29P1 ///SNX29P2	-2.47
219275_at	PDCD5	2.13	218807_at	VAV3	-2.47
224925_at	PREX1	2.11	229147_at	RASSF6	-2.36
212089_at	LMNA	2.11	226456_at	RMI2	-2.35
37028_at	PPP1R15A	2.10	203418_at	CCNA2	-2.35
223376_s_at	BRI3	2.00	218862_at	ASB13	-2.34
200799_at	HSPA1A	1.94	221123_x_at	ZNF395	-2.34
223172_s_at	MTFP1	1.90	219901_at	FGD6	-2.33
201473_at	JUNB	1.89	226249_at	SNX30	-2.32
220118_at	ZBTB32	1.88	219517_at	ELL3	-2.30
201565_s_at	ID2	1.86	213772_s_at	GGA2	-2.30
212563_at	BOP1	1.83	205297_s_at	CD79B	-2.29
206380_s_at	CFP	1.80	225637_at	DEF8	-2.29
226121_at	DHRS13	1.78	235400_at	FCRLA	-2.28
33736_at	STOML1	1.76	243109_at	MCTP2	-2.27
214752_x_at	FLNA	1.75	209995_s_at	TCL1A	-2.24
220688_s_at	MRTO4	1.74	201753_s_at	ADD3	-2.23
225440_at	AGPAT3	1.74	39318_at	TCL1A	-2.22
209366_x_at	CYB5A	1.73	231455_at	LINC00487	-2.22
215726_s_at	CYB5A	1.71	227224_at	RALGPS2	-2.21
227804_at	TLCD1	1.71	203434_s_at	MME	-2.21
201858_s_at	SRGN	1.69	205882_x_at	ADD3	-2.21
218982_s_at	MRPS17	1.66	230128_at	IGLL5	-2.20
214011_s_at	NOP16	1.64	221044_s_at	TRIM6-TRIM34	-2.19
201391_at	TRAP1	1.64	204993_at	GNAZ	-2.19
204015_s_at	DUSP4	1.59	1554343_a_at	STAP1	-2.19
212680_x_at	PPP1R14B	1.57	242785_at	EML6	-2.19
			235353_at	SEL1L3	-2.18
			227189_at	CPNE5	-2.18
			220214_at	ZNF215	-2.16
			213326_at	VAMP1	-2.16
			218149_s_at	ZNF395	-2.16
			214047_s_at	MBD4	-2.16
			209200_at	MEF2C	-2.14
			38521_at	CD22	-2.13
			1553102_a_at	CCDC69	-2.11
			226431_at	FAM117B	-2.10
			208913_at	GGA2	-2.09
			229656_s_at	EML6	-2.08
			205922_at	VNN2	-2.08

	210279_at	GPR18	-2.06
	209580_s_at	MBD4	-2.06
	222589_at	NLK	-2.05
	223750_s_at	TLR10	-2.05
	212886_at	CCDC69	-2.05
	209447_at	SYNE1	-2.04
	228551_at	DENND5B	-2.03
	225327_at	KIAA1370	-2.02
	208442_s_at	ATM	-2.01
	225136_at	PLEKHA2	-2.00
	235372_at	FCRLA	-2.00
	1568752_s_at	RGS13	-2.00
	226158_at	KLHL24	-1.99
	217825_s_at	UBE2J1	-1.99
	205997_at	ADAM28	-1.99
	205124_at	MEF2BNB-MEF2B	-1.97
	217824_at	UBE2J1	-1.97
	203806_s_at	FANCA	-1.97
	203140_at	BCL6	-1.97
	210640_s_at	GPER	-1.96
	225763_at	RCSD1	-1.96
	212311_at	SEL1L3	-1.96
	205034_at	CCNE2	-1.95
	213674_x_at	IGHD	-1.94
	204581_at	CD22	-1.94
	236562_at	ZNF439	-1.93
	201688_s_at	TPD52	-1.93
	220059_at	STAP1	-1.92
	227122_at	LOC100507237	-1.91
	218031_s_at	FOXN3	-1.91
	208021_s_at	RFC1	-1.91
	210347_s_at	BCL11A	-1.90
	219498_s_at	BCL11A	-1.90
	218073_s_at	TMEM48	-1.90
	235310_at	GCET2	-1.89
	222891_s_at	BCL11A	-1.89
	227684_at	S1PR2	-1.88
	228030_at	RBM6	-1.88
	225558_at	GIT2	-1.87
	220377_at	KIAA0125	-1.87
	202759_s_at	AKAP2	-1.87
	231093_at	FCRL3	-1.87
	1556579_s_at	IGSF10	-1.86
	226630_at	MIS18BP1	-1.86

213305_s_at	PPP2R5C	-1.86
209085_x_at	RFC1	-1.83
205301_s_at	OGG1	-1.83
225045_at	CCDC88A	-1.82
239355_at	GMCL1	-1.81
212672_at	ATM	-1.81
209709_s_at	HMMR	-1.80
234192_s_at	GKAP1	-1.80
210448_s_at	P2RX5	-1.79
206206_at	CD180	-1.79
201697_s_at	DNMT1	-1.78
200940_s_at	RERE	-1.78
229552_at	LOC283454	-1.78
222233_s_at	DCLRE1C	-1.78
231810_at	BRI3BP	-1.77
221922_at	GPSM2	-1.76
203805_s_at	FANCA	-1.76
209083_at	CORO1A	-1.75
204951_at	RHOH	-1.75
213510_x_at	USP32P2	-1.74
212399_s_at	VGLL4	-1.73
224811_at	LPP	-1.73
213005_s_at	KANK1	-1.72
202213_s_at	CUL4B	-1.72
37577_at	ARHGAP19	-1.72
227134_at	SYTL1	-1.72
202548_s_at	ARHGEF7	-1.72
226001_at	KLHL5	-1.71
218782_s_at	ATAD2	-1.71
203117_s_at	PAN2	-1.71
215058_at	DENND5B	-1.70
209827_s_at	IL16	-1.70
222285_at	IGHD	-1.67
202664_at	WIPF1	-1.66
230193_at	WDR66	-1.66
226641_at	ANKRD44	-1.66
1552623_at	HSH2D	-1.66
240159_at	SLC15A2	-1.65
204674_at	LRMP	-1.64
212276_at	LPIN1	-1.64
235061_at	PPM1K	-1.64
209271_at	BPTF	-1.63
211711_s_at	PTEN	-1.62
228298_at	FAM113B	-1.61

	229937_x_at	LILRB1	-1.59
	212274_at	LPIN1	-1.58
	209141_at	UBE2G1	-1.57

Chapter 8

References

8 References

ADLER, B., SCHAADT, E., KEMPKES, B., ZIMBER-STROBL, U., BAIER, B. & BORNKAMM, G. W. 2002. Control of Epstein-Barr virus reactivation by activated CD40 and viral latent membrane protein 1. *Proc Natl Acad Sci U S A,* 99**,** 437-42.

ALDINUCCI, D., GLOGHINI, A., PINTO, A., DE FILIPPI, R. & CARBONE, A. 2010. The classical Hodgkin's lymphoma microenvironment and its role in promoting tumour growth and immune escape. *J Pathol,* 221**,** 248-63.

ALIZADEH, A. A., EISEN, M. B., DAVIS, R. E., MA, C., LOSSOS, I. S., ROSENWALD, A., BOLDRICK, J. C., SABET, H., TRAN, T., YU, X., POWELL, J. I., YANG, L., MARTI, G. E., MOORE, T., HUDSON, J., JR., LU, L., LEWIS, D. B., TIBSHIRANI, R., SHERLOCK, G., CHAN, W. C., GREINER, T. C., WEISENBURGER, D. D., ARMITAGE, J. O., WARNKE, R., LEVY, R., WILSON, W., GREVER, M. R., BYRD, J. C., BOTSTEIN, D., BROWN, P. O. & STAUDT, L. M. 2000. Distinct types of diffuse large B-cell lymphoma identified by gene expression profiling. *Nature,* 403**,** 503-11.

ALLEN, C. D., ANSEL, K. M., LOW, C., LESLEY, R., TAMAMURA, H., FUJII, N. & CYSTER, J. G. 2004. Germinal center dark and light zone organization is mediated by CXCR4 and CXCR5. *Nat Immunol,* 5**,** 943-52.

ALLEN, C. D. C., OKADA, T., TANG, H. L. & CYSTER, J. G. 2007. Imaging of Germinal Center Selection Events During Affinity Maturation. *Science,* 315**,** 528-531.

ALLENDE, M. L., DREIER, J. L., MANDALA, S. & PROIA, R. L. 2004. Expression of the sphingosine 1-phosphate receptor, S1P1, on T-cells controls thymic emigration. *J Biol Chem,* 279**,** 15396-401.

ALLENDE, M. L., TUYMETOVA, G., LEE, B. G., BONIFACINO, E., WU, Y. P. & PROIA, R. L. 2010. S1P1 receptor directs the release of immature B cells from bone marrow into blood. *J Exp Med,* 207**,** 1113-24.

AME, J. C., SPENLEHAUER, C. & DE MURCIA, G. 2004. The PARP superfamily. *Bioessays,* 26**,** 882-93.

AMINI, R. M., BERGLUND, M., ROSENQUIST, R., VON HEIDEMAN, A., LAGERCRANTZ, S., THUNBERG, U., BERGH, J., SUNDSTROM, C., GLIMELIUS, B. & ENBLAD, G. 2002. A novel B-cell line (U-2932) established from a patient with diffuse large B-cell lymphoma following Hodgkin lymphoma. *Leuk Lymphoma,* 43**,** 2179-89.

ANDERTON, J. A., BOSE, S., VOCKERODT, M., VRZALIKOVA, K., WEI, W., KUO, M., HELIN, K., CHRISTENSEN, J., ROWE, M., MURRAY, P. G. & WOODMAN, C. B. 2011. The H3K27me3 demethylase, KDM6B, is induced by Epstein-Barr virus and over-expressed in Hodgkin's Lymphoma. *Oncogene,* 30**,** 2037-43.

ARIKAWA, K., TAKUWA, N., YAMAGUCHI, H., SUGIMOTO, N., KITAYAMA, J., NAGAWA, H., TAKEHARA, K. & TAKUWA, Y. 2003. Ligand-dependent inhibition of B16 melanoma cell migration and invasion via endogenous S1P2 G protein-coupled receptor. Requirement of inhibition of cellular RAC activity. *J Biol Chem,* 278**,** 32841-51.

BABCOCK, G. J., HOCHBERG, D. & THORLEY-LAWSON, A. D. 2000. The expression pattern of Epstein-Barr virus latent genes in vivo is dependent upon the differentiation stage of the infected B cell. *Immunity,* 13**,** 497-506.

BAER, R., BANKIER, A. T., BIGGIN, M. D., DEININGER, P. L., FARRELL, P. J., GIBSON, T. J., HATFULL, G., HUDSON, G. S., SATCHWELL, S. C., SEGUIN, C. & ET AL. 1984. DNA sequence and expression of the B95-8 Epstein-Barr virus genome. *Nature,* 310**,** 207-11.

BARGOU, R. C., EMMERICH, F., KRAPPMANN, D., BOMMERT, K., MAPARA, M. Y., ARNOLD, W., ROYER, H. D., GRINSTEIN, E., GREINER, A., SCHEIDEREIT, C. & DORKEN, B. 1997.

Constitutive nuclear factor-kappaB-RelA activation is required for proliferation and survival of Hodgkin's disease tumor cells. *J Clin Invest,* 100**,** 2961-9.

BARON, B. W., NUCIFORA, G., MCCABE, N., ESPINOSA, R., 3RD, LE BEAU, M. M. & MCKEITHAN, T. W. 1993. Identification of the gene associated with the recurring chromosomal translocations t(3;14)(q27;q32) and t(3;22)(q27;q11) in B-cell lymphomas. *Proc Natl Acad Sci U S A,* 90**,** 5262-6.

BARTHOLDY, B. & MATTHIAS, P. 2004. Transcriptional control of B cell development and function. *Gene,* 327**,** 1-23.

BASSO, K. & DALLA-FAVERA, R. 2010. BCL6: master regulator of the germinal center reaction and key oncogene in B cell lymphomagenesis. *Adv Immunol,* 105**,** 193-210.

BASSO, K. & DALLA-FAVERA, R. 2012. Roles of BCL6 in normal and transformed germinal center B cells. *Immunol Rev,* 247**,** 172-83.

BEA, S., ZETTL, A., WRIGHT, G., SALAVERRIA, I., JEHN, P., MORENO, V., BUREK, C., OTT, G., PUIG, X., YANG, L., LOPEZ-GUILLERMO, A., CHAN, W. C., GREINER, T. C., WEISENBURGER, D. D., ARMITAGE, J. O., GASCOYNE, R. D., CONNORS, J. M., GROGAN, T. M., BRAZIEL, R., FISHER, R. I., SMELAND, E. B., KVALOY, S., HOLTE, H., DELABIE, J., SIMON, R., POWELL, J., WILSON, W. H., JAFFE, E. S., MONTSERRAT, E., MULLER-HERMELINK, H. K., STAUDT, L. M., CAMPO, E. & ROSENWALD, A. 2005. Diffuse large B-cell lymphoma subgroups have distinct genetic profiles that influence tumor biology and improve gene-expression-based survival prediction. *Blood,* 106**,** 3183-90.

BECHTEL, D., KURTH, J., UNKEL, C. & KUPPERS, R. 2005. Transformation of BCR-deficient germinal-center B cells by EBV supports a major role of the virus in the pathogenesis of Hodgkin and posttransplantation lymphomas. *Blood,* 106**,** 4345-50.

BELL, A. I., GROVES, K., KELLY, G. L., CROOM-CARTER, D., HUI, E., CHAN, A. T. & RICKINSON, A. B. 2006. Analysis of Epstein-Barr virus latent gene expression in endemic Burkitt's lymphoma and nasopharyngeal carcinoma tumour cells by using quantitative real-time PCR assays. *J Gen Virol,* 87**,** 2885-90.

BEN-BASSAT, H., GOLDBLUM, N., MITRANI, S., GOLDBLUM, T., YOFFEY, J. M., COHEN, M. M., BENTWICH, Z., RAMOT, B., KLEIN, E. & KLEIN, G. 1977. Establishment in continuous culture of a new type of lymphocyte from a "Burkitt like" malignant lymphoma (line D.G.-75). *Int J Cancer,* 19**,** 27-33.

BERTRAND, S., BERGER, R., PHILIP, T., BERNHEIM, A., BRYON, P. A., BERTOGLIO, J., DORE, J. F., BRUNAT-MENTIGNY, M. & LENOIR, G. M. 1981. Variant translocation in a non endemic case of Burkitt's lymphoma: t (8;22) in an Epstein--Barr virus negative tumour and in a derived cell line. *Eur J Cancer,* 17**,** 577-84.

BISHOP, G. A. 2004. The multifaceted roles of TRAFs in the regulation of B-cell function. *Nat Rev Immunol,* 4**,** 775-86.

BOHNHORST, J. O., BJORGAN, M. B., THOEN, J. E., NATVIG, J. B. & THOMPSON, K. M. 2001. Bm1-Bm5 classification of peripheral blood B cells reveals circulating germinal center founder cells in healthy individuals and disturbance in the B cell subpopulations in patients with primary Sjogren's syndrome. *J Immunol,* 167**,** 3610-8.

BOLSTAD, B. M., IRIZARRY, R. A., ASTRAND, M. & SPEED, T. P. 2003. A comparison of normalization methods for high density oligonucleotide array data based on variance and bias. *Bioinformatics,* 19**,** 185-93.

BOSE, S., STARCZYNSKI, J., CHUKWUMA, M., BAUMFORTH, K., WEI, W., MORGAN, S., BYRD, P., YING, J., GRUNDY, R., MANN, J. R., TAO, Q., TAYLOR, A. M., MURRAY, P. G. & STANKOVIC, T. 2007. Down-regulation of ATM protein in HRS cells of nodular sclerosis Hodgkin's lymphoma in children occurs in the absence of ATM gene inactivation. *J Pathol,* 213**,** 329-36.

BRAUNINGER, A., SCHMITZ, R., BECHTEL, D., RENNE, C., HANSMANN, M. L. & KUPPERS, R. 2006. Molecular biology of Hodgkin's and Reed/Sternberg cells in Hodgkin's lymphoma. *Int J Cancer,* 118**,** 1853-61.

BRAUNINGER, A., WACKER, H. H., RAJEWSKY, K., KUPPERS, R. & HANSMANN, M. L. 2003. Typing the histogenetic origin of the tumor cells of lymphocyte-rich classical Hodgkin's lymphoma in relation to tumor cells of classical and lymphocyte-predominance Hodgkin's lymphoma. *Cancer Res,* 63**,** 1644-51.

BROWN, K. D., HOSTAGER, B. S. & BISHOP, G. A. 2001. Differential signaling and tumor necrosis factor receptor-associated factor (TRAF) degradation mediated by CD40 and the Epstein-Barr virus oncoprotein latent membrane protein 1 (LMP1). *J Exp Med,* 193**,** 943-54.

BROWN, K. D., HOSTAGER, B. S. & BISHOP, G. A. 2002. Regulation of TRAF2 signaling by self-induced degradation. *J Biol Chem,* 277**,** 19433-8.

BRUNE, V., TIACCI, E., PFEIL, I., DORING, C., ECKERLE, S., VAN NOESEL, C. J., KLAPPER, W., FALINI, B., VON HEYDEBRECK, A., METZLER, D., BRAUNINGER, A., HANSMANN, M. L. & KUPPERS, R. 2008. Origin and pathogenesis of nodular lymphocyte-predominant Hodgkin lymphoma as revealed by global gene expression analysis. *J Exp Med,* 205**,** 2251-68.

BUETTNER, M., MEYER, B., SCHRECK, S. & NIEDOBITEK, G. 2007. Expression of RANTES and MCP-1 in epithelial cells is regulated via LMP1 and CD40. *Int J Cancer,* 121**,** 2703-10.

CABANNES, E., KHAN, G., AILLET, F., JARRETT, R. F. & HAY, R. T. 1999. Mutations in the IkBa gene in Hodgkin's disease suggest a tumour suppressor role for IkappaBalpha. *Oncogene,* 18**,** 3063-70.

CALDWELL, R. G., WILSON, J. B., ANDERSON, S. J. & LONGNECKER, R. 1998. Epstein-Barr virus LMP2A drives B cell development and survival in the absence of normal B cell receptor signals. *Immunity,* 9**,** 405-11.

CAMPO, E., SWERDLOW, S. H., HARRIS, N. L., PILERI, S., STEIN, H. & JAFFE, E. S. 2011. The 2008 WHO classification of lymphoid neoplasms and beyond: evolving concepts and practical applications. *Blood,* 117**,** 5019-32.

CARBONE, A., GLOGHINI, A., GATTEI, V., ALDINUCCI, D., DEGAN, M., DE PAOLI, P., ZAGONEL, V. & PINTO, A. 1995a. Expression of functional CD40 antigen on Reed-Sternberg cells and Hodgkin's disease cell lines. *Blood,* 85**,** 780-789.

CARBONE, A., GLOGHINI, A., GRUSS, H. J. & PINTO, A. 1995b. CD40 ligand is constitutively expressed in a subset of T cell lymphomas and on the microenvironmental reactive T cells of follicular lymphomas and Hodgkin's disease. *Am J Pathol,* 147**,** 912-22.

CARDESA-SALZMANN, T. M., COLOMO, L., GUTIERREZ, G., CHAN, W. C., WEISENBURGER, D., CLIMENT, F., GONZALEZ-BARCA, E., MERCADAL, S., ARENILLAS, L., SERRANO, S., TUBBS, R., DELABIE, J., GASCOYNE, R. D., CONNORS, J. M., MATE, J. L., RIMSZA, L., BRAZIEL, R., ROSENWALD, A., LENZ, G., WRIGHT, G., JAFFE, E. S., STAUDT, L., JARES, P., LOPEZ-GUILLERMO, A. & CAMPO, E. 2011. High microvessel density determines a poor outcome in patients with diffuse large B-cell lymphoma treated with rituximab plus chemotherapy. *Haematologica,* 96**,** 996-1001.

CARON, G., LE GALLOU, S., LAMY, T., TARTE, K. & FEST, T. 2009. CXCR4 expression functionally discriminates centroblasts versus centrocytes within human germinal center B cells. *J Immunol,* 182**,** 7595-602.

CASOLA, S., OTIPOBY, K. L., ALIMZHANOV, M., HUMME, S., UYTTERSPROT, N., KUTOK, J. L., CARROLL, M. C. & RAJEWSKY, K. 2004. B cell receptor signal strength determines B cell fate. *Nat Immunol,* 5**,** 317-27.

CASTIGLI, E., WILSON, S. A., SCOTT, S., DEDEOGLU, F., XU, S., LAM, K. P., BRAM, R. J., JABARA, H. & GEHA, R. S. 2005. TACI and BAFF-R mediate isotype switching in B cells. *J Exp Med,* 201**,** 35-9.

CATTORETTI, G., CHANG, C. C., CECHOVA, K., ZHANG, J., YE, B. H., FALINI, B., LOUIE, D. C., OFFIT, K., CHAGANTI, R. S. & DALLA-FAVERA, R. 1995. BCL-6 protein is expressed in germinal-center B cells. *Blood,* 86**,** 45-53.

CATTORETTI, G., MANDELBAUM, J., LEE, N., CHAVES, A. H., MAHLER, A. M., CHADBURN, A., DALLA-FAVERA, R., PASQUALUCCI, L. & MACLENNAN, A. J. 2009. Targeted disruption of the S1P2 sphingosine 1-phosphate receptor gene leads to diffuse large B-cell lymphoma formation. *Cancer Res,* 69**,** 8686-92.

CHAGANTI, S., BELL, A. I., PASTOR, N. B., MILNER, A. E., DRAYSON, M., GORDON, J. & RICKINSON, A. B. 2005. Epstein-Barr virus infection in vitro can rescue germinal center B cells with inactivated immunoglobulin genes. *Blood,* 106**,** 4249-52.

CHEN, P., GUO, X., ZHOU, H., ZHANG, W., ZENG, Z., LIAO, Q., LI, X., XIANG, B., YANG, J., MA, J., ZHOU, M., PENG, S., XIANG, J., LI, X., L, E. C., XIONG, W., MCCARTHY, J. B. & LI, G. 2013. SPLUNC1 regulates cell progression and apoptosis through the miR-141-PTEN/p27 pathway, but is hindered by LMP1. *PLoS One,* 8**,** e56929.

CHIBA, K., YANAGAWA, Y., MASUBUCHI, Y., KATAOKA, H., KAWAGUCHI, T., OHTSUKI, M. & HOSHINO, Y. 1998. FTY720, a novel immunosuppressant, induces sequestration of circulating mature lymphocytes by acceleration of lymphocyte homing in rats. I. FTY720 selectively decreases the number of circulating mature lymphocytes by acceleration of lymphocyte homing. *J Immunol,* 160**,** 5037-44.

COHEN, J. H., REVILLARD, J. P., MAGAUD, J. P., LENOIR, G., VUILLAUME, M., MANEL, A. M., VINCENT, C. & BRYON, P. A. 1987. B-cell maturation stages of Burkitt's lymphoma cell lines according to Epstein-Barr virus status and type of chromosome translocation. *J Natl Cancer Inst,* 78**,** 235-42.

COIFFIER, B. 2001. Diffuse large cell lymphoma. *Curr Opin Oncol,* 13**,** 325-34.

COMPAGNO, M., LIM, W. K., GRUNN, A., NANDULA, S. V., BRAHMACHARY, M., SHEN, Q., BERTONI, F., PONZONI, M., SCANDURRA, M., CALIFANO, A., BHAGAT, G., CHADBURN, A., DALLA-FAVERA, R. & PASQUALUCCI, L. 2009. Mutations of multiple genes cause deregulation of NF-kappaB in diffuse large B-cell lymphoma. *Nature,* 459**,** 717-21.

CYSTER, J. G. 2005. Chemokines, sphingosine-1-phosphate, and cell migration in secondary lymphoid organs. *Annu Rev Immunol,* 23**,** 127-59.

CYSTER, J. G. 2010. B cell follicles and antigen encounters of the third kind. *Nat Immunol,* 11**,** 989-96.

CYSTER, J. G., ANSEL, K. M., REIF, K., EKLAND, E. H., HYMAN, P. L., TANG, H. L., LUTHER, S. A. & NGO, V. N. 2000. Follicular stromal cells and lymphocyte homing to follicles. *Immunol Rev,* 176**,** 181-93.

DAVIS, R. E., BROWN, K. D., SIEBENLIST, U. & STAUDT, L. M. 2001. Constitutive Nuclear Factor κB Activity Is Required for Survival of Activated B Cell–like Diffuse Large B Cell Lymphoma Cells. *The Journal of Experimental Medicine,* 194**,** 1861-1874.

DAVIS, R. E., NGO, V. N., LENZ, G., TOLAR, P., YOUNG, R. M., ROMESSER, P. B., KOHLHAMMER, H., LAMY, L., ZHAO, H., YANG, Y., XU, W., SHAFFER, A. L., WRIGHT, G., XIAO, W., POWELL, J., JIANG, J. K., THOMAS, C. J., ROSENWALD, A., OTT, G., MULLER-HERMELINK, H. K., GASCOYNE, R. D., CONNORS, J. M., JOHNSON, N. A., RIMSZA, L. M., CAMPO, E., JAFFE, E. S., WILSON, W. H., DELABIE, J., SMELAND, E. B., FISHER, R. I., BRAZIEL, R. M., TUBBS, R. R., COOK, J. R., WEISENBURGER, D. D., CHAN, W. C., PIERCE, S. K. & STAUDT, L. M. 2010. Chronic active B-cell-receptor signalling in diffuse large B-cell lymphoma. *Nature,* 463**,** 88-92.

DIEHL, V., KIRCHNER, H. H., BURRICHTER, H., STEIN, H., FONATSCH, C., GERDES, J., SCHAADT, M., HEIT, W., UCHANSKA-ZIEGLER, B., ZIEGLER, A., HEINTZ, F. & SUENO, K. 1982. Characteristics of Hodgkin's disease-derived cell lines. *Cancer Treat Rep,* 66**,** 615-32.

DIRMEIER, U., HOFFMANN, R., KILGER, E., SCHULTHEISS, U., BRISENO, C., GIRES, O., KIESER, A., EICK, D., SUGDEN, B. & HAMMERSCHMIDT, W. 2005. Latent membrane protein 1 of Epstein-Barr virus coordinately regulates proliferation with control of apoptosis. *Oncogene,* 24**,** 1711-7.

DISANTO, J. P., BONNEFOY, J. Y., GAUCHAT, J. F., FISCHER, A. & DE SAINT BASILE, G. 1993. CD40 ligand mutations in x-linked immunodeficiency with hyper-IgM. *Nature,* 361**,** 541-3.

DU, W., TAKUWA, N., YOSHIOKA, K., OKAMOTO, Y., GONDA, K., SUGIHARA, K., FUKAMIZU, A., ASANO, M. & TAKUWA, Y. 2010. S1P(2), the G protein-coupled receptor for sphingosine-1-phosphate, negatively regulates tumor angiogenesis and tumor growth in vivo in mice. *Cancer Res,* 70**,** 772-81.

DUTTON, A., O'NEIL, J. D., MILNER, A. E., REYNOLDS, G. M., STARCZYNSKI, J., CROCKER, J., YOUNG, L. S. & MURRAY, P. G. 2004. Expression of the cellular FLICE-inhibitory protein (c-FLIP) protects Hodgkin's lymphoma cells from autonomous Fas-mediated death. *Proceedings of the National Academy of Sciences of the United States of America,* 101**,** 6611-6616.

DUTTON, A., REYNOLDS, G. M., DAWSON, C. W., YOUNG, L. S. & MURRAY, P. G. 2005. Constitutive activation of phosphatidyl-inositide 3 kinase contributes to the survival of Hodgkin's lymphoma cells through a mechanism involving Akt kinase and mTOR. *J Pathol,* 205**,** 498-506.

DUTTON, A., WOODMAN, C. B., CHUKWUMA, M. B., LAST, J. I., WEI, W., VOCKERODT, M., BAUMFORTH, K. R., FLAVELL, J. R., ROWE, M., TAYLOR, A. M., YOUNG, L. S. & MURRAY, P. G. 2007. Bmi-1 is induced by the Epstein-Barr virus oncogene LMP1 and regulates the expression of viral target genes in Hodgkin lymphoma cells. *Blood,* 109**,** 2597-603.

EMMERICH, F., MEISER, M., HUMMEL, M., DEMEL, G., FOSS, H. D., JUNDT, F., MATHAS, S., KRAPPMANN, D., SCHEIDEREIT, C., STEIN, H. & DORKEN, B. 1999. Overexpression of I kappa B alpha without inhibition of NF-kappaB activity and mutations in the I kappa B alpha gene in Reed-Sternberg cells. *Blood,* 94**,** 3129-34.

EMMERICH, F., THEURICH, S., HUMMEL, M., HAEFFKER, A., VRY, M. S., DOHNER, K., BOMMERT, K., STEIN, H. & DORKEN, B. 2003. Inactivating I kappa B epsilon mutations in Hodgkin/Reed-Sternberg cells. *J Pathol,* 201**,** 413-20.

EPSTEIN, A. L., LEVY, R., KIM, H., HENLE, W., HENLE, G. & KAPLAN, H. S. 1978. Biology of the human malignant lymphomas. IV. Functional characterization of ten diffuse histiocytic lymphoma cell lines. *Cancer,* 42**,** 2379-91.

EPSTEIN, M. A., ACHONG, B. G. & BARR, Y. M. 1964. VIRUS PARTICLES IN CULTURED LYMPHOBLASTS FROM BURKITT'S LYMPHOMA. *Lancet,* 1**,** 702-3.

FALK, M. H., TESCH, H., STEIN, H., DIEHL, V., JONES, D. B., FONATSCH, C. & BORNKAMM, G. W. 1987. Phenotype versus immunoglobulin and T-cell receptor genotype of Hodgkin-derived cell lines: activation of immature lymphoid cells in Hodgkin's disease. *Int J Cancer,* 40**,** 262-9.

FISCHER, M., JUREMALM, M., OLSSON, N., BACKLIN, C., SUNDSTROM, C., NILSSON, K., ENBLAD, G. & NILSSON, G. 2003. Expression of CCL5/RANTES by Hodgkin and Reed-Sternberg cells and its possible role in the recruitment of mast cells into lymphomatous tissue. *Int J Cancer,* 107**,** 197-201.

FRICK, M., DORKEN, B. & LENZ, G. 2011. The molecular biology of diffuse large B-cell lymphoma. *Ther Adv Hematol,* 2**,** 369-79.

GATTO, D. & BRINK, R. 2013. B cell localization: regulation by EBI2 and its oxysterol ligand. *Trends Immunol,* 34**,** 336-41.

GATTO, D., PAUS, D., BASTEN, A., MACKAY, C. R. & BRINK, R. 2009. Guidance of B cells by the orphan G protein-coupled receptor EBI2 shapes humoral immune responses. *Immunity,* 31**,** 259-69.

GEIGER, T. R. & MARTIN, J. M. 2006. The Epstein-Barr virus-encoded LMP-1 oncoprotein negatively affects Tyk2 phosphorylation and interferon signaling in human B cells. *J Virol,* 80**,** 11638-50.

GEORGAKIS, G. V., LI, Y., RASSIDAKIS, G. Z., MEDEIROS, L. J., MILLS, G. B. & YOUNES, A. 2006. Inhibition of the phosphatidylinositol-3 kinase/Akt promotes G1 cell cycle arrest and apoptosis in Hodgkin lymphoma. *Br J Haematol,* 132**,** 503-11.

GIRES, O., KOHLHUBER, F., KILGER, E., BAUMANN, M., KIESER, A., KAISER, C., ZEIDLER, R., SCHEFFER, B., UEFFING, M. & HAMMERSCHMIDT, W. 1999. Latent membrane protein 1 of Epstein-Barr virus interacts with JAK3 and activates STAT proteins. *EMBO J,* 18**,** 3064-73.

GIRES, O., ZIMBER-STROBL, U., GONNELLA, R., UEFFING, M., MARSCHALL, G., ZEIDLER, R., PICH, D. & HAMMERSCHMIDT, W. 1997. Latent membrane protein 1 of Epstein-Barr virus mimics a constitutively active receptor molecule. *Embo J,* 16**,** 6131-40.

GOOD-JACOBSON, K. L., SZUMILAS, C. G., CHEN, L., SHARPE, A. H., TOMAYKO, M. M. & SHLOMCHIK, M. J. 2010. PD-1 regulates germinal center B cell survival and the formation and affinity of long-lived plasma cells. *Nat Immunol,* 11**,** 535-42.

GRAHAM, J. P., ARCIPOWSKI, K. M. & BISHOP, G. A. 2010. Differential B-lymphocyte regulation by CD40 and its viral mimic, latent membrane protein 1. *Immunol Rev,* 237**,** 226-48.

GREEN, J. A. & CYSTER, J. G. 2012. S1PR2 links germinal center confinement and growth regulation. *Immunol Rev,* 247**,** 36-51.

GREEN, J. A., SUZUKI, K., CHO, B., WILLISON, L. D., PALMER, D., ALLEN, C. D., SCHMIDT, T. H., XU, Y., PROIA, R. L., COUGHLIN, S. R. & CYSTER, J. G. 2011. The sphingosine 1-phosphate receptor S1P(2) maintains the homeostasis of germinal center B cells and promotes niche confinement. *Nat Immunol,* 12**,** 672-80.

HALUSKA, F. G., TSUJIMOTO, Y. & CROCE, C. M. 1987. The t(8;14) chromosome translocation of the Burkitt lymphoma cell line Daudi occurred during immunoglobulin gene rearrangement and involved the heavy chain diversity region. *Proceedings of the National Academy of Sciences,* 84**,** 6835-6839.

HAN, J. I., HUANG, N. N., KIM, D. U. & KEHRL, J. H. 2006. RGS1 and RGS13 mRNA silencing in a human B lymphoma line enhances responsiveness to chemoattractants and impairs desensitization. *J Leukoc Biol,* 79**,** 1357-68.

HAO, Z., DUNCAN, G. S., SEAGAL, J., SU, Y. W., HONG, C., HAIGHT, J., CHEN, N. J., ELIA, A., WAKEHAM, A., LI, W. Y., LIEPA, J., WOOD, G. A., CASOLA, S., RAJEWSKY, K. & MAK, T. W. 2008. Fas receptor expression in germinal-center B cells is essential for T and B lymphocyte homeostasis. *Immunity,* 29**,** 615-27.

HARTL, P. & LIPP, M. 1987. Generation of a variant t(2;8) translocation of Burkitt's lymphoma by site-specific recombination via the kappa light-chain joining signals. *Molecular and Cellular Biology,* 7**,** 2037-2045.

HATZIVASSILIOU, E., MILLER, W. E., RAAB-TRAUB, N., KIEFF, E. & MOSIALOS, G. 1998. A fusion of the EBV latent membrane protein-1 (LMP1) transmembrane domains to the CD40 cytoplasmic domain is similar to LMP1 in constitutive activation of epidermal growth factor receptor expression, nuclear factor-kappa B, and stress-activated protein kinase. *J Immunol,* 160**,** 1116-21.

HATZIVASSILIOU, E. G., KIEFF, E. & MOSIALOS, G. 2007. Constitutive CD40 signaling phenocopies the transforming function of the Epstein-Barr virus oncoprotein LMP1 in vitro. *Leuk Res,* 31**,** 315-20.

HE, Z., XIN, B., YANG, X., CHAN, C. & CAO, L. 2000. Nuclear factor-kappaB activation is involved in LMP1-mediated transformation and tumorigenesis of rat-1 fibroblasts. *Cancer Res,* 60**,** 1845-8.

HENNINO, A., BERARD, M., KRAMMER, P. H. & DEFRANCE, T. 2001. FLICE-inhibitory protein is a key regulator of germinal center B cell apoptosis. *J Exp Med,* 193**,** 447-58.

HIGUCHI, M., KIEFF, E. & IZUMI, K. M. 2002. The Epstein-Barr virus latent membrane protein 1 putative Janus kinase 3 (JAK3) binding domain does not mediate JAK3 association or activation in B-lymphoma or lymphoblastoid cell lines. *J Virol,* 76**,** 455-9.

HINZ, M., LEMKE, P., ANAGNOSTOPOULOS, I., HACKER, C., KRAPPMANN, D., MATHAS, S., DORKEN, B., ZENKE, M., STEIN, H. & SCHEIDEREIT, C. 2002. Nuclear factor kappaB-dependent gene expression profiling of Hodgkin's disease tumor cells, pathogenetic significance, and link to constitutive signal transducer and activator of transcription 5a activity. *J Exp Med,* 196**,** 605-17.

HODGKIN 1832. On some Morbid Appearances of the Absorbent Glands and Spleen. *Med Chir Trans,* 17**,** 68-114.

HOELLER, S., TZANKOV, A., PILERI, S. A., WENT, P. & DIRNHOFER, S. 2010. Epstein-Barr virus–positive diffuse large B-cell lymphoma in elderly patients is rare in Western populations. *Human pathology,* 41**,** 352-357.

HOGERKORP, C. M. & BORREBAECK, C. A. 2006. The human CD77- B cell population represents a heterogeneous subset of cells comprising centroblasts, centrocytes, and plasmablasts, prompting phenotypical revision. *J Immunol,* 177**,** 4341-9.

HOMIG-HOLZEL, C., HOJER, C., RASTELLI, J., CASOLA, S., STROBL, L. J., MULLER, W., QUINTANILLA-MARTINEZ, L., GEWIES, A., RULAND, J., RAJEWSKY, K. & ZIMBER-STROBL, U. 2008. Constitutive CD40 signaling in B cells selectively activates the noncanonical NF-kappaB pathway and promotes lymphomagenesis. *J Exp Med,* 205**,** 1317-29.

HUMMEL, M., ZIEMANN, K., LAMMERT, H., PILERI, S., SABATTINI, E. & STEIN, H. 1995. Hodgkin's Disease with Monoclonal and Polyclonal Populations of Reed–Sternberg Cells. *New England Journal of Medicine,* 333**,** 901-906.

HWANG, I. Y., HWANG, K. S., PARK, C., HARRISON, K. A. & KEHRL, J. H. 2013. Rgs13 constrains early B cell responses and limits germinal center sizes. *PLoS One,* 8**,** e60139.

IQBAL, J., GREINER, T. C., PATEL, K., DAVE, B. J., SMITH, L., JI, J., WRIGHT, G., SANGER, W. G., PICKERING, D. L., JAIN, S., HORSMAN, D. E., SHEN, Y., FU, K., WEISENBURGER, D. D., HANS, C. P., CAMPO, E., GASCOYNE, R. D., ROSENWALD, A., JAFFE, E. S., DELABIE, J., RIMSZA, L., OTT, G., MULLER-HERMELINK, H. K., CONNORS, J. M., VOSE, J. M., MCKEITHAN, T., STAUDT, L. M. & CHAN, W. C. 2007. Distinctive patterns of BCL6 molecular alterations and their functional consequences in different subgroups of diffuse large B-cell lymphoma. *Leukemia,* 21**,** 2332-43.

IRIZARRY, R. A., BOLSTAD, B. M., COLLIN, F., COPE, L. M., HOBBS, B. & SPEED, T. P. 2003. Summaries of Affymetrix GeneChip probe level data. *Nucleic Acids Res,* 31**,** e15.

IRSCH, J., WOLF, J., TESCH, H., DIEHL, V., RADBRUCH, A. & STARATSCHEK-JOX, A. 2001. Class switch recombination was specifically targeted to immunoglobulin (Ig)G4 or IgA in Hodgkin's disease-derived cell lines. *Br J Haematol,* 113**,** 785-93.

JEGO, G., ROBILLARD, N., PUTHIER, D., AMIOT, M., ACCARD, F., PINEAU, D., HAROUSSEAU, J. L., BATAILLE, R. & PELLAT-DECEUNYNCK, C. 1999. Reactive plasmacytoses are expansions of plasmablasts retaining the capacity to differentiate into plasma cells. *Blood,* 94**,** 701-12.

JOOS, S., KUPPER, M., OHL, S., VON BONIN, F., MECHTERSHEIMER, G., BENTZ, M., MARYNEN, P., MOLLER, P., PFREUNDSCHUH, M., TRUMPER, L. & LICHTER, P. 2000. Genomic imbalances including amplification of the tyrosine kinase gene JAK2 in CD30+ Hodgkin cells. *Cancer Res,* 60**,** 549-52.

JOOS, S., MENZ, C. K., WROBEL, G., SIEBERT, R., GESK, S., OHL, S., MECHTERSHEIMER, G., TRUMPER, L., MOLLER, P., LICHTER, P. & BARTH, T. F. 2002. Classical Hodgkin lymphoma

is characterized by recurrent copy number gains of the short arm of chromosome 2. *Blood,* 99**,** 1381-7.

JUNDT, F., ACIKGOZ, O., KWON, S. H., SCHWARZER, R., ANAGNOSTOPOULOS, I., WIESNER, B., MATHAS, S., HUMMEL, M., STEIN, H., REICHARDT, H. M. & DORKEN, B. 2008. Aberrant expression of Notch1 interferes with the B-lymphoid phenotype of neoplastic B cells in classical Hodgkin lymphoma. *Leukemia,* 22**,** 1587-94.

JUNGNICKEL, B., STARATSCHEK-JOX, A., BRAUNINGER, A., SPIEKER, T., WOLF, J., DIEHL, V., HANSMANN, M. L., RAJEWSKY, K. & KUPPERS, R. 2000. Clonal deleterious mutations in the IkappaBalpha gene in the malignant cells in Hodgkin's lymphoma. *J Exp Med,* 191**,** 395-402.

KAMESAKI, H., FUKUHARA, S., TATSUMI, E., UCHINO, H., YAMABE, H., MIWA, H., SHIRAKAWA, S., HATANAKA, M. & HONJO, T. 1986. Cytochemical, immunologic, chromosomal, and molecular genetic analysis of a novel cell line derived from Hodgkin's disease. *Blood,* 68**,** 285-92.

KANZLER, H., KUPPERS, R., HANSMANN, M. L. & RAJEWSKY, K. 1996. Hodgkin and Reed-Sternberg cells in Hodgkin's disease represent the outgrowth of a dominant tumor clone derived from (crippled) germinal center B cells. *J Exp Med,* 184**,** 1495-505.

KAPP, U., YEH, W. C., PATTERSON, B., ELIA, A. J., KAGI, D., HO, A., HESSEL, A., TIPSWORD, M., WILLIAMS, A., MIRTSOS, C., ITIE, A., MOYLE, M. & MAK, T. W. 1999. Interleukin 13 is secreted by and stimulates the growth of Hodgkin and Reed-Sternberg cells. *J Exp Med,* 189**,** 1939-46.

KATO, M., SANADA, M., KATO, I., SATO, Y., TAKITA, J., TAKEUCHI, K., NIWA, A., CHEN, Y., NAKAZAKI, K., NOMOTO, J., ASAKURA, Y., MUTO, S., TAMURA, A., IIO, M., AKATSUKA, Y., HAYASHI, Y., MORI, H., IGARASHI, T., KUROKAWA, M., CHIBA, S., MORI, S., ISHIKAWA, Y., OKAMOTO, K., TOBINAI, K., NAKAGAMA, H., NAKAHATA, T., YOSHINO, T., KOBAYASHI, Y. & OGAWA, S. 2009. Frequent inactivation of A20 in B-cell lymphomas. *Nature,* 459**,** 712-6.

KAWABE, T., NAKA, T., YOSHIDA, K., TANAKA, T., FUJIWARA, H., SUEMATSU, S., YOSHIDA, N., KISHIMOTO, T. & KIKUTANI, H. 1994. The immune responses in CD40-deficient mice: impaired immunoglobulin class switching and germinal center formation. *Immunity,* 1**,** 167-78.

KAYE, K. M., IZUMI, K. M. & KIEFF, E. 1993. Epstein-Barr virus latent membrane protein 1 is essential for B-lymphocyte growth transformation. *Proc Natl Acad Sci U S A,* 90**,** 9150-4.

KILGER, E., KIESER, A., BAUMANN, M. & HAMMERSCHMIDT, W. 1998. Epstein-Barr virus-mediated B-cell proliferation is dependent upon latent membrane protein 1, which simulates an activated CD40 receptor. *EMBO J,* 17**,** 1700-9.

KIM, L. H., EOW, G. I., PEH, S. C. & POPPEMA, S. 2003. The role of CD30, CD40 and CD95 in the regulation of proliferation and apoptosis in classical Hodgkin's lymphoma. *Pathology,* 35**,** 428-35.

KITANO, M., MORIYAMA, S., ANDO, Y., HIKIDA, M., MORI, Y., KUROSAKI, T. & OKADA, T. 2011. Bcl6 protein expression shapes pre-germinal center B cell dynamics and follicular helper T cell heterogeneity. *Immunity,* 34**,** 961-72.

KLEIN, U., CASOLA, S., CATTORETTI, G., SHEN, Q., LIA, M., MO, T., LUDWIG, T., RAJEWSKY, K. & DALLA-FAVERA, R. 2006. Transcription factor IRF4 controls plasma cell differentiation and class-switch recombination. *Nat Immunol,* 7**,** 773-82.

KLEIN, U. & DALLA-FAVERA, R. 2008. Germinal centres: role in B-cell physiology and malignancy. *Nat Rev Immunol,* 8**,** 22-33.

KLEIN, U., RAJEWSKY, K. & KUPPERS, R. 1998. Human immunoglobulin (Ig)M+IgD+ peripheral blood B cells expressing the CD27 cell surface antigen carry somatically mutated variable

region genes: CD27 as a general marker for somatically mutated (memory) B cells. *J Exp Med,* 188**,** 1679-89.

KLEIN, U., TU, Y., STOLOVITZKY, G. A., KELLER, J. L., HADDAD, J., JR., MILJKOVIC, V., CATTORETTI, G., CALIFANO, A. & DALLA-FAVERA, R. 2003. Transcriptional analysis of the B cell germinal center reaction. *Proc Natl Acad Sci U S A,* 100**,** 2639-44.

KORKOLOPOULOU, P., THYMARA, I., KAVANTZAS, N., VASSILAKOPOULOS, T. P., ANGELOPOULOU, M. K., KOKORIS, S. I., DIMITRIADOU, E. M., SIAKANTARIS, M. P., ANARGYROU, K., PANAYIOTIDIS, P., TSENGA, A., ANDROULAKI, A., DOUSSIS-ANAGNOSTOPOULOU, I. A., PATSOURIS, E. & PANGALIS, G. A. 2005. Angiogenesis in Hodgkin's lymphoma: a morphometric approach in 286 patients with prognostic implications. *Leukemia,* 19**,** 894-900.

KORTHAUER, U., GRAF, D., MAGES, H. W., BRIERE, F., PADAYACHEE, M., MALCOLM, S., UGAZIO, A. G., NOTARANGELO, L. D., LEVINSKY, R. J. & KROCZEK, R. A. 1993. Defective expression of T-cell CD40 ligand causes X-linked immunodeficiency with hyper-IgM. *Nature,* 361**,** 539-41.

KRAPPMANN, D., EMMERICH, F., KORDES, U., SCHARSCHMIDT, E., DORKEN, B. & SCHEIDEREIT, C. 1999. Molecular mechanisms of constitutive NF-kappaB/Rel activation in Hodgkin/Reed-Sternberg cells. *Oncogene,* 18**,** 943-53.

KRAUS, Z. J., NAKANO, H. & BISHOP, G. A. 2009. TRAF5 is a critical mediator of in vitro signals and in vivo functions of LMP1, the viral oncogenic mimic of CD40. *Proc Natl Acad Sci U S A,* 106**,** 17140-5.

KUBE, D., HOLTICK, U., VOCKERODT, M., AHMADI, T., HAIER, B., BEHRMANN, I., HEINRICH, P. C., DIEHL, V. & TESCH, H. 2001. STAT3 is constitutively activated in Hodgkin cell lines. *Blood,* 98**,** 762-70.

KULWICHIT, W., EDWARDS, R. H., DAVENPORT, E. M., BASKAR, J. F., GODFREY, V. & RAAB-TRAUB, N. 1998. Expression of the Epstein-Barr virus latent membrane protein 1 induces B cell lymphoma in transgenic mice. *Proc Natl Acad Sci U S A,* 95**,** 11963-8.

KUPPERS, R. 2005. Mechanisms of B-cell lymphoma pathogenesis. *Nat Rev Cancer,* 5**,** 251-62.

KUPPERS, R. 2009. The biology of Hodgkin's lymphoma. *Nat Rev Cancer,* 9**,** 15-27.

KUPPERS, R., ENGERT, A. & HANSMANN, M. L. 2012. Hodgkin lymphoma. *J Clin Invest,* 122**,** 3439-47.

KÜPPERS, R., HANSMANN, M. L. & RAJEWSKY, K. 1998. Clonality and germinal centre B-cell derivation of Hodgkin/Reed-Sternberg cells in Hodgkin's disease. *Annals of Oncology,* 9**,** S17-S20.

KUPPERS, R., KLEIN, U., HANSMANN, M. L. & RAJEWSKY, K. 1999. Cellular origin of human B-cell lymphomas. *N Engl J Med,* 341**,** 1520-9.

KUPPERS, R., RAJEWSKY, K., ZHAO, M., SIMONS, G., LAUMANN, R., FISCHER, R. & HANSMANN, M. L. 1994. Hodgkin disease: Hodgkin and Reed-Sternberg cells picked from histological sections show clonal immunoglobulin gene rearrangements and appear to be derived from B cells at various stages of development. *Proc Natl Acad Sci U S A,* 91**,** 10962-6.

KURTH, J., HANSMANN, M. L., RAJEWSKY, K. & KUPPERS, R. 2003. Epstein-Barr virus-infected B cells expanding in germinal centers of infectious mononucleosis patients do not participate in the germinal center reaction. *Proc Natl Acad Sci U S A,* 100**,** 4730-5.

LAGRESLE, C., BELLA, C., DANIEL, P. T., KRAMMER, P. H. & DEFRANCE, T. 1995. Regulation of germinal center B cell differentiation. Role of the human APO-1/Fas (CD95) molecule. *J Immunol,* 154**,** 5746-56.

LAM, N. & SUGDEN, B. 2003. CD40 and its viral mimic, LMP1: similar means to different ends. *Cell Signal,* 15**,** 9-16.

LAMPRECHT, B., KREHER, S., ANAGNOSTOPOULOS, I., JÖHRENS, K., MONTELEONE, G., JUNDT, F., STEIN, H., JANZ, M., DÖRKEN, B. & MATHAS, S. 2008. Aberrant expression of the Th2

cytokine IL-21 in Hodgkin lymphoma cells regulates STAT3 signaling and attracts Treg cells via regulation of MIP-3α. *Blood,* 112**,** 3339-3347.

LENZ, G., DAVIS, R. E., NGO, V. N., LAM, L., GEORGE, T. C., WRIGHT, G. W., DAVE, S. S., ZHAO, H., XU, W., ROSENWALD, A., OTT, G., MULLER-HERMELINK, H. K., GASCOYNE, R. D., CONNORS, J. M., RIMSZA, L. M., CAMPO, E., JAFFE, E. S., DELABIE, J., SMELAND, E. B., FISHER, R. I., CHAN, W. C. & STAUDT, L. M. 2008a. Oncogenic CARD11 mutations in human diffuse large B cell lymphoma. *Science,* 319**,** 1676-9.

LENZ, G., WRIGHT, G., DAVE, S. S., XIAO, W., POWELL, J., ZHAO, H., XU, W., TAN, B., GOLDSCHMIDT, N., IQBAL, J., VOSE, J., BAST, M., FU, K., WEISENBURGER, D. D., GREINER, T. C., ARMITAGE, J. O., KYLE, A., MAY, L., GASCOYNE, R. D., CONNORS, J. M., TROEN, G., HOLTE, H., KVALOY, S., DIERICKX, D., VERHOEF, G., DELABIE, J., SMELAND, E. B., JARES, P., MARTINEZ, A., LOPEZ-GUILLERMO, A., MONTSERRAT, E., CAMPO, E., BRAZIEL, R. M., MILLER, T. P., RIMSZA, L. M., COOK, J. R., POHLMAN, B., SWEETENHAM, J., TUBBS, R. R., FISHER, R. I., HARTMANN, E., ROSENWALD, A., OTT, G., MULLER-HERMELINK, H. K., WRENCH, D., LISTER, T. A., JAFFE, E. S., WILSON, W. H., CHAN, W. C. & STAUDT, L. M. 2008b. Stromal gene signatures in large-B-cell lymphomas. *N Engl J Med,* 359**,** 2313-23.

LENZ, G., WRIGHT, G. W., EMRE, N. C. T., KOHLHAMMER, H., DAVE, S. S., DAVIS, R. E., CARTY, S., LAM, L. T., SHAFFER, A. L., XIAO, W., POWELL, J., ROSENWALD, A., OTT, G., MULLER-HERMELINK, H. K., GASCOYNE, R. D., CONNORS, J. M., CAMPO, E., JAFFE, E. S., DELABIE, J., SMELAND, E. B., RIMSZA, L. M., FISHER, R. I., WEISENBURGER, D. D., CHAN, W. C. & STAUDT, L. M. 2008c. Molecular subtypes of diffuse large B-cell lymphoma arise by distinct genetic pathways. *Proceedings of the National Academy of Sciences,* 105**,** 13520-13525.

LEONARD, S., WEI, W., ANDERTON, J., VOCKERODT, M., ROWE, M., MURRAY, P. G. & WOODMAN, C. B. 2011. Epigenetic and Transcriptional Changes Which Follow Epstein-Barr Virus Infection of Germinal Center B Cells and Their Relevance to the Pathogenesis of Hodgkin's Lymphoma. *Journal of Virology,* 85**,** 9568-9577.

LEPLEY, D., PAIK, J. H., HLA, T. & FERRER, F. 2005. The G protein-coupled receptor S1P2 regulates Rho/Rho kinase pathway to inhibit tumor cell migration. *Cancer Res,* 65**,** 3788-95.

LI, D. H., TUNG, J. W., TARNER, I. H., SNOW, A. L., YUKINARI, T., NGERNMANEEPOTHONG, R., MARTINEZ, O. M. & PARNES, J. R. 2006. CD72 Down-Modulates BCR-Induced Signal Transduction and Diminishes Survival in Primary Mature B Lymphocytes. *The Journal of Immunology,* 176**,** 5321-5328.

LINTERMAN, M. A., BEATON, L., YU, D., RAMISCAL, R. R., SRIVASTAVA, M., HOGAN, J. J., VERMA, N. K., SMYTH, M. J., RIGBY, R. J. & VINUESA, C. G. 2010. IL-21 acts directly on B cells to regulate Bcl-6 expression and germinal center responses. *J Exp Med,* 207**,** 353-63.

LIU, Y. J., JOSHUA, D. E., WILLIAMS, G. T., SMITH, C. A., GORDON, J. & MACLENNAN, I. C. 1989. Mechanism of antigen-driven selection in germinal centres. *Nature,* 342**,** 929-31.

LIVAK, K. J. & SCHMITTGEN, T. D. 2001. Analysis of relative gene expression data using real-time quantitative PCR and the 2(-Delta Delta C(T)) Method. *Methods,* 25**,** 402-8.

LOSSOS, I. S., ALIZADEH, A. A., EISEN, M. B., CHAN, W. C., BROWN, P. O., BOTSTEIN, D., STAUDT, L. M. & LEVY, R. 2000. Ongoing immunoglobulin somatic mutation in germinal center B cell-like but not in activated B cell-like diffuse large cell lymphomas. *Proc Natl Acad Sci U S A,* 97**,** 10209-13.

LUFTIG, M., PRINARAKIS, E., YASUI, T., TSICHRITZIS, T., CAHIR-MCFARLAND, E., INOUE, J., NAKANO, H., MAK, T. W., YEH, W. C., LI, X., AKIRA, S., SUZUKI, N., SUZUKI, S., MOSIALOS, G. & KIEFF, E. 2003. Epstein-Barr virus latent membrane protein 1 activation of NF-kappaB through IRAK1 and TRAF6. *Proc Natl Acad Sci U S A,* 100**,** 15595-600.

MA, X., YANG, L., XIAO, L., TANG, M., LIU, L., LI, Z., DENG, M., SUN, L. & CAO, Y. 2011. Down-regulation of EBV-LMP1 radio-sensitizes nasal pharyngeal carcinoma cells via NF-kappaB regulated ATM expression. *PLoS One,* 6**,** e24647.

MACLENNAN, I. C. 1994. Germinal centers. *Annu Rev Immunol,* 12**,** 117-39.

MANCAO, C., ALTMANN, M., JUNGNICKEL, B. & HAMMERSCHMIDT, W. 2005. Rescue of "crippled" germinal center B cells from apoptosis by Epstein-Barr virus. *Blood,* 106**,** 4339-44.

MARAFIOTI, T., HUMMEL, M., FOSS, H. D., LAUMEN, H., KORBJUHN, P., ANAGNOSTOPOULOS, I., LAMMERT, H., DEMEL, G., THEIL, J., WIRTH, T. & STEIN, H. 2000. Hodgkin and reed-sternberg cells represent an expansion of a single clone originating from a germinal center B-cell with functional immunoglobulin gene rearrangements but defective immunoglobulin transcription. *Blood,* 95**,** 1443-50.

MARTIN-SUBERO, J. I., GESK, S., HARDER, L., SONOKI, T., TUCKER, P. W., SCHLEGELBERGER, B., GROTE, W., NOVO, F. J., CALASANZ, M. J., HANSMANN, M. L., DYER, M. J. & SIEBERT, R. 2002. Recurrent involvement of the REL and BCL11A loci in classical Hodgkin lymphoma. *Blood,* 99**,** 1474-7.

MARTIN-SUBERO, J. I., KLAPPER, W., SOTNIKOVA, A., CALLET-BAUCHU, E., HARDER, L., BASTARD, C., SCHMITZ, R., GROHMANN, S., HOPPNER, J., RIEMKE, J., BARTH, T. F., BERGER, F., BERND, H. W., CLAVIEZ, A., GESK, S., FRANK, G. A., KAPLANSKAYA, I. B., MOLLER, P., PARWARESCH, R. M., RUDIGER, T., STEIN, H., KUPPERS, R., HANSMANN, M. L. & SIEBERT, R. 2006. Chromosomal breakpoints affecting immunoglobulin loci are recurrent in Hodgkin and Reed-Sternberg cells of classical Hodgkin lymphoma. *Cancer Res,* 66**,** 10332-8.

MARTINEZ-VALDEZ, H., GURET, C., DE BOUTEILLER, O., FUGIER, I., BANCHEREAU, J. & LIU, Y. J. 1996. Human germinal center B cells express the apoptosis-inducing genes Fas, c-myc, P53, and Bax but not the survival gene bcl-2. *J Exp Med,* 183**,** 971-7.

MATHAS, S., JANZ, M., HUMMEL, F., HUMMEL, M., WOLLERT-WULF, B., LUSATIS, S., ANAGNOSTOPOULOS, I., LIETZ, A., SIGVARDSSON, M., JUNDT, F., JOHRENS, K., BOMMERT, K., STEIN, H. & DORKEN, B. 2006. Intrinsic inhibition of transcription factor E2A by HLH proteins ABF-1 and Id2 mediates reprogramming of neoplastic B cells in Hodgkin lymphoma. *Nat Immunol,* 7**,** 207-15.

MATHAS, S., LIETZ, A., ANAGNOSTOPOULOS, I., HUMMEL, F., WIESNER, B., JANZ, M., JUNDT, F., HIRSCH, B., JOHRENS-LEDER, K., VORNLOCHER, H. P., BOMMERT, K., STEIN, H. & DORKEN, B. 2004. c-FLIP mediates resistance of Hodgkin/Reed-Sternberg cells to death receptor-induced apoptosis. *J Exp Med,* 199**,** 1041-52.

MATLOUBIAN, M., LO, C. G., CINAMON, G., LESNESKI, M. J., XU, Y., BRINKMANN, V., ALLENDE, M. L., PROIA, R. L. & CYSTER, J. G. 2004. Lymphocyte egress from thymus and peripheral lymphoid organs is dependent on S1P receptor 1. *Nature,* 427**,** 355-60.

MCADAM, A. J., GREENWALD, R. J., LEVIN, M. A., CHERNOVA, T., MALENKOVICH, N., LING, V., FREEMAN, G. J. & SHARPE, A. H. 2001. ICOS is critical for CD40-mediated antibody class switching. *Nature,* 409**,** 102-5.

MCCLORY, S., HUGHES, T., FREUD, A. G., BRIERCHECK, E. L., MARTIN, C., TRIMBOLI, A. J., YU, J., ZHANG, X., LEONE, G., NUOVO, G. & CALIGIURI, M. A. 2012. Evidence for a stepwise program of extrathymic T cell development within the human tonsil. *J Clin Invest,* 122**,** 1403-15.

MIDDELDORP, J. M. & PEGTEL, D. M. 2008. Multiple roles of LMP1 in Epstein-Barr virus induced immune escape. *Semin Cancer Biol,* 18**,** 388-96.

MONTES-MORENO, S., ODQVIST, L., DIAZ-PEREZ, J. A., LOPEZ, A. B., DE VILLAMBROSIA, S. G., MAZORRA, F., CASTILLO, M. E., LOPEZ, M., PAJARES, R., GARCIA, J. F., MOLLEJO, M., CAMACHO, F. I., RUIZ-MARCELLAN, C., ADRADOS, M., ORTIZ, N., FRANCO, R., ORTIZ-

HIDALGO, C., SUAREZ-GAUTHIER, A., YOUNG, K. H. & PIRIS, M. A. 2012. EBV-positive diffuse large B-cell lymphoma of the elderly is an aggressive post-germinal center B-cell neoplasm characterized by prominent nuclear factor-kB activation. *Mod Pathol,* 25**,** 968-82.

MOORTHY, R. K. & THORLEY-LAWSON, D. A. 1993. All three domains of the Epstein-Barr virus-encoded latent membrane protein LMP-1 are required for transformation of rat-1 fibroblasts. *J Virol,* 67**,** 1638-46.

MORIN, R. D., JOHNSON, N. A., SEVERSON, T. M., MUNGALL, A. J., AN, J., GOYA, R., PAUL, J. E., BOYLE, M., WOOLCOCK, B. W., KUCHENBAUER, F., YAP, D., HUMPHRIES, R. K., GRIFFITH, O. L., SHAH, S., ZHU, H., KIMBARA, M., SHASHKIN, P., CHARLOT, J. F., TCHERPAKOV, M., CORBETT, R., TAM, A., VARHOL, R., SMAILUS, D., MOKSA, M., ZHAO, Y., DELANEY, A., QIAN, H., BIROL, I., SCHEIN, J., MOORE, R., HOLT, R., HORSMAN, D. E., CONNORS, J. M., JONES, S., APARICIO, S., HIRST, M., GASCOYNE, R. D. & MARRA, M. A. 2010. Somatic mutations altering EZH2 (Tyr641) in follicular and diffuse large B-cell lymphomas of germinal-center origin. *Nat Genet,* 42**,** 181-5.

MORRISON, J. A., GULLEY, M. L., PATHMANATHAN, R. & RAAB-TRAUB, N. 2004. Differential Signaling Pathways Are Activated in the Epstein-Barr Virus-Associated Malignancies Nasopharyngeal Carcinoma and Hodgkin Lymphoma. *Cancer Research,* 64**,** 5251-5260.

MOTTOK, A., RENNE, C., WILLENBROCK, K., HANSMANN, M. L. & BRAUNINGER, A. 2007. Somatic hypermutation of SOCS1 in lymphocyte-predominant Hodgkin lymphoma is accompanied by high JAK2 expression and activation of STAT6. *Blood,* 110**,** 3387-90.

MUSCHEN, M., RAJEWSKY, K., BRAUNINGER, A., BAUR, A. S., OUDEJANS, J. J., ROERS, A., HANSMANN, M. L. & KUPPERS, R. 2000. Rare occurrence of classical Hodgkin's disease as a T cell lymphoma. *J Exp Med,* 191**,** 387-94.

MÜSCHEN, M., RE, D., JUNGNICKEL, B., DIEHL, V., RAJEWSKY, K. & KÜPPERS, R. 2000. Somatic Mutation of the Cd95 Gene in Human B Cells as a Side-Effect of the Germinal Center Reaction. *The Journal of Experimental Medicine,* 192**,** 1833-1840.

NGO, V. N., DAVIS, R. E., LAMY, L., YU, X., ZHAO, H., LENZ, G., LAM, L. T., DAVE, S., YANG, L., POWELL, J. & STAUDT, L. M. 2006. A loss-of-function RNA interference screen for molecular targets in cancer. *Nature,* 441**,** 106-10.

NGO, V. N., YOUNG, R. M., SCHMITZ, R., JHAVAR, S., XIAO, W., LIM, K. H., KOHLHAMMER, H., XU, W., YANG, Y., ZHAO, H., SHAFFER, A. L., ROMESSER, P., WRIGHT, G., POWELL, J., ROSENWALD, A., MULLER-HERMELINK, H. K., OTT, G., GASCOYNE, R. D., CONNORS, J. M., RIMSZA, L. M., CAMPO, E., JAFFE, E. S., DELABIE, J., SMELAND, E. B., FISHER, R. I., BRAZIEL, R. M., TUBBS, R. R., COOK, J. R., WEISENBURGER, D. D., CHAN, W. C. & STAUDT, L. M. 2011. Oncogenically active MYD88 mutations in human lymphoma. *Nature,* 470**,** 115-9.

OHSHIMA, K., AKAIWA, M., UMESHITA, R., SUZUMIYA, J., IZUHARA, K. & KIKUCHI, M. 2001. Interleukin-13 and interleukin-13 receptor in Hodgkin's disease: possible autocrine mechanism and involvement in fibrosis. *Histopathology,* 38**,** 368-375.

OK, C. Y., PAPATHOMAS, T. G., MEDEIROS, L. J. & YOUNG, K. H. 2013. EBV-positive diffuse large B-cell lymphoma of the elderly. *Blood,* 122**,** 328-40.

OSADA, M., YATOMI, Y., OHMORI, T., IKEDA, H. & OZAKI, Y. 2002. Enhancement of sphingosine 1-phosphate-induced migration of vascular endothelial cells and smooth muscle cells by an EDG-5 antagonist. *Biochem Biophys Res Commun,* 299**,** 483-7.

OTTO, C., GIEFING, M., MASSOW, A., VATER, I., GESK, S., SCHLESNER, M., RICHTER, J., KLAPPER, W., HANSMANN, M. L., SIEBERT, R. & KUPPERS, R. 2012. Genetic lesions of the TRAF3 and MAP3K14 genes in classical Hodgkin lymphoma. *Br J Haematol,* 157**,** 702-8.

OYAMA, T., ICHIMURA, K., SUZUKI, R., SUZUMIYA, J., OHSHIMA, K., YATABE, Y., YOKOI, T., KOJIMA, M., KAMIYA, Y., TAJI, H., KAGAMI, Y., OGURA, M., SAITO, H., MORISHIMA, Y. &

NAKAMURA, S. 2003. Senile EBV+ B-cell lymphoproliferative disorders: a clinicopathologic study of 22 patients. *Am J Surg Pathol,* 27**,** 16-26.

OYAMA, T., YAMAMOTO, K., ASANO, N., OSHIRO, A., SUZUKI, R., KAGAMI, Y., MORISHIMA, Y., TAKEUCHI, K., IZUMO, T., MORI, S., OHSHIMA, K., SUZUMIYA, J., NAKAMURA, N., ABE, M., ICHIMURA, K., SATO, Y., YOSHINO, T., NAOE, T., SHIMOYAMA, Y., KAMIYA, Y., KINOSHITA, T. & NAKAMURA, S. 2007. Age-related EBV-associated B-cell lymphoproliferative disorders constitute a distinct clinicopathologic group: a study of 96 patients. *Clin Cancer Res,* 13**,** 5124-32.

PALANICHAMY, A., BARNARD, J., ZHENG, B., OWEN, T., QUACH, T., WEI, C., LOONEY, R. J., SANZ, I. & ANOLIK, J. H. 2009. Novel human transitional B cell populations revealed by B cell depletion therapy. *J Immunol,* 182**,** 5982-93.

PANAGOPOULOS, D., VICTORATOS, P., ALEXIOU, M., KOLLIAS, G. & MOSIALOS, G. 2004. Comparative analysis of signal transduction by CD40 and the Epstein-Barr virus oncoprotein LMP1 in vivo. *J Virol,* 78**,** 13253-61.

PARK, S., LEE, J., KO, Y. H., HAN, A., JUN, H. J., LEE, S. C., HWANG, I. G., PARK, Y. H., AHN, J. S., JUNG, C. W., KIM, K., AHN, Y. C., KANG, W. K., PARK, K. & KIM, W. S. 2007. The impact of Epstein-Barr virus status on clinical outcome in diffuse large B-cell lymphoma. *Blood,* 110**,** 972-8.

PASCUAL, V., LIU, Y. J., MAGALSKI, A., DE BOUTEILLER, O., BANCHEREAU, J. & CAPRA, J. D. 1994. Analysis of somatic mutation in five B cell subsets of human tonsil. *J Exp Med,* 180**,** 329-39.

PASQUALUCCI, L., COMPAGNO, M., HOULDSWORTH, J., MONTI, S., GRUNN, A., NANDULA, S. V., ASTER, J. C., MURTY, V. V., SHIPP, M. A. & DALLA-FAVERA, R. 2006. Inactivation of the PRDM1/BLIMP1 gene in diffuse large B cell lymphoma. *J Exp Med,* 203**,** 311-7.

PASQUALUCCI, L., MIGLIAZZA, A., FRACCHIOLLA, N., WILLIAM, C., NERI, A., BALDINI, L., CHAGANTI, R. S. K., KLEIN, U., KÜPPERS, R., RAJEWSKY, K. & DALLA-FAVERA, R. 1998. BCL-6 mutations in normal germinal center B cells: Evidence of somatic hypermutation acting outside Ig loci. *Proceedings of the National Academy of Sciences,* 95**,** 11816-11821.

PASQUALUCCI, L., NEUMEISTER, P., GOOSSENS, T., NANJANGUD, G., CHAGANTI, R. S., KUPPERS, R. & DALLA-FAVERA, R. 2001. Hypermutation of multiple proto-oncogenes in B-cell diffuse large-cell lymphomas. *Nature,* 412**,** 341-6.

PEPERZAK, V., VIKSTROM, I. B. & TARLINTON, D. M. 2012. Through a glass less darkly: apoptosis and the germinal center response to antigen. *Immunol Rev,* 247**,** 93-106.

PEREIRA, J. P., KELLY, L. M. & CYSTER, J. G. 2010. Finding the right niche: B-cell migration in the early phases of T-dependent antibody responses. *Int Immunol,* 22**,** 413-9.

PEREIRA, J. P., KELLY, L. M., XU, Y. & CYSTER, J. G. 2009. EBI2 mediates B cell segregation between the outer and centre follicle. *Nature,* 460**,** 1122-6.

PHAM, L. V., TAMAYO, A. T., YOSHIMURA, L. C., LO, P., TERRY, N., REID, P. S. & FORD, R. J. 2002. A CD40 Signalosome anchored in lipid rafts leads to constitutive activation of NF-kappaB and autonomous cell growth in B cell lymphomas. *Immunity,* 16**,** 37-50.

PHAN, R. T. & DALLA-FAVERA, R. 2004. The BCL6 proto-oncogene suppresses p53 expression in germinal-centre B cells. *Nature,* 432**,** 635-9.

PHAN, R. T., SAITO, M., BASSO, K., NIU, H. & DALLA-FAVERA, R. 2005. BCL6 interacts with the transcription factor Miz-1 to suppress the cyclin-dependent kinase inhibitor p21 and cell cycle arrest in germinal center B cells. *Nat Immunol,* 6**,** 1054-60.

PYNE, N. J. & PYNE, S. 2010. Sphingosine 1-phosphate and cancer. *Nat Rev Cancer,* 10**,** 489-503.

RASTELLI, J., HOMIG-HOLZEL, C., SEAGAL, J., MULLER, W., HERMANN, A. C., RAJEWSKY, K. & ZIMBER-STROBL, U. 2008. LMP1 signaling can replace CD40 signaling in B cells in vivo

and has unique features of inducing class-switch recombination to IgG1. *Blood,* 111**,** 1448-55.

REIF, K., EKLAND, E. H., OHL, L., NAKANO, H., LIPP, M., FORSTER, R. & CYSTER, J. G. 2002. Balanced responsiveness to chemoattractants from adjacent zones determines B-cell position. *Nature,* 416**,** 94-9.

RENNE, C., HINSCH, N., WILLENBROCK, K., FUCHS, M., KLAPPER, W., ENGERT, A., KUPPERS, R., HANSMANN, M. L. & BRAUNINGER, A. 2007. The aberrant coexpression of several receptor tyrosine kinases is largely restricted to EBV-negative cases of classical Hodgkin's lymphoma. *Int J Cancer,* 120**,** 2504-9.

RENNE, C., MARTIN-SUBERO, J. I., EICKERNJAGER, M., HANSMANN, M. L., KUPPERS, R., SIEBERT, R. & BRAUNINGER, A. 2006. Aberrant expression of ID2, a suppressor of B-cell-specific gene expression, in Hodgkin's lymphoma. *Am J Pathol,* 169**,** 655-64.

RENNE, C., WILLENBROCK, K., KUPPERS, R., HANSMANN, M. L. & BRAUNINGER, A. 2005. Autocrine- and paracrine-activated receptor tyrosine kinases in classic Hodgkin lymphoma. *Blood,* 105**,** 4051-9.

RENSHAW, B. R., FANSLOW, W. C., 3RD, ARMITAGE, R. J., CAMPBELL, K. A., LIGGITT, D., WRIGHT, B., DAVISON, B. L. & MALISZEWSKI, C. R. 1994. Humoral immune responses in CD40 ligand-deficient mice. *J Exp Med,* 180**,** 1889-900.

RIBATTI, D., NICO, B., RANIERI, G., SPECCHIA, G. & VACCA, A. 2013. The role of angiogenesis in human non-Hodgkin lymphomas. *Neoplasia,* 15**,** 231-8.

ROSEN, H., ALFONSO, C., SURH, C. D. & MCHEYZER-WILLIAMS, M. G. 2003. Rapid induction of medullary thymocyte phenotypic maturation and egress inhibition by nanomolar sphingosine 1-phosphate receptor agonist. *Proc Natl Acad Sci U S A,* 100**,** 10907-12.

ROSENWALD, A., WRIGHT, G., CHAN, W. C., CONNORS, J. M., CAMPO, E., FISHER, R. I., GASCOYNE, R. D., MULLER-HERMELINK, H. K., SMELAND, E. B., GILTNANE, J. M., HURT, E. M., ZHAO, H., AVERETT, L., YANG, L., WILSON, W. H., JAFFE, E. S., SIMON, R., KLAUSNER, R. D., POWELL, J., DUFFEY, P. L., LONGO, D. L., GREINER, T. C., WEISENBURGER, D. D., SANGER, W. G., DAVE, B. J., LYNCH, J. C., VOSE, J., ARMITAGE, J. O., MONTSERRAT, E., LÓPEZ-GUILLERMO, A., GROGAN, T. M., MILLER, T. P., LEBLANC, M., OTT, G., KVALOY, S., DELABIE, J., HOLTE, H., KRAJCI, P., STOKKE, T. & STAUDT, L. M. 2002. The Use of Molecular Profiling to Predict Survival after Chemotherapy for Diffuse Large-B-Cell Lymphoma. *New England Journal of Medicine,* 346**,** 1937-1947.

ROUGHAN, J. E. & THORLEY-LAWSON, D. A. 2009. The intersection of Epstein-Barr virus with the germinal center. *J Virol,* 83**,** 3968-76.

SCHAADT, M., DIEHL, V., STEIN, H., FONATSCH, C. & KIRCHNER, H. H. 1980. Two neoplastic cell lines with unique features derived from Hodgkin's disease. *Int J Cancer,* 26**,** 723-31.

SCHEEREN, F. A., DIEHL, S. A., SMIT, L. A., BEAUMONT, T., NASPETTI, M., BENDE, R. J., BLOM, B., KARUBE, K., OHSHIMA, K., VAN NOESEL, C. J. & SPITS, H. 2008. IL-21 is expressed in Hodgkin lymphoma and activates STAT5: evidence that activated STAT5 is required for Hodgkin lymphomagenesis. *Blood,* 111**,** 4706-15.

SCHMITZ, R., HANSMANN, M. L., BOHLE, V., MARTIN-SUBERO, J. I., HARTMANN, S., MECHTERSHEIMER, G., KLAPPER, W., VATER, I., GIEFING, M., GESK, S., STANELLE, J., SIEBERT, R. & KUPPERS, R. 2009a. TNFAIP3 (A20) is a tumor suppressor gene in Hodgkin lymphoma and primary mediastinal B cell lymphoma. *J Exp Med,* 206**,** 981-9.

SCHMITZ, R., STANELLE, J., HANSMANN, M. L. & KUPPERS, R. 2009b. Pathogenesis of classical and lymphocyte-predominant Hodgkin lymphoma. *Annu Rev Pathol,* 4**,** 151-74.

SCHULTHEISS, U., PUSCHNER, S., KREMMER, E., MAK, T. W., ENGELMANN, H., HAMMERSCHMIDT, W. & KIESER, A. 2001. TRAF6 is a critical mediator of signal transduction by the viral oncogene latent membrane protein 1. *EMBO J,* 20**,** 5678-91.

SCHWERING, I., BRAUNINGER, A., KLEIN, U., JUNGNICKEL, B., TINGUELY, M., DIEHL, V., HANSMANN, M. L., DALLA-FAVERA, R., RAJEWSKY, K. & KUPPERS, R. 2003. Loss of the B-lineage-specific gene expression program in Hodgkin and Reed-Sternberg cells of Hodgkin lymphoma. *Blood,* 101**,** 1505-12.

SCHWICKERT, T. A., LINDQUIST, R. L., SHAKHAR, G., LIVSHITS, G., SKOKOS, D., KOSCO-VILBOIS, M. H., DUSTIN, M. L. & NUSSENZWEIG, M. C. 2007. In vivo imaging of germinal centres reveals a dynamic open structure. *Nature,* 446**,** 83-7.

SCIAMMAS, R., SHAFFER, A. L., SCHATZ, J. H., ZHAO, H., STAUDT, L. M. & SINGH, H. 2006. Graded expression of interferon regulatory factor-4 coordinates isotype switching with plasma cell differentiation. *Immunity,* 25**,** 225-36.

SEITZ, V., HUMMEL, M., MARAFIOTI, T., ANAGNOSTOPOULOS, I., ASSAF, C. & STEIN, H. 2000. Detection of clonal T-cell receptor gamma-chain gene rearrangements in Reed-Sternberg cells of classic Hodgkin disease. *Blood,* 95**,** 3020-4.

SHAFFER, A. L., ROSENWALD, A., HURT, E. M., GILTNANE, J. M., LAM, L. T., PICKERAL, O. K. & STAUDT, L. M. 2001. Signatures of the immune response. *Immunity,* 15**,** 375-85.

SHI, G. X., HARRISON, K., WILSON, G. L., MORATZ, C. & KEHRL, J. H. 2002. RGS13 regulates germinal center B lymphocytes responsiveness to CXC chemokine ligand (CXCL)12 and CXCL13. *J Immunol,* 169**,** 2507-15.

SIEMER, D., KURTH, J., LANG, S., LEHNERDT, G., STANELLE, J. & KUPPERS, R. 2008. EBV transformation overrides gene expression patterns of B cell differentiation stages. *Mol Immunol,* 45**,** 3133-41.

SIMS, G. P., ETTINGER, R., SHIROTA, Y., YARBORO, C. H., ILLEI, G. G. & LIPSKY, P. E. 2005. Identification and characterization of circulating human transitional B cells. *Blood,* 105**,** 4390-8.

SKINNIDER, B. F., ELIA, A. J., GASCOYNE, R. D., PATTERSON, B., TRUMPER, L., KAPP, U. & MAK, T. W. 2002. Signal transducer and activator of transcription 6 is frequently activated in Hodgkin and Reed-Sternberg cells of Hodgkin lymphoma. *Blood,* 99**,** 618-626.

SMYTH, G. K. 2004. Linear models and empirical bayes methods for assessing differential expression in microarray experiments. *Stat Appl Genet Mol Biol,* 3**,** Article3.

SOUZA, T. A., STOLLAR, B. D., SULLIVAN, J. L., LUZURIAGA, K. & THORLEY-LAWSON, D. A. 2005. Peripheral B cells latently infected with Epstein-Barr virus display molecular hallmarks of classical antigen-selected memory B cells. *Proc Natl Acad Sci U S A,* 102**,** 18093-8.

STEIDL, C., TELENIUS, A., SHAH, S. P., FARINHA, P., BARCLAY, L., BOYLE, M., CONNORS, J. M., HORSMAN, D. E. & GASCOYNE, R. D. 2010. Genome-wide copy number analysis of Hodgkin Reed-Sternberg cells identifies recurrent imbalances with correlations to treatment outcome. *Blood,* 116**,** 418-27.

STEIN, H., MARAFIOTI, T., FOSS, H. D., LAUMEN, H., HUMMEL, M., ANAGNOSTOPOULOS, I., WIRTH, T., DEMEL, G. & FALINI, B. 2001. Down-regulation of BOB.1/OBF.1 and Oct2 in classical Hodgkin disease but not in lymphocyte predominant Hodgkin disease correlates with immunoglobulin transcription. *Blood,* 97**,** 496-501.

STUNZ, L. L., BUSCH, L. K., MUNROE, M. E., SIGMUND, C. D., TYGRETT, L. T., WALDSCHMIDT, T. J. & BISHOP, G. A. 2004. Expression of the cytoplasmic tail of LMP1 in mice induces hyperactivation of B lymphocytes and disordered lymphoid architecture. *Immunity,* 21**,** 255-66.

TAFURI, A., SHAHINIAN, A., BLADT, F., YOSHINAGA, S. K., JORDANA, M., WAKEHAM, A., BOUCHER, L. M., BOUCHARD, D., CHAN, V. S., DUNCAN, G., ODERMATT, B., HO, A., ITIE, A., HORAN, T., WHORISKEY, J. S., PAWSON, T., PENNINGER, J. M., OHASHI, P. S. & MAK, T. W. 2001. ICOS is essential for effective T-helper-cell responses. *Nature,* 409**,** 105-9.

TAKAHASHI, Y., OHTA, H. & TAKEMORI, T. 2001. Fas is required for clonal selection in germinal centers and the subsequent establishment of the memory B cell repertoire. *Immunity,* 14**,** 181-92.

TAM, W., GOMEZ, M., CHADBURN, A., LEE, J. W., CHAN, W. C. & KNOWLES, D. M. 2006. Mutational analysis of PRDM1 indicates a tumor-suppressor role in diffuse large B-cell lymphomas. *Blood,* 107**,** 4090-100.

THORLEY-LAWSON, D. A. 2001. Epstein-Barr virus: exploiting the immune system. *Nat Rev Immunol,* 1**,** 75-82.

THORLEY-LAWSON, D. A. & BABCOCK, G. J. 1999. A model for persistent infection with Epstein-Barr virus: the stealth virus of human B cells. *Life Sci,* 65**,** 1433-53.

THORLEY-LAWSON, D. A. & GROSS, A. 2004. Persistence of the Epstein-Barr virus and the origins of associated lymphomas. *N Engl J Med,* 350**,** 1328-37.

TIACCI, E., DORING, C., BRUNE, V., VAN NOESEL, C. J., KLAPPER, W., MECHTERSHEIMER, G., FALINI, B., KUPPERS, R. & HANSMANN, M. L. 2012. Analyzing primary Hodgkin and Reed-Sternberg cells to capture the molecular and cellular pathogenesis of classical Hodgkin lymphoma. *Blood,* 120**,** 4609-20.

TORLAKOVIC, E., TIERENS, A., DANG, H. D. & DELABIE, J. 2001. The transcription factor PU.1, necessary for B-cell development is expressed in lymphocyte predominance, but not classical Hodgkin's disease. *Am J Pathol,* 159**,** 1807-14.

TZANKOV, A., BOURGAU, C., KAISER, A., ZIMPFER, A., MAURER, R., PILERI, S. A., WENT, P. & DIRNHOFER, S. 2005. Rare expression of T-cell markers in classical Hodgkin's lymphoma. *Mod Pathol,* 18**,** 1542-9.

UCHIDA, J., YASUI, T., TAKAOKA-SHICHIJO, Y., MURAOKA, M., KULWICHIT, W., RAAB-TRAUB, N. & KIKUTANI, H. 1999. Mimicry of CD40 signals by Epstein-Barr virus LMP1 in B lymphocyte responses. *Science,* 286**,** 300-3.

VAN KOOTEN, C. & BANCHEREAU, J. 2000. CD40-CD40 ligand. *J Leukoc Biol,* 67**,** 2-17.

VAN ROOSBROECK, K., COX, L., TOUSSEYN, T., LAHORTIGA, I., GIELEN, O., CAUWELIER, B., DE PAEPE, P., VERHOEF, G., MARYNEN, P., VANDENBERGHE, P., DE WOLF-PEETERS, C., COOLS, J. & WLODARSKA, I. 2011. JAK2 rearrangements, including the novel SEC31A-JAK2 fusion, are recurrent in classical Hodgkin lymphoma. *Blood,* 117**,** 4056-64.

VICTORA, G. D., DOMINGUEZ-SOLA, D., HOLMES, A. B., DEROUBAIX, S., DALLA-FAVERA, R. & NUSSENZWEIG, M. C. 2012. Identification of human germinal center light and dark zone cells and their relationship to human B-cell lymphomas. *Blood,* 120**,** 2240-8.

VICTORA, G. D. & NUSSENZWEIG, M. C. 2012. Germinal centers. *Annu Rev Immunol,* 30**,** 429-57.

VOCKERODT, M., MORGAN, S. L., KUO, M., WEI, W., CHUKWUMA, M. B., ARRAND, J. R., KUBE, D., GORDON, J., YOUNG, L. S., WOODMAN, C. B. & MURRAY, P. G. 2008. The Epstein-Barr virus oncoprotein, latent membrane protein-1, reprograms germinal centre B cells towards a Hodgkin's Reed-Sternberg-like phenotype. *J Pathol,* 216**,** 83-92.

VRZALIKOVA, K., VOCKERODT, M., LEONARD, S., BELL, A., WEI, W., SCHRADER, A., WRIGHT, K. L., KUBE, D., ROWE, M., WOODMAN, C. B. & MURRAY, P. G. 2011. Down-regulation of BLIMP1alpha by the EBV oncogene, LMP-1, disrupts the plasma cell differentiation program and prevents viral replication in B cells: implications for the pathogenesis of EBV-associated B-cell lymphomas. *Blood,* 117**,** 5907-17.

WAN, J., SUN, L., MENDOZA, J. W., CHUI, Y. L., HUANG, D. P., CHEN, Z. J., SUZUKI, N., SUZUKI, S., YEH, W. C., AKIRA, S., MATSUMOTO, K., LIU, Z. G. & WU, Z. 2004. Elucidation of the c-Jun N-terminal kinase pathway mediated by Estein-Barr virus-encoded latent membrane protein 1. *Mol Cell Biol,* 24**,** 192-9.

WANG, D., LIEBOWITZ, D. & KIEFF, E. 1985. An EBV membrane protein expressed in immortalized lymphocytes transforms established rodent cells. *Cell,* 43**,** 831-40.

WENIGER, M. A., MELZNER, I., MENZ, C. K., WEGENER, S., BUCUR, A. J., DORSCH, K., MATTFELDT, T., BARTH, T. F. & MOLLER, P. 2006. Mutations of the tumor suppressor gene SOCS-1 in classical Hodgkin lymphoma are frequent and associated with nuclear phospho-STAT5 accumulation. *Oncogene,* 25**,** 2679-84.

WOLF, J., KAPP, U., BOHLEN, H., KORNACKER, M., SCHOCH, C., STAHL, B., MUCKE, S., VON KALLE, C., FONATSCH, C., SCHAEFER, H. E., HANSMANN, M. L. & DIEHL, V. 1996. Peripheral blood mononuclear cells of a patient with advanced Hodgkin's lymphoma give rise to permanently growing Hodgkin-Reed Sternberg cells. *Blood,* 87**,** 3418-28.

WRIGHT, G., TAN, B., ROSENWALD, A., HURT, E. H., WIESTNER, A. & STAUDT, L. M. 2003. A gene expression-based method to diagnose clinically distinct subgroups of diffuse large B cell lymphoma. *Proc Natl Acad Sci U S A,* 100**,** 9991-6.

WU, L., NAKANO, H. & WU, Z. 2006. The C-terminal activating region 2 of the Epstein-Barr virus-encoded latent membrane protein 1 activates NF-kappaB through TRAF6 and TAK1. *J Biol Chem,* 281**,** 2162-9.

WURSTER, A. L., TANAKA, T. & GRUSBY, M. J. 2000. The biology of Stat4 and Stat6. *Oncogene,* 19**,** 2577-2584.

YAGI, H., KAMBA, R., CHIBA, K., SOGA, H., YAGUCHI, K., NAKAMURA, M. & ITOH, T. 2000. Immunosuppressant FTY720 inhibits thymocyte emigration. *Eur J Immunol,* 30**,** 1435-44.

YE, B. H., RAO, P. H., CHAGANTI, R. S. & DALLA-FAVERA, R. 1993. Cloning of bcl-6, the locus involved in chromosome translocations affecting band 3q27 in B-cell lymphoma. *Cancer Res,* 53**,** 2732-5.

YOUNG, L. S. & MURRAY, P. G. 2003. Epstein-Barr virus and oncogenesis: from latent genes to tumours. *Oncogene,* 22**,** 5108-21.

YOUNG, L. S. & RICKINSON, A. B. 2004. Epstein-Barr virus: 40 years on. *Nat Rev Cancer,* 4**,** 757-68.

ZHENG, B., FIUMARA, P., LI, Y. V., GEORGAKIS, G., SNELL, V., YOUNES, M., VAUTHEY, J. N., CARBONE, A. & YOUNES, A. 2003. MEK/ERK pathway is aberrantly active in Hodgkin disease: a signaling pathway shared by CD30, CD40, and RANK that regulates cell proliferation and survival. *Blood,* 102**,** 1019-27.

ZIMBER-STROBL, U., KEMPKES, B., MARSCHALL, G., ZEIDLER, R., VAN KOOTEN, C., BANCHEREAU, J., BORNKAMM, G. W. & HAMMERSCHMIDT, W. 1996. Epstein-Barr virus latent membrane protein (LMP1) is not sufficient to maintain proliferation of B cells but both it and activated CD40 can prolong their survival. *EMBO J,* 15**,** 7070-8.

ZOTOS, D. & TARLINTON, D. M. 2012. Determining germinal centre B cell fate. *Trends Immunol,* 33**,** 281-8.